# Grey Wolf Optimization based Integral-Backstepping Controller for an Unmanned Aerial Vehicle

Hawi Aboma Kebebew

A Thesis Submitted to

The Department of Electrical Power and Control Engineering

School of Electrical Engineering and Computing

Presented in Partial Fulfillment of the Requirement for the Degree of Master's in Electrical Power and Control Engineering (Control Engineering)

Office of Graduate Studies

Adama Science and Technology University

June 2022

Adama, Ethiopia

# Grey Wolf Optimization based Integral-Backstepping Controller for an Unmanned Aerial Vehicle

Hawi Aboma Kebebew

Advisor: Dr. Endalew Ayenew

A Thesis Submitted to

The Department of Electrical Power and Control Engineering
School of Electrical Engineering and Computing

Presented in Partial Fulfillment of the Requirement for the Degree of Master's in Electrical Power and Control Engineering (Control Engineering)

Office of Graduate Studies

Adama Science and Technology University

June 2022

Adama, Ethiopia

# DECLARATION

I hereby declare that this Master Thesis entitled "Grey Wolf Optimization based Integral-Backstepping Controller for an Unmanned Aerial Vehicle" is my original work. That is, it has not been submitted for the award of any academic degree, diploma, or certificate in any other university. All sources of materials that are used for this thesis have been duly acknowledged through citation

<u>Hawi Aboma Kebebew</u> ______________________ _________________

Name of student Signature Date

# RECOMMENDATION

I, the advisor of this thesis, hereby certify that I have read the revised version of the thesis entitled "Grey Wolf Optimization based Integral-Backstepping Controller for an Unmanned Aerial Vehicle" prepared under my guidance by Hawi Aboma Kebebew submitted in partial fulfillment of the requirements for the degree of Mater's of Science in Control Engineering. Therefore, I recommend the submission of a revised version of the thesis to the department following the applicable procedures.

| Dr. Endalew Ayenew | __________________ | ________________ |
|---|---|---|
| Major Advisor/Supervisor | Signature | Date |

# APPROVAL SHEET

I, the advisor of the thesis entitled "Grey Wolf Optimization based Integral-Backstepping Controller for an Unmanned Aerial Vehicle" and developed by Hawi Aboma Kebebew, hereby certify that the recommendation and suggestions made by the board of examiners are appropriately incorporated into the final version of the thesis.

| | | |
|---|---|---|
| Dr. Endalew Ayenew | ____________________ | ________________ |
| Major Advisor/Supervisor | Signature | Date |

We, the undersigned, members of the Board of Examiners of the thesis by Hawi Aboma Kebebew, have read and evaluated the thesis entitled "Grey Wolf Optimization based Integral-Backstepping Controller for an Unmanned Aerial Vehicle" and examined the candidate during the open defense. This is, therefore, to certify that the thesis is accepted for partial fulfillment of the requirement of the degree of Master of Science in Control Engineering.

| | | |
|---|---|---|
| ____________________ | ____________________ | ________________ |
| Chairperson | Signature | Date |
| Dr. Lebsework Negash | | June 24/2022 |
| External Examiner | Signature | Date |
| Prof. Gang Gyoo Jin | | June 24/2022 |
| Internal Examiner | Signature | Date |

Finally, approval and acceptance of the thesis are contingent upon the submission of its final copy to the Office of Postgraduate Studies (OPGS) through the Department Graduate Council (DGC) and School Graduate Committee (SGC).

| | | |
|---|---|---|
| ____________________ | ____________________ | ________________ |
| Department Head | Signature | Date |
| ____________________ | ____________________ | ________________ |
| School Dean | Signature | Date |
| ____________________ | ____________________ | ________________ |
| Office of Postgraduate Studies, | Dean Signature | Date |

# ACKNOWLEDGEMENTS

First, I would like to thank God for giving me the strength, and opportunity and making it possible to undertake and complete this thesis. Next, I would like to give my deepest thanks to my adviser and mentor, **Dr. Endalew Ayenew**, for his continuous support and advice at all times. He has given me invaluable guidance, inspiration, and, suggestions throughout doing this thesis, and I am so thankful.

Besides my advisor, my thanks are extended to Adama Science and Technology University (ASTU), the School of Electrical Engineering and Computing, the Department of Power and Control engineering, chair for the opportunity they have given me to attend this Master's program. Space Technology Institute (STI) Center of Excellence teams for their continuous support, and sharing of their knowledge. To my family, for their support, motivation, and immense knowledge. My acknowledgment would be incomplete without thanking the biggest source of my strength, and my friends for all the love, support, and encouragement. It would have been impossible without having you around.

Thank you.

Hawi Aboma Kebebew

# TABLE OF CONTENTS

## CONTENTS

# LIST OF TABLES

# LIST OF FIGURES

# LIST OF ACRONYMS

| | |
|---|---|
| $(\phi, \theta, \psi) \in R^3$ | Euler angles |
| $R_B$ | Rigid body frame |
| $R_E$ | Flat earth frame |
| $\xi \in R^3$ | Position of center of mass in flat earth coordinate |
| $\eta \in R^3$ | Attitude angles of body frame in the flat earth coordinate |
| $\omega_i \in R$ | Angular velocity of the $i$ propeller |
| $V \in R^3$ | Velocity in the body frame |
| $R \in R^{3\times3}$ | Rotation transform matrix |
| $\Omega \in R^3$ | Angular velocity in the body frame |
| $F \in R^3$ | Force acting on the quadcopter |
| $M \in R^3$ | Momentum acting on the quadcopter |
| $I \in R^{3\times3}$ | Symmetrical inertia matrix |
| $m \in R$ | Mass of the quadcopter |
| $g \in R$ | Gravitational acceleration |
| $b \in R$ | Trust constant |
| $C_d \in R^3$ | Translational drag coefficients |
| $\ell \in R$ | Distance between the motor and the center of the mass |
| $d \in R$ | Drag factor |
| $C_a \in R^3$ | Aerodynamic friction coefficients |
| $J_r \in R$ | Rotor inertia |
| $T_i \in R$ | The thrust produced by $i$ propellers |

| | |
|---|---|
| $\tau_i \in R^3$ | Torque induced by the rotor |
| $W$ | Weight of the quadcopter |
| $\alpha$ | The first best function of grey wolf optimization |
| $\beta$ | The second-best function of grey wolf optimization |
| $\delta$ | The third best function of grey wolf optimization |

# LIST OF ABBREVIATION

| | |
|---|---|
| ASTU | Adama Science and Technology University |
| BS | Backstepping Control |
| BLDC | Brushless Direct Current |
| CW | Clock-wise |
| CCW | Counter Clockwise |
| Cg | Center of gravity |
| DOF | Degrees of Freedom |
| GA | Genetic Algorithm |
| GWO | Grey Wolf Optimization |
| HTOL | Horizontal Takeoff and Landing |
| IBS | Integral based nonlinear Backstepping Control |
| IBC | Integrator Backstepping Control |
| LQR | Linear Quadratic Regulator |
| MATLAB | Matrix Laboratory |
| MIMO | Multiple-Input-Multiple –Output |
| MPC | Model Predictive Control |
| ODE | Ordinary Differential Equation |
| PSO | Particle Swarm Optimization |
| PID | Proportional-Integral-Derivative |
| RMSE | Root Mean Square Error |
| SMC | Sliding Mode Control |
| STI | Space Technology Institute |
| UAS | Unmanned Aerial Systems |

| | |
|---|---|
| UAV | Unmanned Aerial Vehicle |
| VTOL | Vertical takeoff and landing |

# ABSTRACT

*The quadcopter is a small rotary-wing unmanned aerial vehicle made up of four identical motors with end-fixed individual propellers. It is highly nonlinear, strongly coupled, and affected by wind, and parameter uncertainty makes it unstable. Due to the high input-output interaction, designing a robust and effective control mechanism to handle parameter uncertainty is the most challenging. In this thesis, grey wolf optimization and the integral-based nonlinear backstepping control (GWO-IBS) method are designed to improve the problems. The nonlinear mathematical model of the quadcopter was formulated by using the Newton-Euler mechanism. The model was represented in a nonlinear state space form suitable to drive the integral nonlinear backstepping control law for all state output. The integral and backstepping gains are optimized using the Grey Wolf optimization technique. The overall system analysis is performed using MATLAB 2021a. Simulink and helical trajectory are also designed for trajectory tracking of the horizontal motion of the system. The performance of the robustness and stability of the proposed controller was tested by applying a wind disturbance for 25 seconds with varying magnitudes and loads. The result shows that the proposed control can reject disturbances and handle uncertainty. Finally, the proposed controller is compared with Integral-based Backstepping (IBS) and evaluated their degree of stability in terms of RMSE. From the evaluation, the new proposed GWO-IBS gives small RMSE and a better improvement of 81.68% for x-trajectory, 93.65% for y-trajectory, 99.86% for altitude, and 48.38% for roll angle, 41.29% for yaw angle and 88.75% for yaw angle than IBS. In addition, it shows better performance in unknown disturbance rejection and load mass in all scenarios.*



***Keywords:*** *UAV, Quadcopter, GWO-IBS, wind disturbance, parameter uncertainties, integral action, Lyapunov stability, helical trajectory*

# CHAPTER ONE

# 1. INTRODUCTION

## 1.1. Background

UAV is the shortest form of Unmanned Aerial Vehicle. It is a small robot that can fly without any order from the pilot on board. It is a flying vehicle system that has capable of sustained flight with no direct human control and performs a specific task (Yang et al., 2018). It plays a vital role in specific tasks where risks to pilots are too high and beyond normal human's fast emergency is necessary. Starting from World War I up to half of the 19$^{th}$ century, UAVs were used only for aviation academies, which means they were designed and built for only military purposes. However, here in the 21$^{st}$ century, this technology become a point of sophistication that UAVs are being given attention than other areas of aviation (Zhou et al., 2019).

### 1.1.1. Unmanned Aerial Vehicles (UAVs)

In aerospace, flying machines are frequently referred to as small unmanned aerial vehicles(UAVs), while the entire infrastructures, human, and systems components required to operate such systems for a given operational goal are often called unmanned aerial systems (UASs) (Can & Içmez, 2014). Contain receiver transmitter and connect to communicate by using radio frequency flight control and receive the information that tells UAV what to do using the transmitter. In recent years, these aircraft have been commonly applied in our day-to-day life activities. UAVs can be very small in size, space, and weight compared to manned air vehicles. The latest development of Micro-electro technology and human crew with a significant weight and space can be substituted by the very small device in UAVs. Before all, we knew those UAVs can able to deliver and transport equipment from one place to another. The UAV includes anything additional such as a camera, sensor, and poly load for delivery purposes.

### 1.1.2. Classification of UAVs

Several groups have been proposed according to the international UAS community. From those groups and classifications of UAV schemes, the current systems are based on the operation principle and their capabilities to fly in the air. Figure 1.1 shows as the UAV classification into the different groups is as follows (Hsieh et al., 2020). These vehicles are being increasingly used in many civil domains, especially for agriculture, healthcare, environmental research, security, film industry, and many others.

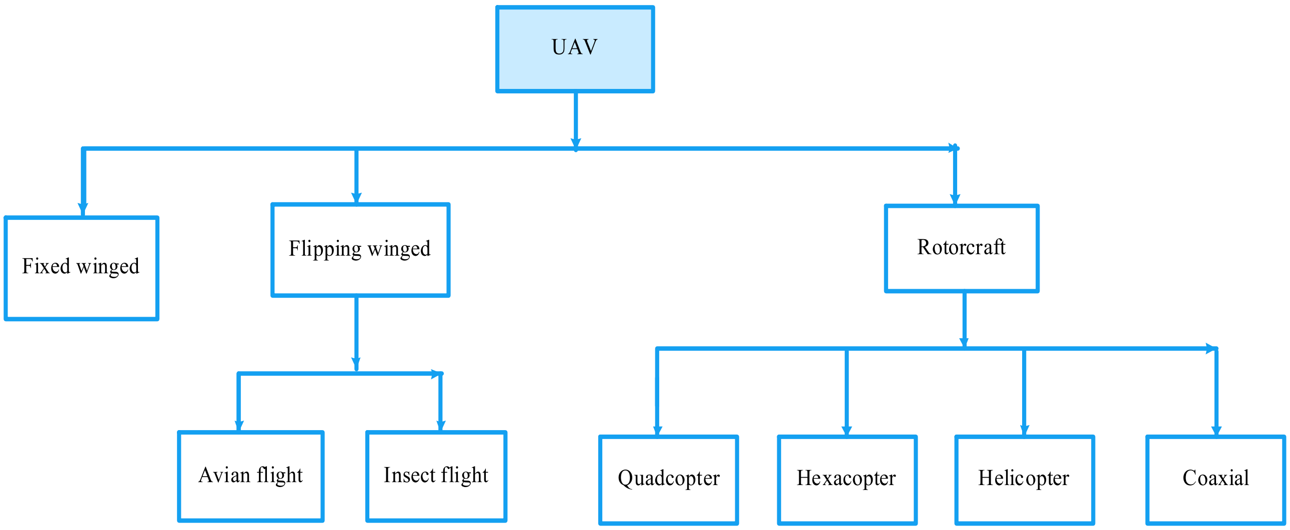


Figure 1.1: Types of a UAV system

### 1.1.3. Based on Aerodynamics

Fixed-wing, multi-copter, motor parachute, single-copter, and glider are just a few of the categories of the UAV systems that have been designed and are in the development stage.

**Fixed-wing UAV: -** Fixed wings can help the vehicle to generate lift to generate propulsion and the simplest structure. They are more comfortable, have long Battery life, are better for large areas, consume less power, are aerodynamically stable systems, and have a thrust loading of lower than 1. To regulate the orientation of an aircraft, rudders, ailerons, and elevators are employed to control yaw, roll, and pitch angles. However, hard to design and implement and may need a launcher device and needs open area for takeoff and landing. Such UAVs cannot hover at a single location as a multi-rotor UAV can. Fixed wings are the main lift generating elements in response to forwarding accelerating speed.

**Rotary wing UAV: -** Rotorcraft, or rotary-wing aircraft, is a heavier-than-air flying machine that uses lift generated by wings, called rotary wings or rotor blades. The rotary wing is the most popular, and it may have a single rotor, two rotors, three rotors, and more than four. Unlike fixed-wing, the thrust force is produced by the main rotor blade, which is used for both lift and propelling, and use the system has the ability of vertical takeoff and landing and hove. The system has vertical takeoff and landing and hovering capabilities.

**Multi-Rotor UAV: -** Such vehicles have multiple rotors and propellers and are actors for VTOL. There is a further subdivision of multi-rotor based on the number of rotors:

i. Quadcopter (4 rotors)
ii. Hex copter (6 rotors)
iii. Octocopter (8 rotors)
iv. Decacopter (10 rotors)
v. Dodecacopter (12 rotors)

Their ability to hover and maintain speed makes them for surveillance purposes and monitoring. Figure 1.2 shows the class of fixed-wing UAVs on the right-hand side and rotary-wing on the left side.

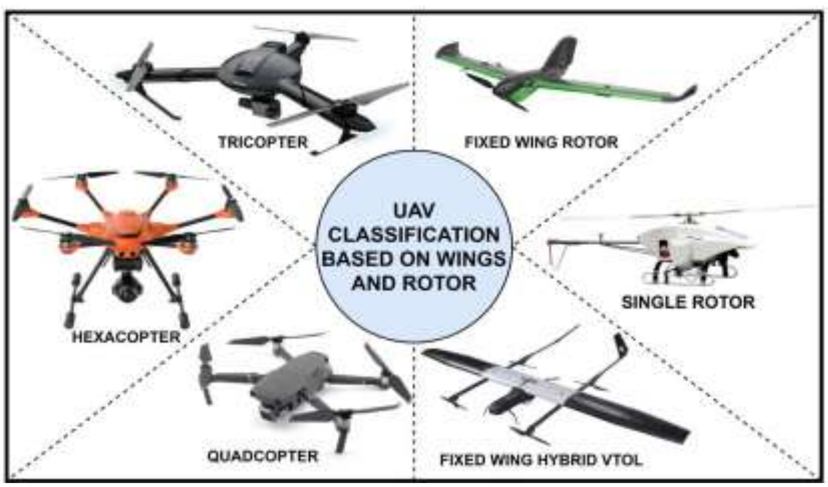


Figure 1.2: UAV Classification based on wings and Rotor (Chamola et al., 2021)

### 1.1.4. Based on Landing

Based on the ability to have UAV landing and takeoff classified into two main parts. The first one is Horizontal takeoff and landing (HTOL), which has high cruise speed and a smooth landing and is categorized as a fixed-wing aircraft's extension and the second one is vertical takeoff and landing (VTOL) (Singhal et al., 2018). Under the category of rotorcraft UAVs, four-rotor has acquired much attention among researchers in recent years because of their low cost, ability to change position, hover, simplicity of their structure, vertical take-off ability, and landing (VTOL). The system also can complete a variety of tasks in control and aerospace engineering.

### 1.1.5. History of Quadcopters-type UAV

In 1920 the first rotorcraft design experiment was done by Etienne Oehmichen (Sabatino, 2015). This scientist did various six experiments designs is tried, and among them, his multi-copter had 4- rotors Figure 1.3(a) and 8-propellers. All are driven by one engine, and he used steel and tube frame with 2- bladed which is mounted on the rotors at the end of all arms. Among the 8-propellers are spinning horizontally and stabilizing the machine. The other propeller was fixed on the nose for steering, and the couple of them was used for forwarding actuation. The amount and quality of stability and controllability are undertaken. He tried above thousand flight tests in the middle of a year. The first recorded distance for the helicopters is 360m, and 1 kilometer closed-circuit is done flight rotorcraft.

(a) 
(b) 

(c) 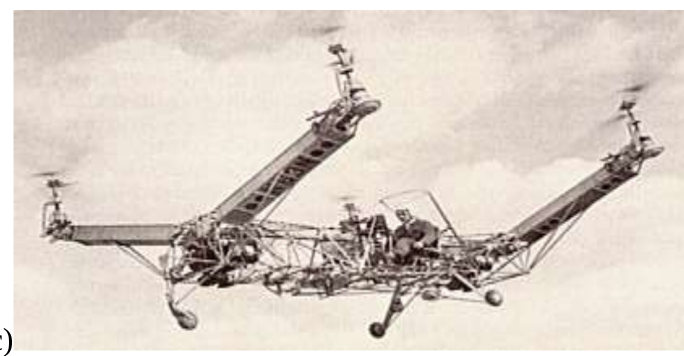

Figure 1.3:(a) Oehmichen No.2 Quadrotor (b) de Bothezat Quadrotor (c) Model A quadrotor

Figure 1.3(b) showed that another aircraft was designed after Oehmichen by two scientists known as Dr. George de Bothezat and Ivan Jerome. In 1922 flew into the air for the first time, and almost 100 flights were made before the end of two years. The inverted system has an x-shape and is 6-bladed with ended by mounted rotors. The system had two propellers used to control trust and yaw movement with variable movement pitch. Despite exhibiting feasibility, it was underpowered, mechanically complex, and prone to reliability issues. The side motion was unacceptable because the operations workload was very high when it hove and has 5m altitude. In the Reference (Sabatino, 2015), the model has 2-engine used to drive the 4-rotors fixed wings prototype that was developed in 1956 for a military quadrotor helicopter. Control its motion by changing the trust among rotors. The operation is completed and the quadrotors flayed successfully for the first time. Convert wings proposed a Model E that would have a maximum weight of 19,000 kg with a payload of 4900 kg, as shown in Figure 1.3(c).

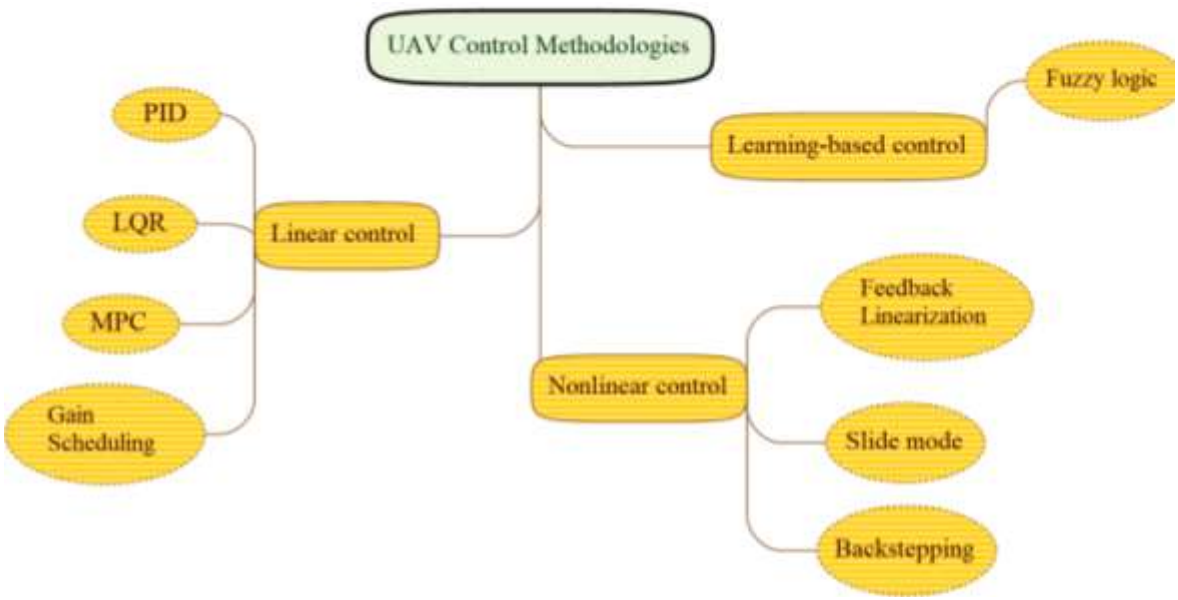


Figure 1.4: Classification of control methodologies for UAV control

Due to the complicity of quadcopter-type UAV being highly nonlinear and having many inputs with multiple outputs, selecting a suitable Control strategy is the most important, and Figure 1.4 shows the different control methods of UAV. The Control system begins development from where the quadcopter was invented to meet the desired performance. From classical control mechanisms, there is a linear controller such aa s PID controller (Siti et al., 2019) (Leal et al., 2021); designed controllers include a linear PID controller and a modeling and genetic algorithm-based PID controller (Alkamachi & Erçelebi, 2017), a linear secondary controller (LQR) (Kim et al., 2019), in those controllers, there is the gain which calculated by try and error. Those methods are time consume and lead to high steady-state error to reduce limitations are optimization mechanisms like Ziegler-Nichols (Z-N), genetic algorithm (GA) with PID, and Particle Swarm Optimization (PSO) (Vishal & Ohri, 2015). Adaptive digital PID control algorithm (Xuan-Mung & Hong, 2019).amount the lathe optimal control mechanisms there Linear Quadratic Regulator (LQR) (Ganapathy Subramanian & Elumalai, 2016)(Lin et al., 2019) and Gain scheduled LQR(Shah et al., 2018). The actual non-linear system and sliding mode control (SMC) (Roy et al., 2021). SMC has the inherent problem of the undesired significant control chattering phenomenon caused by the large switching gain of the discontinuous switching control term (P. Gao et al., 2019). Other control methods for nonlinear systems have been investigated [16]. A reasonable control strategy must guarantee global stability and improve tracking and transient performance (Suresh et al., 2018). The backstepping methods have been widely used to solve the control problems of nonlinear systems. It can guarantee global stability and improvement of tracking and transient performances and is a recursive method that uses the Lyapunov function and a systematic design approach to certain forms of nonlinear systems. The integral control action is added to backstepping control to minimize the tracking error and to have a fast response. The grey wolf optimization also can search for the optimal and global value of the gains.

## 1.2. Statement Problem

Quadcopter-type UAV systems are highly nonlinear, MIMO, and non-minimum phases. The system has four control inputs and six controlled outputs that indicate it is strongly coupled. This system is affected by possible parameter uncertainties and unknown external disturbances. Currently, there are two main control problems to be solved. The first is the usage of linear manipulation techniques like PID from classical control and LQR implemented via the linearization of a non-linear system. During the linearization process, some of the system behaviors are ignored, and the quadcopter does not meet the behavior of a real system. The main drawback of the linearization method is the lack of robustness in the presence of system parameter uncertainties, such as the mass of the quadcopter, and unknown external disturbances. In this situation, the linear controllers are no longer ensured of a global run, and the operating range is limited.

Secondly, even in nonlinear control, the 4DOF (altitude and attitude-roll, pitch, yaw angles) control of the quadcopter independently, the respective controller estimates the attitude and altitude to the desired value. This may be a better hover controller, but it is still not enough. In the existence of wind gusts through this system, the wind might initially introduce a little roll angle, but our roll controller removes that error and gets the quadcopter back to level flight with the ground. However, the thrust vector is not straight up and down for a very brief time during the roll. Therefore, the quadcopter will have moved a little bit horizontally. A little bit of gust comes and causes another roll and pitch error, and the quadcopter walks away for a little more. This controller still allows it to meander away slowly; there is no way in the control scheme that will bring the quadcopter back to its reference position.

To overcome those problems, the implementation of active disturbance rejection and uncertainty handling in a nonlinear position control law is a must be needed.

## 1.3. The Objective of This Thesis

### 1.3.1. General Objective

The main objective of this thesis is to develop a grey wolf optimization based Integral-based non-linear backstepping controller for quadcopter-type UAV

### 1.3.2. Specific Objective

- ✓ Develop a mathematical model of the quadcopter
- ✓ Design Integral-Backstepping controller for altitude and position control of the quadcopter
- ✓ Design an Integral-Backstepping controller for attitude control of the quadcopter
- ✓ Tuning the proposed controller gains using Grey Wolf Optimization
- ✓ Investigate performance of proposed controller in terms of RMSE

## 1.4. Scope of Thesis

The scope of this thesis, deriving a mathematical model of system dynamics and designing an Integral-based Non-linear Backstepping controller with a grey wolf optimization algorithm for tuning the gain of control for controlling the altitude, helical trajectory passes for horizontal motions of the quadcopter, and attitude of a quadcopter-type UAV and implementation is done on MATLAB2021a/Simulink to simulate, and test the controller performance with the quadcopter.

There is no hardware implementation. Because implement this system also needs high cost acquired, time, and availability of a component.

## 1.5. The motivation of the Thesis

Today Quadcopter-type UAVs are being used in several areas for various purposes especially in healthcare to deliver medical supplies in emergency cases. Thus, the design of control algorithms takes an important role in designing these advanced technology systems. Currently, Ethiopians are also starting to develop and build unmanned aerial robots. The innovation foundations are having second and Initiatives to utilize privately created drones is one of them. Since the system access to electricity even in the health centers is low, storing vaccines in suitable environments has been unsustainable. Quadcopter-type UAVs are used to transport vaccines from proper storage areas to remote health centers. The advancement and introduction of the making a strong technology in drones have developed a new field of research. This kind of vehicle can maneuver in small spaces and is used to perform a large set of tasks.

## 1.6. Significant of Thesis

Currently, these types of research are implemented in many countries due to multi-purpose application areas and the advantages of multi-rotor UAVs. In August 2018, the service of health of Ethiopia declared designs to utilize UAVs to convey clinical equipment and supplies to far-off areas of Ethiopia. This would assist with disseminating medication and blood supplies to regions where admittance to the street is hard and costly. This would help to distribute medicine and blood supplies to areas where access to the road is hard and expensive. Controlling the Unmanned Aerial Vehicle position, altitude and orientation is a very interesting research field in control system areas and this thesis research develops a robust controller to achieve the solution. Additionally, for Adama science and technology university (ASTU), the Space Technology Institute (STI) Center of Excellence could be important due to the research and development teams trying to design and develop their quadcopter UAV in the Ethiopian market.

## 1.7. Thesis Organization

This thesis research consists of five chapters with well organized. Chapter 1 introduces the system's historical background and quadcopter-type UAV. It also includes a statement of the problem, the detailed objective of the thesis, scope with limitation of study, motivation, and significance of the thesis. Chapter 2: deals with the review of the literature on control schemes of the quadcopter-type UAVs. The theoretical background of the backstepping controller and the advantages of GWO over other algorithms. Chapter 3 contains the methodology, materials, nonlinear kinematics, and dynamics model of the quadcopter for each rotational and translational equation of motions. Chapter 4: detail about the open-loop response of the system, and the proposed control strategies Integral-based non-linear Backstepping control for the nonlinear dynamic model of the quadcopter system. Chapter 5: in this section, the simulation results with detailed analysis, and the conclusion, recommendation, and prospective work for future researchers are finalized.

# CHAPTER TWO

# 2. LITERATURE REVIEW AND THEORETICAL BACKGROUND

## 2.1. Introduction

This chapter consists of a discussion and summary of what works in previous research based on the control mechanism of quadcopter-type UAV. The reviews debug drawn-backpack designed controllers in that research works. Finally, closely related works along with their admirable quality and faults are reviewed and discussed. Additionally, the principle and architecture of quadcopter-type unmanned aerial vehicles (UAVs) are discussed with its advantage when quadcopter-type UAVs are applicable in healthcare. Finally, discuss how the backstepping controller is integrated with integral action and grey wolf optimization. Closed by with mention some advantage of GWO over anthers optimization mechanisms.

## 2.2. Related Works on Quadcopter-type UAV Control Systems

In the beyond few years, exceptional manipulation techniques have been explored for the mindset and position manipulation of the quadrotor (DING et al., 2019). Therefore, those controllers' simplest paintings are higher while the quadrotor is close to the equilibrium state. Such a controller no longer carries out properly at some point of the life of unknown outside disturbance and is not always assured stability. The controller design is linear; consequently, it displays numerous results while carried out in a real non-linear system. System obstacles additionally propagate undesired overall performance of the machine in real-time applications.

(Saibi et al., 2022)Backstepping Control for 6-DOF and Genetic Algorithm-Based Tuning of Backstepping Controller (Rodríguez-Abreo et al., 2020) for quadcopter-type UAV is done. The quadrotor dynamics for 6-DOF and PID numerical results and comparison with backstepping. The proposed control system shows high performance in the face of parametric uncertainties, as is clear from the time of establishment on different reference inputs and errors of different magnitudes than the classical one. There is a lack of robustness in the system during disturbance and uncertainty existence. The controls are performed only for the linear system; even if the system is non-linear dynamic, it needs a linearization method. The research focused on Design Controller for Altitude Only of multi-copter UAVs (Setyawan et al., 2019)

(Basri et al., 2018) This paper focused on the Design of Backstepping-based Non- Linear Control for Quadrotor helicopters. To design control to stabilize the vehicle in a hovering mode. Modeling the system with the ‘X’ quadcopter structure for 4 degrees of freedom (DOF) and the designed controller adapts the Lyapunov stability criteria. Achievement, the designed control method has stabilized the vehicle at a hovering state, and the attitude of the quadcopter is stabilized around the desired value. The paper cannot test the robustness of the controller. The classical backstepping controller has two main disadvantages. First, the controller's gain is selected via the time-consuming trial and error method. Secondary, Luck of robustness because of not robust under external disturbance and parameter uncertainty.

(Shah et al., 2018)The main objective of this research paper is to design an optimal control method for controlling altitude and angular motion of quadcopter through applying Gain scheduled LQR on Based on the dynamics of quadcopter linearized model to obtain linear state space for the design of LQR controller. Minimize the steady-state error by adding integral control action. Control trajectory tracking of the quadcopter is done using helical. Compare the new control method with the conventional LQR. The authors got a minimum of the steady-state errors during the gain scheduled controller, which has better performance than LQR. In paper work, there are three main visible limitations. The most fulfilling approach LQR manipulate implemented via the linearization system of a non-linear system. That method is controlled and reflects different effects on the system, and the second is Q and R are the weighted matrices of the state vector, and the input vector is chosen arbitrarily and not optimized. At last, the controller's performance during sudden disturbance and modeled parameters of the system in real-time applications were not tested.

(Liu et al., 2016) Design PID and LQR Trajectory Tracking Control for an Unmanned Quadrotor Helicopter. The author’ Achievement Simulations were carried out to compare the effectiveness of the designed control strategies. LQR controller is smoother and has less disturbance than PID. The limitations of this work are that most of the prevailing control systems use linear manipulation techniques like PID from the classical management and top-of-the-lineline approach LQR manipulation implemented through the linearization system of a nonlinear and Luck of robustness. Table 2.1 summarizes the controller in the previous related works and the limitation of their works.

Table 2.1: Summary from previous related work on control of Quadcopter-type UAV

| Control algorithm | Type | Robustness | Additivity | Optimality | tracking ability | Fast convergences | Disturbance reject | Unmolded-Parameter handling | Chattering/energy | Limitation |
|---|---|---|---|---|---|---|---|---|---|---|
| PID in (Liu et al., 2016) | Linear | ∗ | ↓ | ↓ | ∗ | ∗ | ↓ | ↓ | ↓ | Reflects dissimilar, luck of robustness |
| LQR in (Shah et al., 2018) | Linear | ↓ | ↑ | ∗ | ∗ | ∗ | ∗ | ↓ | ↓ | Q, R vector is chosen arbitrarily, Reflects dissimilar Not tested and only designed for 4DOF |
| MPC.in(Cheng & Yang, 2017) | Linear | ↓ | ↑ | ↑ | ∗ | ∗ | ∗ | ∗ | ↓ | Designed for pass plan only The required high data store memory |
| SMC(Mamo , 2020) | Non-linear | ∗ | ↑ | ∗ | ↑ | ↑ | ↑ | ∗ | ↑ | Not optimal, for 4dof only, high gain need |
| BS in (Saibi et al., 2022) (Rodríguez-Abreo et al., 2020) (Basri et al., 2018) | Non-linear | ∗ | ↑ | ↓ | ↑ | ∗ | ↑ | ↑ | ↓ | No integral action, high steady state errors No-optimization algorithm |

Note: ↓ stand for low, ↑ stand for high, and ∗ is average

(Cheng & Yang, 2017) This work's objective is to design Model Predictive Control to track the reference trajectory of the outer loop or position loop. The achievement of this work is that MPC controllers are designed, and PID controllers are designed to track the reference attitude. Results validate the effectiveness s of the proposed control approach, and there are also limitations. A linear state space MPC used method. The weighted matrices Q, R, and PID gains are chosen arbitrarily without any optimization algorithm. Generally, the above control strategies may be divided into groups. The first institution linearizes the version and uses linear regulation to lay out the controller. Whereas the second one is the nonlinear idea of the layout of the controller. Linear model predictive control (LMPC) is applied to solve the path tracking problem for a quadrotor (Y. Gao et al., 2022). The proposed controller good performance and the system track the given path. The robustness and balance nonetheless want to be improved. However, MPC is a complex algorithm control algorithm that needs a longer time than the other controller.

## 2.3. The Theoretical Background Quadcopter-type of UAV System

### 2.3.1. Working principle of Quadcopter-type UAV System

A special class of multi-rotor having four rotors with individually end-mounted propellers has four motors. Each motor contains the individual propellers matched to a separately powered motor. The light of a quadcopter-type UAV works over different principles with varying degrees of autonomy. Initially, the working and naming of multi-rotor unmanned vehicles are based on the number of rotors and control of their movement through the rotor of the motors either under the supervision of a human operator or independently by the onboard computer. Rotating motor with varying speed and torque produced by the rotor, then based on the direction of motor rotation motion of the quadcopter-type UAV is performed. This vehicle has four motors and is used to perform the motion. That is what we call a quadrotor. This particular case of multi-rotor has four rotors with individually end-mounted propellers. Those rotors are fixed at the end of the vehicle arms in a different placement which can form different shapes of quadcopter-type UAVs.

This flying robot has six degrees of freedom with only four actuators, and there are two configurations, “X” (cross) and (plus) “+” based on the definition of the body frame, as shown in Figure 2.1. X, an arrangement of parts, is more stable when compared with the “+” (Bjälemark, 2013). Quadcopter required a yaw control input during the flight, and its control mechanism is the same for all configurations, but the pitch and roll control mechanism is about 30% greater in the case of X-configuration. The propellers and rotors are located on the end of the frame (Kandeel et al., 2022).

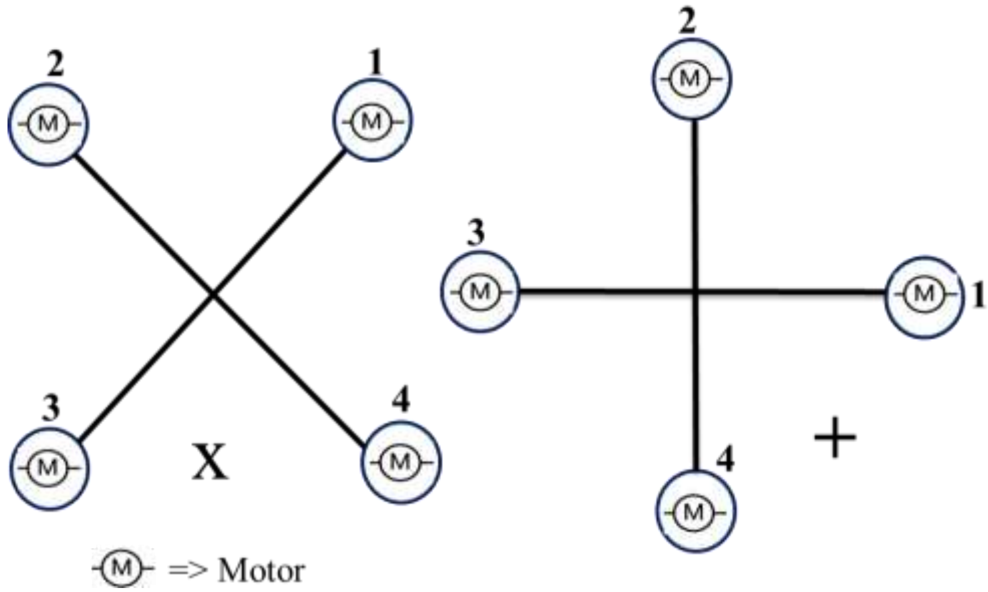


Figure 2.1: “×” and “+” configuration of the quadcopter

The direction that the propellers are spinning in the opposite direction of torque induced by motors. The four motors are named numerically by 1, 2, 3, and 4. Also, there is facing towards the front of the quadcopter, motors 1 and 3 spin clockwise, whereas motors 2 and 4 spin counterclockwise. Each movement attempts to reach its stable position by balancing different forces acting on it. From Figure 2.2 all possible movements of X-configuration of the quadcopter with associated the rotor speed. In the case of flight, there are four forces all four main forces acting on quadcopter motion are thrust, lift, and torque is shown in Figure 2.2 as follows (Akhtar, 2017). Thrust is a pushing force and can act in any direction. The thrust is generated by the propellers, and Weight is the force of gravity. It acts in a downward direction toward the center of the Earth. Lift is a force that directly opposes the weight of aircraft, so gravity will try and lift will keep it up in the air. Drag is the force that acts opposite to the direction of motion. Drag tends to slow down the flying machine and is caused by friction in air pressure (Niemiec & Gandhi, 2016).

Table 2.2: Possible movements of the quadrotor with associated the rotor speed

| Types-of motions | Motor 1 Clockwise | Motor 2 Anti-clockwise | Motor 3 Clockwise | Motor 4 Anti-clockwise |
|---|---|---|---|---|
| Take off | ↑ | ↑ | ↑ | ↑ |
| Landing | ↓ | ↓ | ↓ | ↓ |
| Right | ↓ | ↑ | ↑ | ↓ |
| Left | ↑ | ↓ | ↓ | ↑ |
| Forward | ↓ | ↓ | ↑ | ↑ |
| Backward | ↑ | ↑ | ↓ | ↓ |
| clockwise | ↑ | ↓ | ↑ | ↓ |
| Anticlockwise | ↓ | ↑ | ↑ | ↓ |

Note: ↓ is decreasing motors speed, ↑ is increasing the motor speed

According to the 3rd law of Newton, when every object is in action, there is another action that is equal in magnitude but opposite in the direction of motion of an object. This law is applied in the motion of every aircraft, and quadcopter propellers will also rotate the body in the opposite direction, and balancing going to be important in understanding working principles.

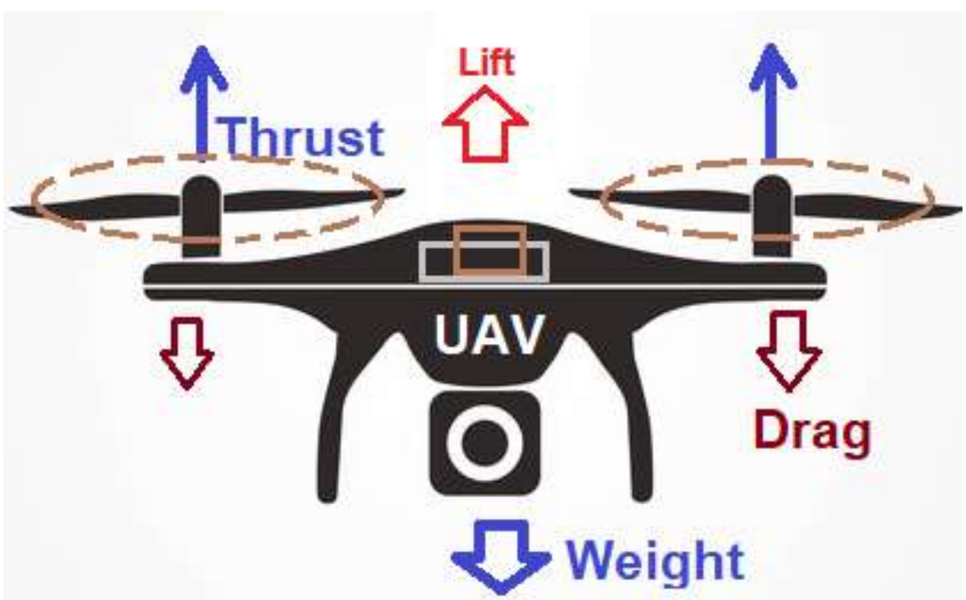


Figure 2.2: The Four Different types of forces applied to UAVs (Pattern, 2021)

### 2.3.2. Application of Quadcopter-Type UAV in Health Care

In a developing country like Ethiopia, the use of this quadcopter-type UAV is rare, especially in healthcare for the delivery of small emergency medications(USAID, 2019). However, the demand for automated systems is constantly increasing while the technology is limited basically, and to be able to fly autonomously doing an action simplifies human power for contribution, increasing its ability exponentially. UAVs in healthcare also are very thought-provoking. It is an effective life-saving process. It can get into an urgent scene quicker than human beings and ground vehicles which can save many lives. It is easy to use, portable to reliable in providing health care for various purposes. It helps to provide more efficient healthcare to patients from a distance by eliminating some human steps (Balamurugan et al., 2020). Have structure Figure 2.3 and UAVs could deliver medicine to the bedside of a patient from the pharmacy and vaccines and can be used in the transport of blood from the store to the place of surgery and take tests from hard-to-arrive regions to the labs in neighboring towns (Nithyavathy et al., 2020). Additional UAV support carries oxygen supply to people who are suffering from respiratory syndrome.

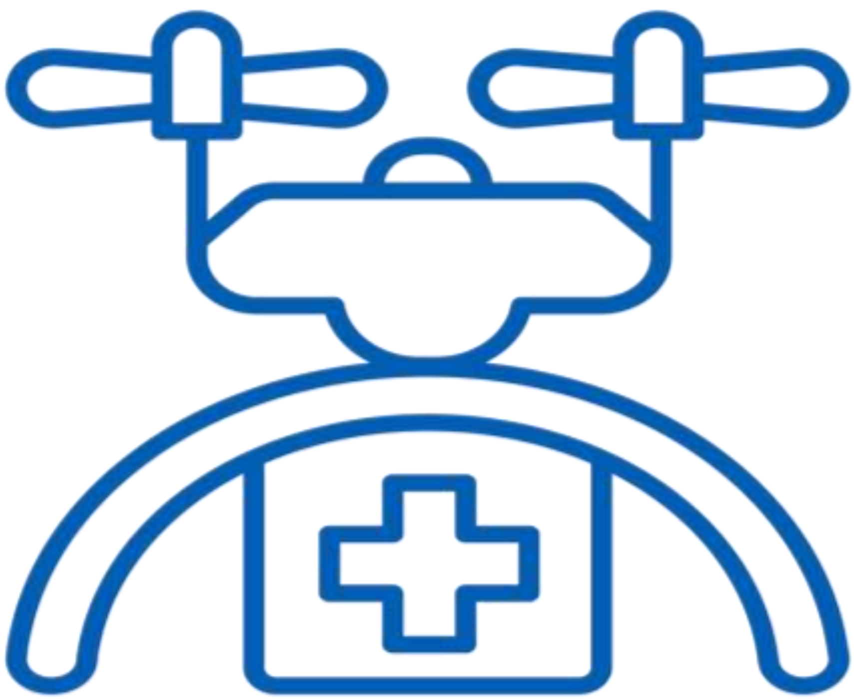

Figure 2.3: Quadcopter-type UAV in healthcare for emergency medications(Tps & Tp, 2018)

## 2.5. Overview of Backstepping Control

From recent nonlinear control theory, backstepping is the most effective recursive structured control mechanism applicable for stabilizing nonlinear systems. Firstly, it was developed by Petar V. Kokotovic in 1990 as a special class of nonlinear dynamic systems to stabilize and improve the problem(Luis & Moncayo, 2021). The backstepping method has been of great interest since its proposal and has been widely applied to control problems arising from aerospace engineering. The backstepping control approach is divide a system into subsystems that do not reach the order of the system and design the control law to stabilize each subsystem(Sheng & Wei-qi, 2017). During the designing of this controller, the user can start the design process at the known-stable system and "back out" new controllers that progressively stabilize each subsystem and stop when the final control laws are achieved. Consider the nonlinear system defined as represented as the block diagram shown in Figure 2.4.

$$\begin{aligned} \dot{\boldsymbol{x}} &= \boldsymbol{f}(\boldsymbol{x}) + \boldsymbol{g}(\boldsymbol{x})\varepsilon \\ \dot{\varepsilon} &= u \end{aligned} \tag{2.1}$$

Consider $\varepsilon$ as a virtual controller. It is assumed that there exists a smooth feedback control law

$$\varepsilon = \gamma(x) \tag{2.2}$$

With $\gamma(0) = 0$ such that $x = 0$ is an asymptotically stable equilibrium of the original system. The strict-feedback plant is described as

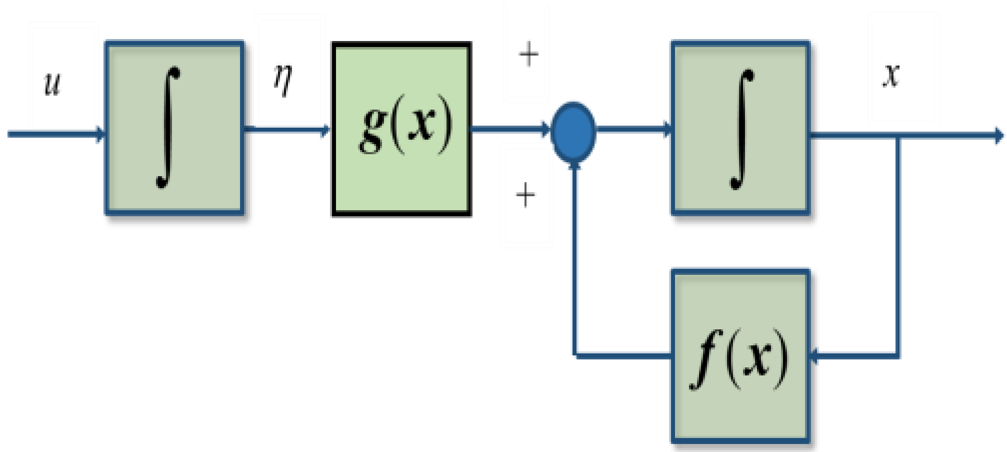


Figure 2.4: Block diagram of the nonlinear system (Luis & Moncayo, 2021)

$$\dot{x}_1 = f_1(x_1) + g_1(x_1)x_2$$
$$\dot{x}_2 = f_2(x_1, x_2) + g_2(x_1, x_2)u \tag{2.3}$$

where $x_1, x_2 \in R^m$ are the states, $u \in R^m$ is the control law, $f_1 : R^m \to R^m$, $f_2 : R^m \times R^m \to R^m$, are smooth nonlinear vector fields, and the matrix-valued function, $g_1 : R^m \to R^{m\times m}$ and $g_2 : R^m \times R^m \to R^{m\times m}$, are smooth and have the inverse. The controller is adapting the Lyapunov stability behaviors and improves the performance of the controller and system (Gouta et al., 2016). The backstepping technique applied once quadcopter model developed. The choice of this method is considering the major advantages it presents (Bouadi et al., 2007):

- ✓ It ensures Lyapunov stability.
- ✓ It ensures the handling of all system nonlinearities
- ✓ It ensures the robustness of all properties of the desired dynamics.

### 2.5.1. Lyapunov function and Lyapunov stability

Lyapunov functions are scalar functions that may be used to prove the stability of equilibrium of an ODE and the most crucial function to check the stability of systems in control theory ("Lyapunov Function," 2008). Lyapunov functions have sufficient and necessary conditions for stability. The main merit of Lyapunov function-based stability analysis is that the actual solution, whether analytical or numerical of the ODE is not required. Define a Lyapunov function as:

$$V(x) = \frac{1}{2}x^2 \tag{2.4}$$

Which is a positive definite ( $V\ (0) = 0$ and $V\ (x) > 0$ with $x = 0$ ) and if $V(x) \to +\infty\ for\ ||x|| \to +\infty$ is called radially unbounded. Asymptotical stability of nonlinear systems if there is $V\ (x)$ that is globally positive definite and radially unbounded such that $\dot{V}(x) \le 0$ is globally negative definite, then which satisfies Condition of globally asymptotically stable.

### 2.5.2. Integral action

The integral actions are used to eliminate the steady-state errors of the system, reduce response time and restrain overshoot of the control parameters(Leal et al., 2021). The main limitation of the backstepping control algorithm is that its robustness is not good. To increase the robustness of this algorithm in the existence of disturbances and parameter uncertainty, the integrator control action defines as:

$$\text{integtral } (p) = \int_0^t e(\tau) d\tau \tag{2.5}$$

To solve the tracking problem $\text{limit}_{t\to\infty}\ [x_1(t) - x_d(t)] = 0$, where $x_d(t)$ is a bounded smooth reference signal and $x_1(t)$ system state then the stabilizing function, the convergence of the tracking error to zero at the steady state can be enforced despite the presence of the disturbance and model uncertainty in the motion control system. Integrator is added and the algorithm becomes Integrator nonlinear backstepping control (IBS) as articulated by (Han, 2021). The main target of this control is to design the robust control law such that the outputs of the quadcopter system track their desired smooth and bounded reference.

## 2.6. Grey Wolf Optimization (GWO) Algorithm

Grey wolf optimizer is mimic the leadership hierarchy, an intelligent optimization algorithm proposed by Seyedali Mirjalili in 2014 (Mirjalili et al., 2014)(Fessi et al.2021). It has based on the hunting mechanism of the grey wolf. It is similar to others meta-heuristics (GA and PSO), and they live in a pack of the group from 5 to 12 wolves, with a strict leadership hierarchy (Turabieh, 2016). They have four types of hierarchy: the first is alpha ($\alpha$) which is responsible for decisions about hunting, sleeping place, and time to work. They have the best skill in management, and their decision is dictated to pack through betas ($\beta$). The searching space which is characterized by $x_k^i = (x_{k,1}^i, x_{k,2}^i, ...x_{k,d}^i)$ prey position is denoted as $x_k^p = (x_{k,d}^p, x_{k,d}^p, ...x_{k,d}^p)$. The fittest solution is the position of the $\alpha$ wolf in the search space in terms of optimization where $\beta$ and $\delta$ are the second and third best functions and have better knowledge about the potential location of is problem optimum of the best search agents. $\omega_{omg}$ used to update their position randomly around the prey (Pan et al.2021). The three best optimum solutions are $x_k^{best,1}, x_k^{best,2}$ and $x_k^{best,3}$ expressed as equations:

$$x_{k+1}^i = \frac{x_k^{best,1} + x_k^{best,2} + x_k^{best,3}}{3}, i \neq \alpha, \beta, \delta \tag{2.6}$$

Where $x_k^{best,1} = x_k^{\alpha} - \Delta_k^{\alpha} v_{1,k}, x_k^{best,2} = x_k^{\beta} - \Delta_k^{\beta} v_{2,k}, x_k^{best,3} = x_k^{\delta} - \Delta_k^{\delta} v_{3,k}$.

The vector $\nu_{1,k}, \nu_{2,k}, \nu_{3,k}, \Delta_k^{\alpha}, \Delta_k^{\beta}$ and $\Delta_k^{\delta}$ can be calculated as:

$$\begin{cases} \nu_{1,k} = 2\kappa_{1,k}\Re(0,1) - \kappa_{1,k}; \nu_{2,k} = 2\kappa_{2,k}\Re(0,1) - \kappa_{2,k}; \nu_{3,k} = 2\kappa_{3,k}\Re(0,1) - \kappa_{3,k} \\ \Delta_k^{\alpha} = \left|\iota_{1,k} x_k^{\alpha} - x_k^i\right|; \Delta_k^{\beta} = \left|\iota_{2,k} x_k^{\beta} - x_k^i\right|; \Delta_k^{\delta} = \left|\iota_{3,k} x_k^{\delta} - x_k^i\right| \end{cases} \tag{2.7}$$

Where $\nu_{j,k} \in \{1,2,3\}$ linearly decreases from 2 to 0 throughout iteration and $\iota_{j,k}^i$ a random number between 2 and 0, $\Re(0,1)$ is uniformly random between the [0,1] (Kohli & Arora, 2018). points and

Table 2.3:Pseudo-code of the grey wolf optimization (Singh & Wolf, 2020)

| |
|---|
| *Begin*<br>Initialize the parameters pop size, Max_iter, up, and lb. where<br>pop size: the size of the population,<br>Max_iter: maximum number of iterations,<br>up: upper bound(s) of the variables,<br>lb.: lower bound(s) of the variables;<br>Generate the initial positions of grey wolves with up and lb.;<br>Initialize $\nu_{j,k}$, $\kappa_{2,k}$, and $\iota_{j,k}^i$<br>Calculate the fitness of each grey wolf;<br>alpha = the grey wolf with the first maximum fitness;<br>beta = the grey wolf with the second maximum fitness;<br>delta = the grey wolf with the third maximum fitness;<br>While<br>for : pop size<br>Update the position of the current grey wolf;<br>end for<br>Update $\nu_{j,k}$, $\kappa_{2,k}$, and $\iota_{j,k}^i$;<br>Calculate the fitness of all grey wolves;<br>Update alpha, beta, and delta;<br>;<br>end while<br>Return alpha;<br>End |

# CHAPTER THREE

# 3. MATERIALS AND METHODOLOGY

## 3.1. Introduction

This chapter contains two parts: the first one is about the method by which the research followed to complete the research work and achieve the objective of the work and the material used in this thesis work. The second part deals with the mathematical modeling of both kinematics and dynamic of the quadcopter-type UAV system based on Euler Newton methods.

## 3.2. Methodology

To meet the above-mentioned objectives of this thesis work, the following formal methodologies of Figure 3.1 can be followed, subjected to changes due course of the work.

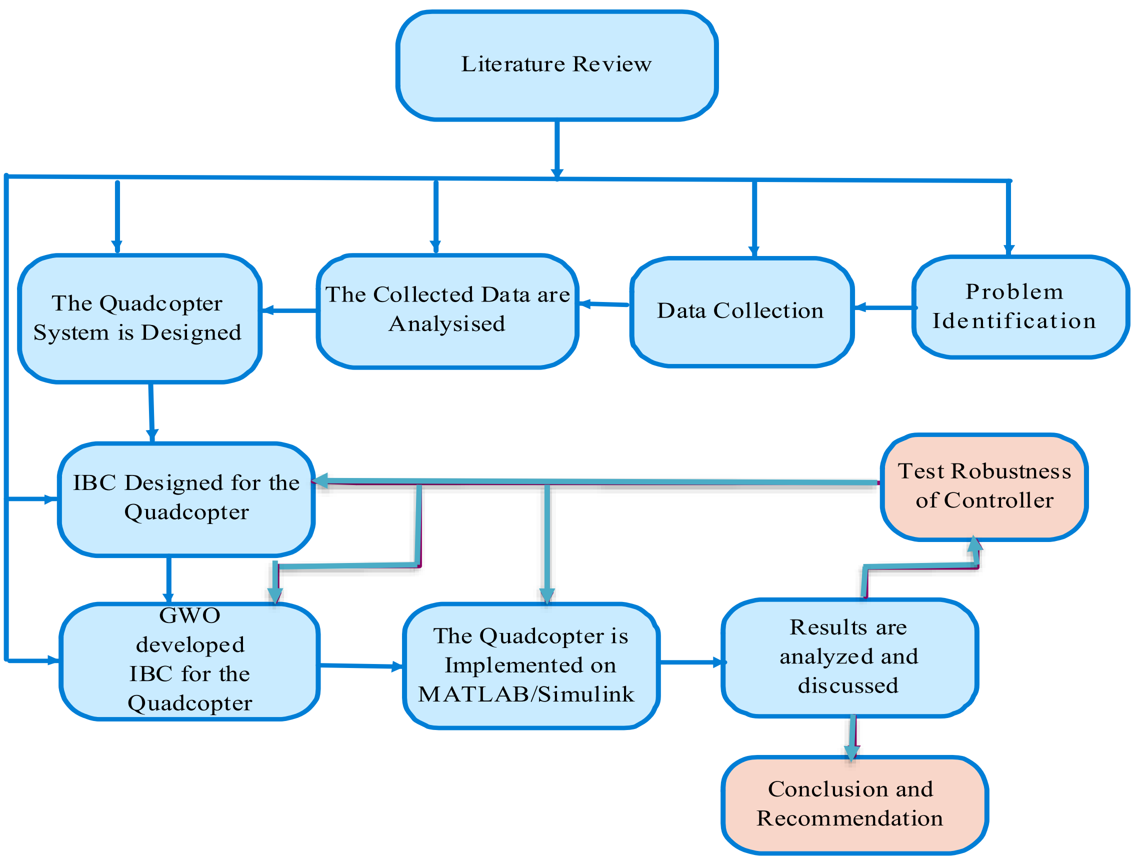


Figure 3.1: Research methodology

## 3.3. Materials

In this thesis, Matlab2021a/Simulink software to implement the proposed controller with the quadcopter-type UAV model to simulate and get response graphically from the system. Software such as Microsoft office word 2016 is used to write and edit the final reporting of the thesis documentation. MathType 7.0c is used for writing mathematical formulas and equations in Microsoft offices word and PowerPoint presentation tools. Additionally, Mendeley 2.61.0 for citation of reference in the thesis document body as well as list the reference in the standard style. The ConceptDraw Office PRO (MINDMAP) was also used to draw the block diagram and chart mentioned in the research report.

## 3.4. Mathematical Modeling of Quadcopter-type UAV System

This section studies a nonlinear model for the kinematics and dynamics of the quadcopter-type UAV is described, and an equation is derived based on the Newton-Euler method. The quadcopter-type UAV has 6 DOF and a rigid body system(Dynamics & Equations, 2018). To develop the mathematical model of the quadcopter which can sensible for an existing system, four basic assumptions must take into account for the established quadcopter and accommodate the controller design (Huang & Wingo, 2016). Those assumptions are as follows:

*Assumption 1.* The structure is rigid and symmetrical.

*Assumption 2.* The propellers are rigid.

*Assumption 3.* The center of gravity constant

*Assumption 4.* The body-fixed frame origin is supposed to be the same.

### 3.4.1. Kinematics of Quadcopter-type UAV System

There are two frames of reference, as shown in Figure 3.2, in which the Quadcopter-type UAV operation is described. The first is the body frame of reference $R_B(x_B;y_B;z_B)$, whereas the second is measured relative to the world frame of reference, which is termed as an inertial or earth frame, $R_E(x_E;y_E;z_E)$. In the case of the body frame, the linear distance is in the vertical and horizontal positions $(x \quad y \quad z)$. Rotation of the axes sequence is needed to generate the relationship of both coordinate frames, and those axes are pointing in the Z-direction with the arms pointing in x and z directions. While in the case of the inertial frame, the rotor axes are pointing in the positive z-direction with the arms pointing in the x and y position, whereas in the inertial frames, the rotor axes are pointing in the positive z-direction with the arms pointing in the x and z directions. The gravity is pointing in the negative dawn ward in the z-direction.

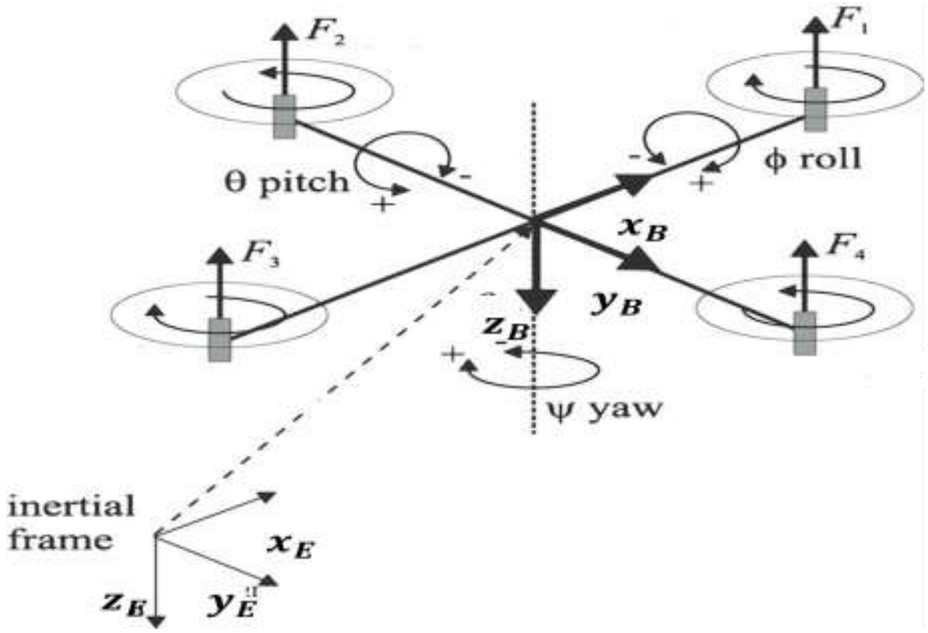


Figure 3.2: Reference frames of Quadcopter-type UAV Coordinate.

The Newton Euler method is the most popular and simplest way to understand and gain insight into the system. Euler angles are defined as $(\phi \quad \theta \quad \psi)$ a sequence of three successive rotations about particular axes that can reflect any ultimate orientation of a reference frame (Rodríguez-Abreo et al., 2020).

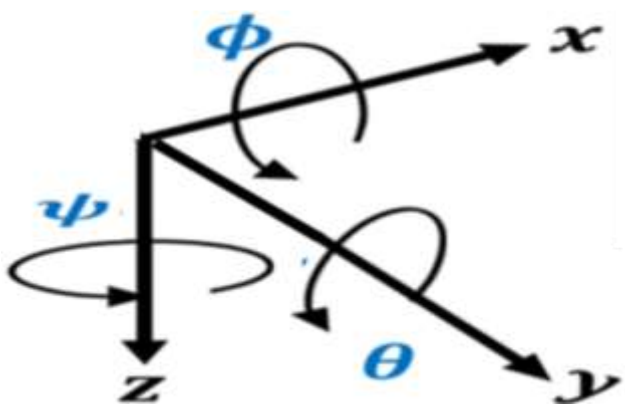


Figure 3.3:The three Euler Angles

### 3.4.2. Transformation matrix

Both reference frame coordinate's representation is simply the vector distance of the body frame from the inertial $\vartheta = [x \quad y \quad z]^T$ and represents the orientation using Euler angles $\eta = [\phi \quad \theta \quad \psi]^T$ , as shown in Figure 3.3. The state variables for velocity are in the body frame, whereas the position is in the global frame (Selby, 2020). Therefore, it is necessary to define a rotation matrix to transform variables between the coordinate systems. Figure 3.4 is the transformation $R_e \Rightarrow R_b$ between the global and body coordinate frames described below:

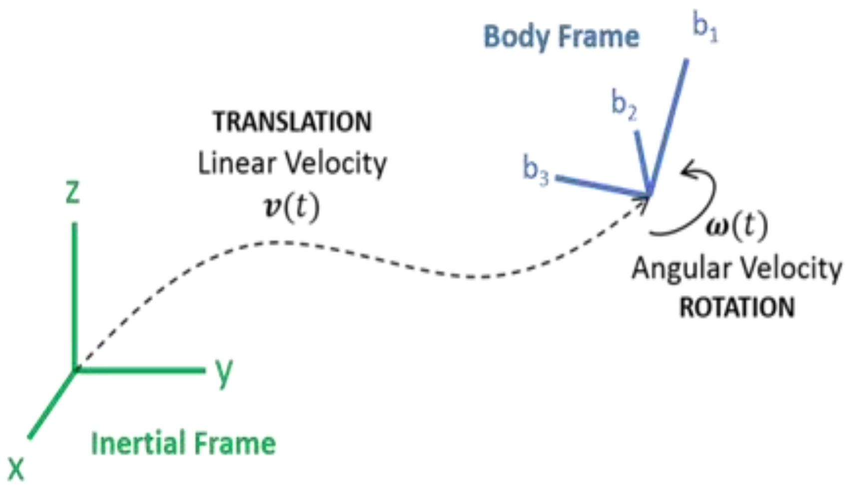


Figure 3.4: Transformation of the inertial frame body frame(Usman, 2020)

As a result, a rotation matrix $R$ must be defined to translate variables across coordinate systems (Selby, 2020). As a result, defining a rotation matrix to translate variables across coordinate systems and how to change the global and body coordinate frames are described and derived in appendix A. The body frame has been transformed from the inertial frame using a transformation matrix. In this thesis work, the transformation from inertial to body frame is given by:

$$R_e^b = R(\phi)R(\theta)R(\psi) \tag{3.1}$$

$$R_e^b = \begin{pmatrix} \cos\theta\cos\psi & \sin\psi\cos\theta & -\sin\theta \\ \cos\psi\sin\theta\sin\phi - \sin\psi\cos\phi & \sin\theta\sin\psi\sin\phi + \cos\psi\cos\theta & \sin\phi\cos\theta \\ \cos\psi\sin\theta\cos\phi + \sin\psi\sin\phi & \cos\phi\sin\psi\sin\theta - \cos\psi\sin\phi & \cos\theta\cos\phi \end{pmatrix} \tag{3.2}$$

### 3.4.3. Rotational Kinematics of Quadcopter-type UAV System

The rotation matrix derived used to determine the relationship between the angular rates and the time derivatives of the Euler angles. Since the Euler angles vector and its derivative is yield $\dot{\eta}$, it is defined in intermediate coordinate frames, and the angular rates $\boldsymbol{\xi}$ are defined in the body frame. The angular velocities are vectors pointing along each axis of rotation $(\dot{\phi} \;\; \dot{\theta} \;\; \dot{\psi}) \neq (p \; q \; r)$:

$$\boldsymbol{\xi} = R_e^b \dot{\eta} \tag{3.3}$$

$$\boldsymbol{\xi} = \begin{bmatrix} 1 & 0 & -\sin(\theta) \\ 0 & \cos(\phi) & \sin(\theta)\cos(\theta) \\ 0 & -\sin(\phi) & \cos(\phi)\cos(\theta) \end{bmatrix} \begin{bmatrix} \dot{\phi} \\ \dot{\theta} \\ \dot{\psi} \end{bmatrix} \tag{3.4}$$

## 3.5. Rigid Body Dynamics of Quadcopter-type UAV System

The quadrotor dynamics have evolved through the usage of the Newton-Euler method. The force and momentum of the quadcopters are shown in Figure 3.5. The general equation can be expressed as(Abdelhay & Zakriti, 2019)(Saibi et al., 2022).

$$\begin{bmatrix} F \\ M \end{bmatrix} = \begin{bmatrix} mI_{3\times3} & 0_{3\times3} \\ 0_{3\times3} & I \end{bmatrix} \begin{bmatrix} \dot{V} \\ \dot{\Omega} \end{bmatrix} + \begin{bmatrix} \Omega \Lambda m V \\ \Omega \Lambda I \Omega \end{bmatrix} \tag{3.5}$$

The equation (3.5) is divided into two parts; the first one is the translation dynamic applying Newton's second law and the rotational (Euler's rotation equations) dynamic.

- Condition for hovering motion(Dynamics & Equations, 2018):

$$\begin{cases} mg = F_1 + F_2 + F_3 + F_4 \\ \text{All moment } = 0 \end{cases} \tag{3.6}$$

Vertical Rise Motion of quadcopter-type UAV for Conditions for hovering:

$$\begin{cases} mg < F_1 + F_2 + F_3 + F_4 \\ \text{All moments } = 0 \end{cases} \tag{3.7}$$

- Conditions for vertical fall:

$$\begin{cases} mg > F_1 + F_2 + F_3 + F_4 \\ \text{All moments} = 0 \end{cases} \tag{3.8}$$

- The total moment about the X-axis can be:

$$\begin{aligned} M_x &= -F_2\ell + F_4\ell \\ &= -(b\omega_2^2)\ell + (b\omega_4^2)\ell \\ &= b\ell(-\omega_2^2 + \omega_4^2) \end{aligned} \tag{3.9}$$

- For the Y-axis, the moment is defined as:

$$\begin{aligned} M_y &= F_1\ell - F_3\ell \\ &= (b\omega_1^2)\ell - (b\omega_3^2)\ell \\ &= b\ell(\omega_1^2 - \omega_3^2) \end{aligned} \tag{3.10}$$

For about the Z-axis, the thrust of the rotor does not produce a moment. A moment is caused by the rotor rotation using the right-hand rule (Ding et al., 2021). The moment about the body frame's Z-axis can be expressed as:

$$\begin{aligned} M_z &= F_1\ell - F_2\ell + F_3\ell - F_4\ell \\ &= d\omega_1^2 - d\omega_3^2 + d\omega_1^2 - d\omega_3^2 \\ &= d(\omega_1^2 - \omega_2^2 + \omega_3^2 - \omega_4^2) \end{aligned} \tag{3.11}$$

Combining equation (3.10), (3.11) and (3.12):

$$M_B = \begin{bmatrix} b\ell(-\omega_2^2 + \omega_4^2) \\ b\ell(\omega_1^2 - \omega_3^2) \\ d(\omega_1^2 - \omega_2^2 + \omega_3^2 - \omega_4^2) \end{bmatrix} \tag{3.12}$$

Where the term $\ell$ is the moment arm, and which is the distance between the axis of rotation of each rotor to the origin of the body reference frame which should coincide with the center of the quadrotor.

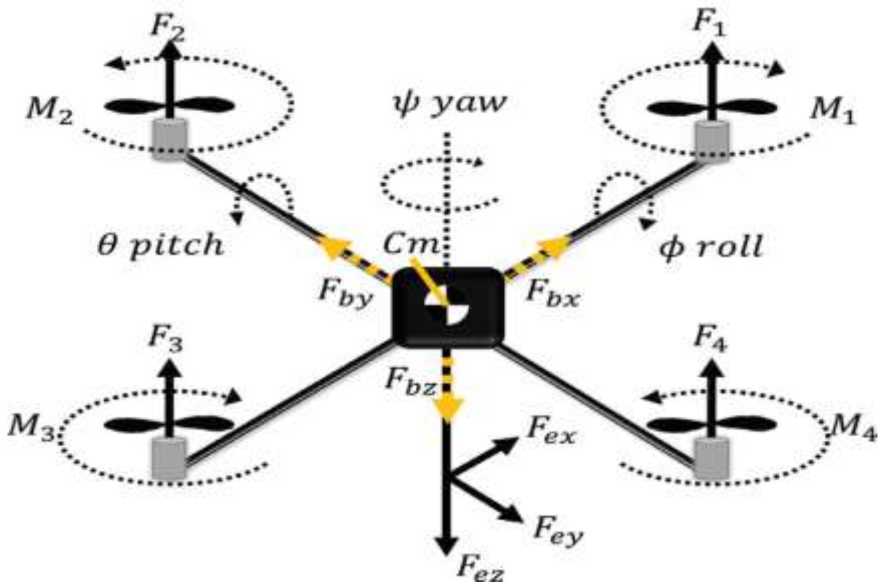


Figure 3.5: Force and momentum acting on the quadcopter (Pérez et al., 2018)

### 3.5.1. Translation dynamic of Quadcopter-type UAV System

The main forces applied to the quadcopter-type UAV system. The weight of the quadcopter:

$$F_g = [0 \quad 0 \quad -mg]^T \tag{3.13}$$

1. The thrust of the rotors:

$$F_t = R\sum_i^4 F_i = b\sum_i^4 \omega_i^2 \begin{bmatrix} \cos\psi \sin\theta \cos\phi + \sin\psi \sin\phi \\ \cos\phi \sin\psi \sin\theta - \cos\psi \sin\phi \\ \cos\theta \cos\phi \end{bmatrix} \tag{3.14}$$

2. The drag force and the air friction:

Drug force exerts on the quadcopter body with air and opposes the quadcopter motion. The velocity of the object increase, and the drag force increase.

$$F_d = k_d \dot{\vartheta} = \begin{bmatrix} -k_{dx} & 0 & 0 \\ 0 & -k_{dy} & 0 \\ 0 & 0 & -k_{dz} \end{bmatrix} \begin{bmatrix} \dot{x} \\ \dot{y} \\ \dot{z} \end{bmatrix} = \begin{bmatrix} -k_{dx}\dot{x} \\ -k_{dy}\dot{y} \\ -k_{dz}\dot{z} \end{bmatrix} \tag{3.15}$$

By applying the second law of Newton:

$$F = m\ddot{\vartheta} = W + F_t - F_d \tag{3.16}$$

The equation of motion that governs the translational motion of the quadcopter-type UAV quadcopter is given by:

$$\begin{cases} \ddot{x} = \dfrac{b}{m}(\omega_1^2 + \omega_2^2 + \omega_3^2 + \omega_4^2)(\cos\phi \cos\psi \sin\theta + \sin\psi \sin\phi) - \dfrac{k_{dx}}{m}\dot{x} \\ \ddot{y} = \dfrac{b}{m}(\omega_1^2 + \omega_2^2 + \omega_3^2 + \omega_4^2)(\cos\phi \sin\theta \sin\psi - \cos\psi \sin\phi) - \dfrac{k_{dy}}{m}\dot{y} \\ \ddot{z} = -g + \dfrac{b}{m}(\omega_1^2 + \omega_2^2 + \omega_3^2 + \omega_4^2)(\cos\theta \cos\phi) - \dfrac{k_{dz}}{m}\dot{z} \end{cases} \tag{3.17}$$

### 3.5.2. Rotational dynamics of the Quadcopter-type UAV System

From Equations (3.9) through (3.11) an Equation (3.12), the equation of the total moments or torque acting on the quadrotor becomes :

$$M_B = \begin{bmatrix} U_2 \\ U_3 \\ U_4 \end{bmatrix} \tag{3.18}$$

The torques acting on the quadcopter are:

- For roll

$$\tau_x = \begin{bmatrix} 0 \\ -\ell \\ 0 \end{bmatrix} \Lambda \begin{bmatrix} 0 \\ 0 \\ F_2 \end{bmatrix} + \begin{bmatrix} 0 \\ \ell \\ 0 \end{bmatrix} \Lambda \begin{bmatrix} 0 \\ 0 \\ F_4 \end{bmatrix} = \begin{bmatrix} \ell b(-\omega_2^2 + \omega_4^2) \\ 0 \\ 0 \end{bmatrix} \tag{3.19}$$

- For pitch:

$$\tau_y = \begin{bmatrix} \ell \\ 0 \\ 0 \end{bmatrix} \Lambda \begin{bmatrix} 0 \\ 0 \\ F_1 \end{bmatrix} + \begin{bmatrix} -\ell \\ 0 \\ 0 \end{bmatrix} \Lambda \begin{bmatrix} 0 \\ 0 \\ F_3 \end{bmatrix} = \begin{bmatrix} 0 \\ \ell b(\omega_1^2 - \omega_3^2) \\ 0 \end{bmatrix} \tag{3.20}$$

- For yaw

$$\tau_z = \begin{bmatrix} 0 \\ 0 \\ d(\omega_1^2 - \omega_2^2 + \omega_3^2 - \omega_4^2) \end{bmatrix} \tag{3.21}$$

The torque resulting from aerodynamic friction acting on the quadcopter body, which can be approximated by drag moment is caused by air friction:

$$\tau_d = k_{dm}\begin{bmatrix}\ddot{\phi}\\ \ddot{\theta}\\ \ddot{\psi}\end{bmatrix} = \begin{bmatrix}k_{dmx} & 0 & 0\\ 0 & k_{dmy} & 0\\ 0 & 0 & k_{dmz}\end{bmatrix}\begin{bmatrix}\dot{\phi}\\ \dot{\theta}\\ \dot{\psi}\end{bmatrix} = \begin{bmatrix}k_{dmx}\dot{\phi}\\ k_{dmy}\dot{\theta}\\ k_{dmz}\dot{\psi}\end{bmatrix} \tag{3.22}$$

The gyroscopic effect of propeller:

$$\tau_{gp} = J_r\dot{\eta}\Lambda\begin{bmatrix}0\\ 0\\ \sum_i^4(-1)^{i+1}\omega_i\end{bmatrix} = J_r\omega_r\begin{bmatrix}\dot{\theta}\\ -\dot{\phi}\\ 0\end{bmatrix} \quad \text{with } \omega_r = \sum_i^4(-1)^{i+1}\omega_i \tag{3.23}$$

Because in the beginning, the system starts by assuming that the structure is assumed quadcopter is symmetrical, the inertia matrix becomes:

$$I = \begin{bmatrix}I_x & 0 & 0\\ 0 & I_y & 0\\ 0 & 0 & I_z\end{bmatrix} \tag{3.24}$$

The aerodynamic coefficient considers an external disturbance on the quadcopter due to the air, and it causes the imbalance during the lift and introduces the up and down oscillation of the rotor blades. By applying Euler's rotation equations and expanding that:

$$\begin{bmatrix}I_x & 0 & 0\\ 0 & I_y & 0\\ 0 & 0 & I_z\end{bmatrix}\begin{bmatrix}\ddot{\phi}\\ \ddot{\theta}\\ \ddot{\psi}\end{bmatrix} + \begin{bmatrix}\dot{\phi}\\ \dot{\theta}\\ \dot{\psi}\end{bmatrix}\times\begin{bmatrix}I_x & 0 & 0\\ 0 & I_y & 0\\ 0 & 0 & I_z\end{bmatrix}\begin{bmatrix}\dot{\phi}\\ \dot{\theta}\\ \dot{\psi}\end{bmatrix} + \begin{bmatrix}\dot{\phi}\\ \dot{\theta}\\ \dot{\psi}\end{bmatrix}\times\begin{bmatrix}0\\ 0\\ J_r\omega_r\end{bmatrix} = \begin{bmatrix}\ell U_2\\ \ell U_3\\ \ell U_4\end{bmatrix} \tag{3.25}$$

Through the rule of matrix multiplication with vector and cross-product, Equation (3.25) and Result simplify to (3.26):

$$\begin{bmatrix}I_x\\ I_y\\ I_z\end{bmatrix}\begin{bmatrix}\ddot{\phi}\\ \ddot{\theta}\\ \ddot{\psi}\end{bmatrix} + \begin{bmatrix}I_z\dot{\theta}\dot{\psi} - \dot{\psi}I_y\dot{\theta}\\ \dot{\psi}I_x\dot{\phi} - \dot{\phi}I_z\dot{\psi}\\ \dot{\phi}I_y\dot{\theta} - \dot{\theta}I_x\dot{\phi}\end{bmatrix} + \begin{bmatrix}J_r\omega_r\dot{\theta}\\ -\dot{\phi}J_r\omega_r\\ 0\end{bmatrix} = \begin{bmatrix}\ell U_2\\ \ell U_3\\ \ell U_4\end{bmatrix} \tag{3.26}$$

Rewriting Equation (3.26) to have the angular accelerations in terms of the other variables. The Equation of motion that governs the rotational motion of the quadcopter is given by:

$$\begin{cases} \ddot{\phi} = \dfrac{(I_y - I_z)}{I_x}\dot{\theta}\dot{\psi} + \dfrac{\ell b(-\omega_2^2 + \omega_4^2)}{I_x} - \dfrac{J_r \omega_r}{I_x}\dot{\theta} \\ \ddot{\theta} = \dfrac{(I_z - I_x)}{I_y}\dot{\phi}\dot{\psi} + \dfrac{\ell b(\omega_1^2 - \omega_3^2)}{I_y} + \dfrac{J_r \omega_r}{I_y}\dot{\phi} \\ \ddot{\psi} = \dfrac{(I_x - I_y)}{I_z}\dot{\theta}\dot{\phi} + \dfrac{d}{I_z}(\omega_1^2 - \omega_2^2 + \omega_3^2 - \omega_4^2) \end{cases} \tag{3.27}$$

### 3.5.3. Overall model of The Quadcopter-type UAV System

Finally, from the Equation (3.17) and(3.27) to the dynamic model of 6-DOF, the quadcopter-type UAV is described as follows:

$$\begin{cases} \ddot{\phi} = \dfrac{(I_y - I_z)}{I_x}\dot{\theta}\dot{\psi} + \dfrac{\ell b(\omega_1^2 - \omega_2^2)}{I_x} - \dfrac{J_r \omega_r}{I_x}\dot{\theta} - \dfrac{k_{dmx}}{I_x}\dot{\phi} \\ \ddot{\theta} = \dfrac{(I_z - I_x)}{I_y}\dot{\phi}\dot{\psi} + \dfrac{\ell b(\omega_4^2 - \omega_3^2)}{I_y} + \dfrac{J_r \omega_r}{I_y}\dot{\phi} - \dfrac{k_{dmy}}{I_y}\dot{\theta} \\ \ddot{\psi} = \dfrac{(I_x - I_y)}{I_z}\dot{\theta}\dot{\phi} + \dfrac{d}{I_z}(\omega_3^2 - \omega_2^2 + \omega_4^2 - \omega_1^2) - \dfrac{k_{dmz}}{I_z}\dot{\psi} \\ \ddot{x} = \dfrac{b}{m}(\omega_1^2 + \omega_2^2 + \omega_3^2 + \omega_4^2)(\cos\phi\cos\psi\sin\theta + \sin\psi\sin\phi) - \dfrac{k_{dx}}{m}\dot{x} \\ \ddot{y} = \dfrac{b}{m}(\omega_1^2 + \omega_2^2 + \omega_3^2 + \omega_4^2)(\cos\phi\sin\theta\sin\psi - \cos\psi\sin\phi) - \dfrac{k_{dy}}{m}\dot{y} \\ \ddot{z} = g - \dfrac{b}{m}(\omega_1^2 + \omega_2^2 + \omega_3^2 + \omega_4^2)(\cos\theta\cos\phi) - \dfrac{k_{dz}}{m}\dot{z} \end{cases} \tag{3.28}$$

### 3.5.4. Control input vector U

Control input vector U consist of four inputs from $U_1$ to $U_4$ defined as:

$$U = [U_1 \quad U_2 \quad U_3 \quad U_4]^T \tag{3.29}$$

Where $U_2, U_3,$ and $U_4$ are the roll, pitch, and yaw torque in the body frame and $U_1$ is the total thrust produced by the four motors, respectively. $U_1$ upward force and produced by four of the rotor and its rate of change of ( $z\ \dot{z}$ ). $U_2$, the difference in the thrust between the motor 2 and motor 4 for moving the quadcopter in roll rotation and its rate of change of ( $\phi\ \dot{\phi}$ ). $U_3$, is the difference in the thrust between the motor 1 one and motor 3 for moving the quadcopter in pitch rotation and its rate of change of ( $\theta\ \dot{\theta}$ ). The difference in the torque between the two clockwise turnings rotate and counterclockwise generating yaw rotation and its rate of change of ( $\psi\ \dot{\psi}$ ).

$$\begin{cases} U_1 = b(\omega_1^2 + \omega_2^2 + \omega_3^2 + \omega_4^2) \\ U_2 = \ell b(-\omega_2^2 + \omega_4^2) \\ U_3 = \ell b(\omega_1^2 - \omega_3^2) \\ U_4 = d(\omega_3^2 - \omega_2^2 + \omega_4^2 - \omega_1^2) \end{cases} \tag{3.30}$$

From Equation (3.30) can be rewritten in the matrix form of Equation (3.31):

$$\begin{bmatrix} U_1 \\ U_2 \\ U_3 \\ U_4 \end{bmatrix} = \begin{bmatrix} b & b & b & b \\ 0 & -\ell b & 0 & \ell b \\ \ell b & 0 & -\ell b & 0 \\ d & -d & d & -d \end{bmatrix} \begin{bmatrix} \omega_1{}^2 \\ \omega_2{}^2 \\ \omega_3{}^2 \\ \omega_4{}^2 \end{bmatrix} \tag{3.31}$$

If the rotor velocities are needed to be calculated from the control inputs, an inverse relationship between the control inputs and the rotors' velocities is needed, which can be acquired by inverting the matrix in Equation (3.31) to give. By using transformation using the inverted Matrix Method, the rotor speed is expressed by the input $U_1, U_2, U_3,\ U_4$ as:

$$\begin{cases} \omega_1^2 = \dfrac{1}{4b}U_1 - \dfrac{1}{2b\ell}U_3 - \dfrac{1}{4d}U_4 \\ \omega_2^2 = \dfrac{1}{4b}U_1 - \dfrac{1}{2b\ell}U_2 + \dfrac{1}{4d}U_4 \\ \omega_3^2 = \dfrac{1}{4b}U_1 + \dfrac{1}{2b\ell}U_2 - \dfrac{1}{4d}U_4 \\ \omega_4^2 = \dfrac{1}{4b}U_1 + \dfrac{1}{2b\ell}U_2 + \dfrac{1}{4d}U_4 \end{cases} \tag{3.32}$$

### 3.5.4. State-space Representation of Quadcopter-type UAV System

The mathematical model expressed in the Equation (3.28) is a nonlinear dynamic model of the quadcopter-type UAV for both rotational and translational. It can be re-written in the form of state space with the state variable of 12. The state vector can be defined as;

$$X = \begin{bmatrix} x_1 \ldots & x_{12} \end{bmatrix}^T = \begin{bmatrix} \phi & \dot{\phi} & \theta & \dot{\theta} & \psi & \dot{\psi} & z & \dot{z} & y & \dot{y} & x & \dot{x} \end{bmatrix}^T \tag{3.33}$$

Then the Equation (3.33) describes the equation where both the Euler angle $(\phi, \theta, \psi)$ and its rates $(\dot{\phi}, \dot{\theta}, \dot{\psi})$ are used in both translations on $(x, y, z)$ and rotational equation of quadcopter motion.

$$f(x,U) = \begin{cases} x_2 \\ \dfrac{U_2}{I_x} + \dfrac{(I_y - I_z)}{I_x} x_4 x_6 - \dfrac{J_r}{I_x} x_4 \omega_r \\ x_4 \\ \dfrac{U_3}{I_y} + \dfrac{(I_z - I_x)}{I_y} x_2 x_6 + \dfrac{J_r}{I_y} x_2 \omega_r \\ x_5 \\ \dfrac{(I_x - I_y)}{I_z} x_4 x_2 + \dfrac{U_4}{I_z} \\ x_8 \\ g - \dfrac{U_1}{m}(\cos(x_1)\cos(x_3)) \\ x_{10} \\ \dfrac{u_1}{m}(\cos(x_1)\sin(x_3)\cos(x_5) - \sin(x_1)\cos(x_5)) \\ x_{12} \\ \dfrac{U_1}{m}(\cos(x_1)\sin(x_3)\cos(x_5) + \sin(x_1)\sin(x_5)) \end{cases} \tag{3.34}$$

To simplify the model, the state-space form model of the system:

$$a_1 = \frac{I_y - I_z}{I_x}, a_2 = -\frac{J_r}{I_x}, a_3 = \frac{I_z - I_x}{I_y} \quad a_4 = \frac{J_r}{I_y}, a_5 = \frac{I_x - I_y}{I_z} \quad b_1 = \frac{1}{I_x}, b_2 = \frac{1}{I_y}, b_3 = \frac{1}{I_z}$$

The virtual control $u_x, u_y$ define as:

$$\begin{cases} u_x = (\cos\psi \sin\theta \cos\phi + \sin\psi \sin\phi) \\ u_y = (\cos\psi \sin\theta \cos\phi - \cos\psi \sin\phi) \end{cases} \tag{3.35}$$

The final state space form re-written as:

$$\begin{cases} \dot{x}_1 = \dot{\phi} = x_2 \\ \dot{x}_2 = \ddot{\phi} = b_1 u_2 + a_1 x_4 x_6 + a_2 x_4 \omega_r \\ \dot{x}_3 = \dot{\theta} = x_4 \\ \dot{x}_4 = \ddot{\theta} = b_2 u_3 + a_3 x_2 x_6 + a_4 x_2 \omega_r \\ \dot{x}_5 = x_6 = \dot{\psi} \\ \dot{x}_6 = \ddot{\psi} = a_5 x_2 x_4 + b_3 u_4 \\ \dot{x}_7 = \dot{z} = x_8 \\ \dot{x}_8 = \ddot{z} = g - \dfrac{u_1}{m}(\cos(x_1)\cos(x_3)) \\ \dot{x}_9 = \dot{y} = x_{10} \\ \dot{x}_{10} = \ddot{y} = \dfrac{u_1}{m} u_y \\ \dot{x}_{11} = \dot{x} = x_{12} \\ \dot{x}_{12} = \ddot{x} = \dfrac{u_1}{m} u_x \end{cases} \tag{3.36}$$

# CHAPTER FOUR

# 4. CONTROL SYSTEM DESIGN

Designing a control mechanism for a nonlinear system is the most important for stabilizing the system. The quadcopter-type UAV system covered this thesis is highly nonlinear and under actuators affected by various external and internal disturbances, including aerodynamics. In this chapter, belief explains the steps to design the integral-based nonlinear backstepping controllers for attitude, altitude, and position control using a nonlinear dynamic model of quadcopter-type UAV are explained.

## 4.1. Open-Loop Analysis

The open-loop dynamic shows the effect of input on the output state and the system instability. Without applying any feedback control mechanism, the system is analyzed by varying the motors' rotor speed to perform all motions. The nonlinear dynamic model of the system is implemented in Matlab/Simulink R2021a environment. Figure 4.1 shows the generic block diagram of the open-loop simulations of the quadcopter.

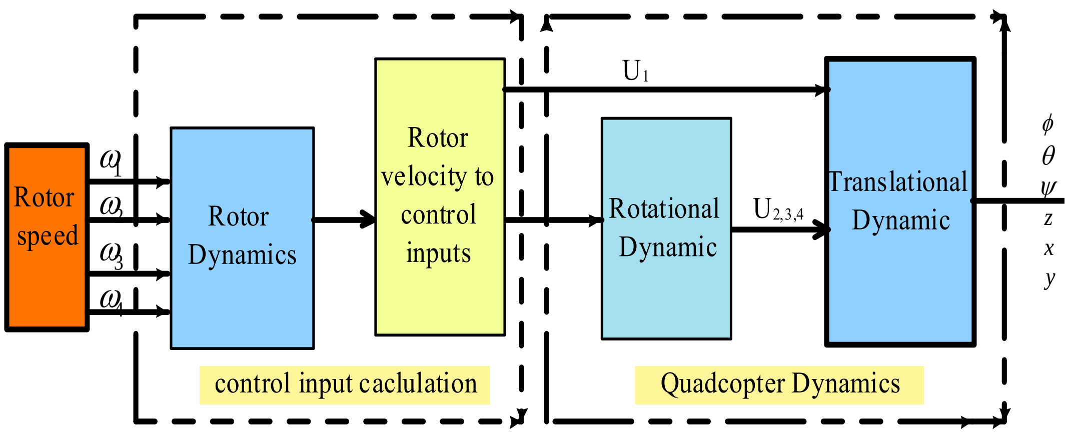


Figure 4.1: Block diagram of open-loop simulation

The open-loop control system is a manual control mechanism in that the controlled object acts based on what the operator order; there is no error correction, no handling of parameter uncertainty, and the existence of disturbance. Motor speed $\omega_1$ and $\omega_3$ rotate clockwise (CW), whereas $\omega_2$ and $\omega_4$ are rotated counterclockwise (CCW). According to international standards, clockwise direction is assumed to be a negative sign, whereas counterclockwise a positive sign. The force and momentum produced by speed of motor $\omega_1$ and $\omega_3$ are the opposite directions of the force and momentum produced by the speed of motor $\omega_2$ and $\omega_4$. There is the matrix for the control input of motor calculation from Equation (3.31) and (3.32) is given by:

$$\begin{bmatrix} U_1 \\ U_2 \\ U_3 \\ U_4 \end{bmatrix} = 10^{-4} \times \begin{bmatrix} 0.3130 & 0.313 & 0.3130 & 0.3130 \\ 0 & -0.1705 & 0 & 0.1705 \\ 0.1722 & 0 & -0.1705 & 0 \\ 0.0075 & -0.0075 & 0.0075 & -0.0075 \end{bmatrix} \begin{bmatrix} \omega_1^2 \\ \omega_2^2 \\ \omega_3^2 \\ \omega_4^2 \end{bmatrix} \tag{4.1}$$

$$\begin{bmatrix} \omega_1^2 \\ \omega_2^2 \\ \omega_3^2 \\ \omega_4^2 \end{bmatrix} = 10^{5} \times \begin{bmatrix} 0.0806 & 0 & -0.2933 & -3.3333 \\ 0.0806 & -0.2933 & 0 & 3.3333 \\ 0.0806 & 0.2933 & 0 & -3.3333 \\ 0.0806 & 0.2933 & 0 & 3.3333 \end{bmatrix} \begin{bmatrix} U_1 \\ U_2 \\ U_3 \\ U_4 \end{bmatrix} \tag{4.2}$$

**Vertical motion of quadcopter-type UAV**

Quadcopters are moved vertically, lift, and down in the vertical direction used to indicate the quadcopter's altitude. The lift force is generated by all four propellers and speeds in equal amounts, but they have opposite directions. Lifting the quadcopter up increases all four motor speeds in equal magnitude, and the lift is greater than the weight of the quadcopter the craft rise into the air. The BLDC motor has a speed of 3000rpm and is equal to 314.16rad/sec (Oh & Yoo, 2021). Downward is decreasing all four motor speeds in equal magnitude. And, the vertical motion of the quadcopter is shown in Figure 4.2, and the quadcopter hovers when the total lift force generated by all four propellers is equal to the amount of weight of the quadcopter. All motor used in the quadcopter system is identical $\omega_1 = \omega_3 = 314.16 rad/\sec$, $\omega_2 = \omega_4 = 314.16 \text{rad/sec}$. During the quadcopter, it flies in a vertical motion, all motor speeds are equal, and the quadcopter moves up in the air from the flat earth's surface without any angle. The vertical downward movement of the quadcopter is performed simply by decreasing the speed of all four motors at the same time

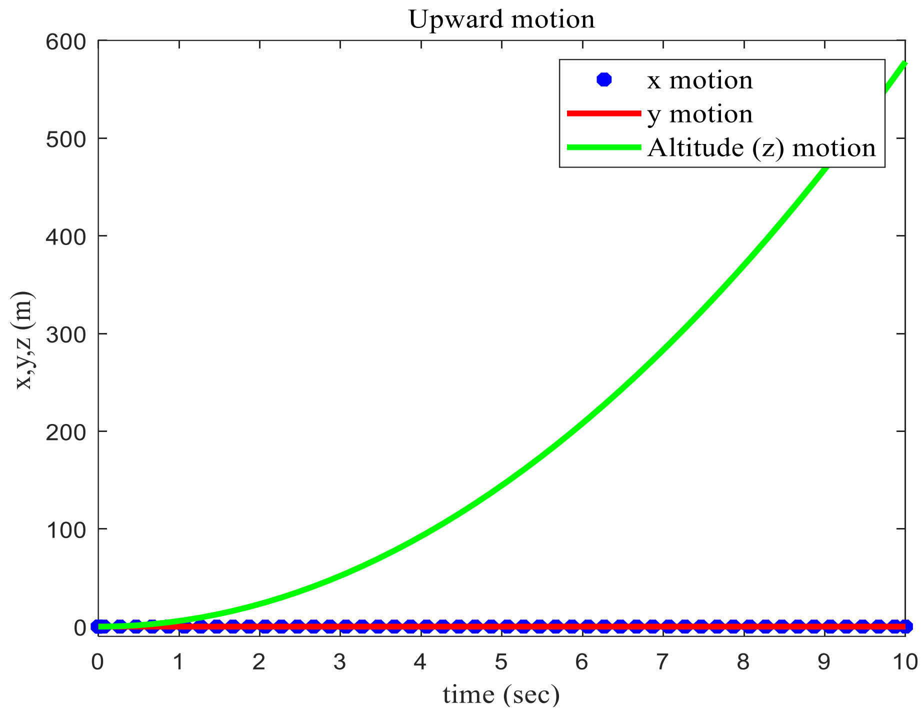


Figure 4.2: Open-loop Response of Vertical upward translational motion**.**

**Pitch angle motion**

Pitch angle rotation is the movement of a quadcopter, either forward or backward. To move the quad forward direction, simply push the throttle stick forward and the quadcopter away from the initial point. That means when the system moves forward motion decrease the speed of the first motor and second motor $\omega_1(CW) = \omega_2(CCW) = 313 rad/\sec$, $\omega_3 = \omega_4 = 314.16 rad/\sec$. Figure 4.3 and Figure 4.4 show the simulation of the open-loop response of $\theta$, dynamic and the effect of its input $U_2$ on x-position when the quadcopter moves in the forward direction. The open-loop response shows that the output of a system goes to infinity with the time and unitability of the system.

**The backward motion of the quadcopter**

When the system moves backward motion $\omega_1(CW) = \omega_2(CCW) = 314.16 rad/\sec$ $\omega_3(CW) =$ $\omega_4(CCW) = 313 rad/\sec$. Pitch angle rotation. Figure 4.5 and Figure 4.6 show the result of the open-loop response of theta $\theta$ or pitch angle dynamic and the effect of its control input $U_2$ on $x$ motion when the quadcopter moves in the backward direction.

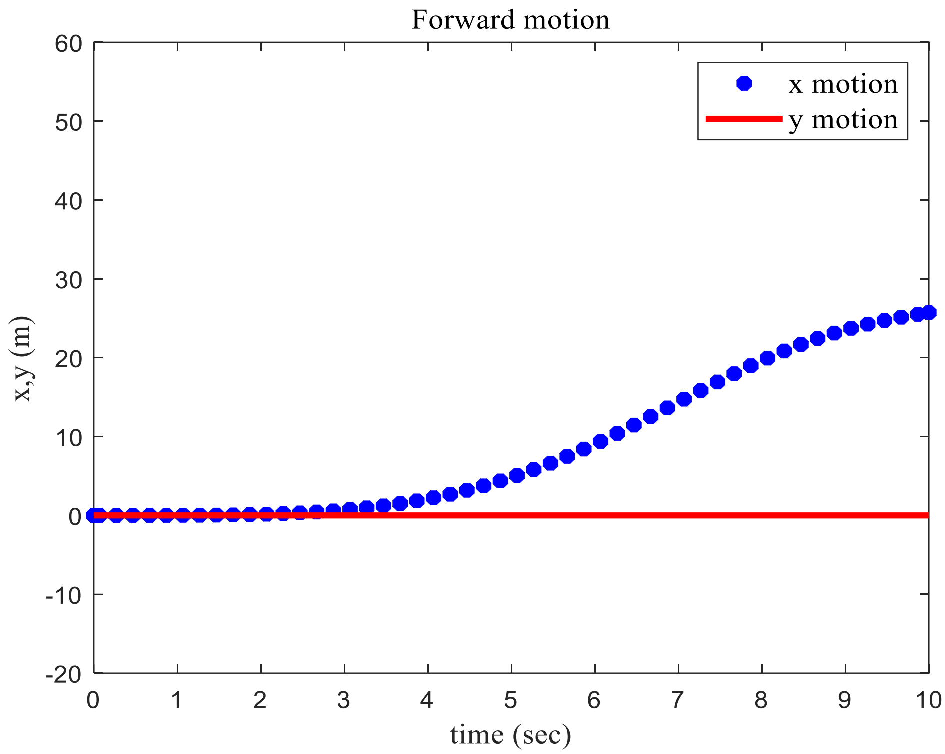


Figure 4.3: Open-loop response of translational x-position

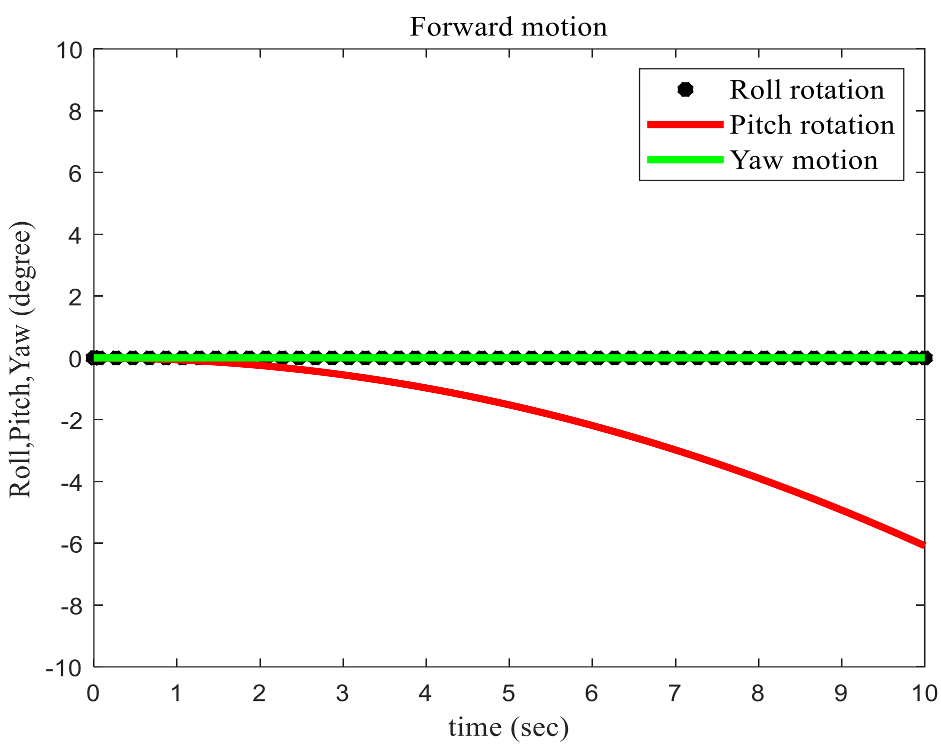


Figure 4.4: Open-loop response for angular motion $\theta$

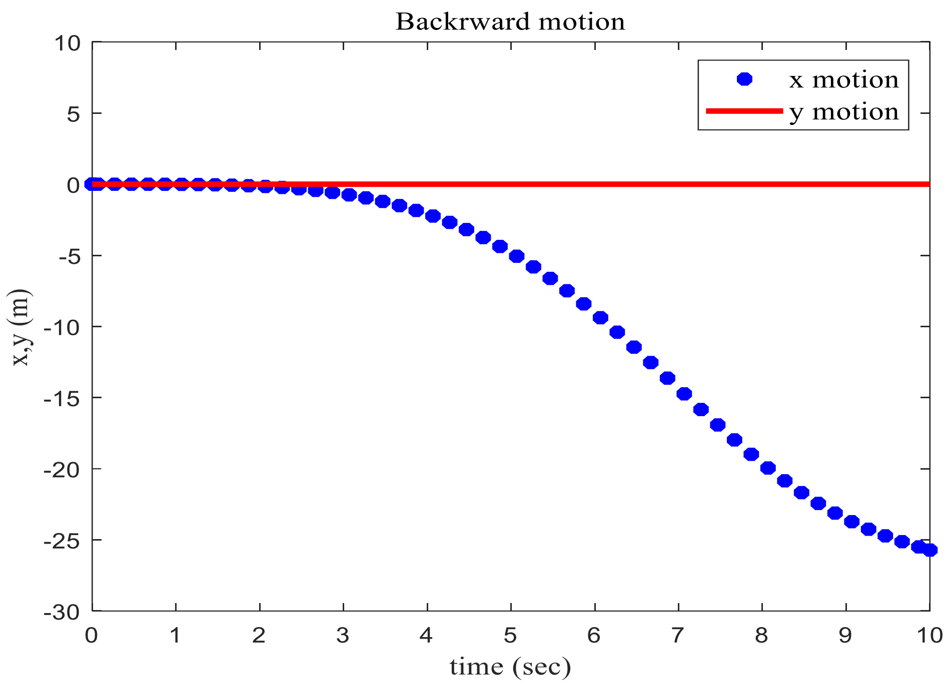


Figure 4.5: Open-loop response of backward motion

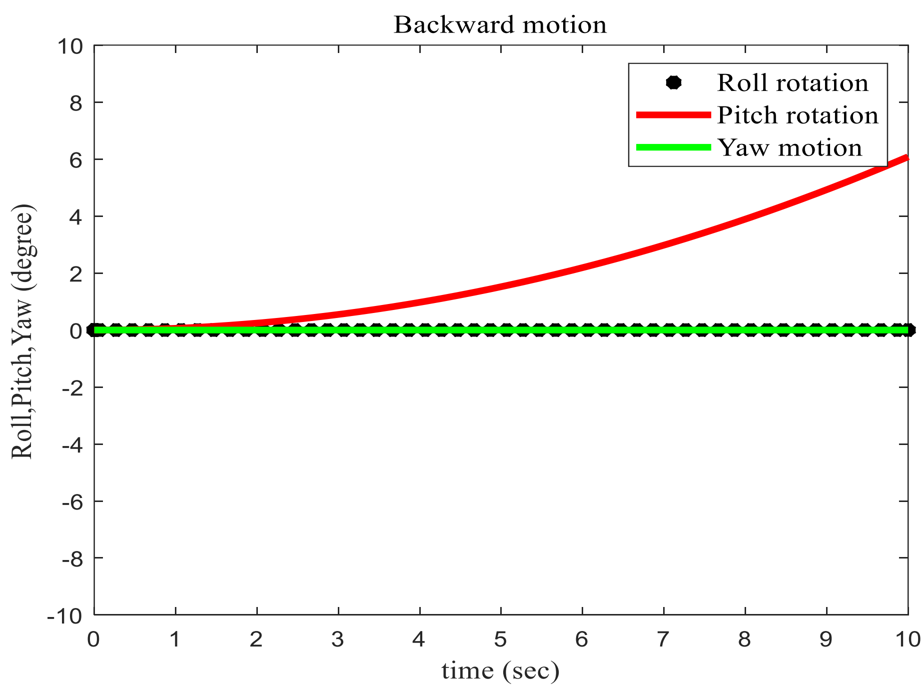


Figure 4.6: Open-loop response of Backward motion $\theta$ when

Roll –means to tilt the quadcopter left or right side. The left two motors have spun down, and the right two motors have spun up. The right two motors will create more lift than the left two motors, which causes the system to roll left, and again the torque cancels out. When using the right stick, push that left to roll left or right to roll right. The motion of the quadcopter to the right is performed when $\omega_1 = \omega_4 = 313 rad/\sec$, $\omega_2 = \omega_3 = 314.16 rad/\sec$. Figure 4.7 and Figure 4.8 show the characteristics of open-loop and effect of small change on $U_2$ on the Y-position on and when the quadcopter moves right side motion and $\phi$ orientation. To the left side motion of quadcopter when $\omega_1 = \omega_4 =, 314.16 rad/\sec$, $\omega_2 = \omega_3 = 313 rad/\sec$.

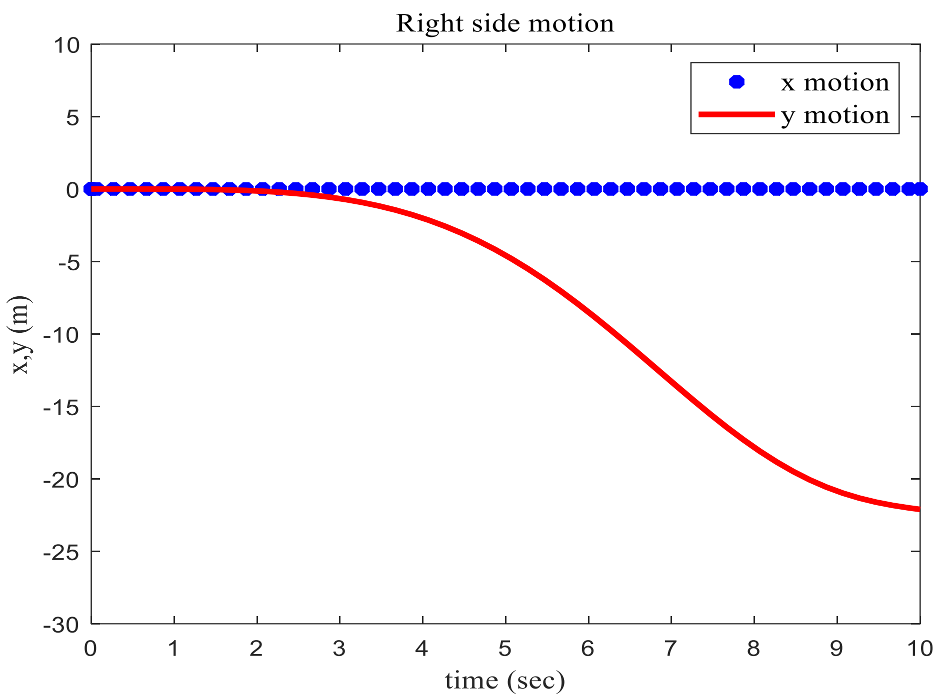


Figure 4.7: Open-loop response of Right side motion x

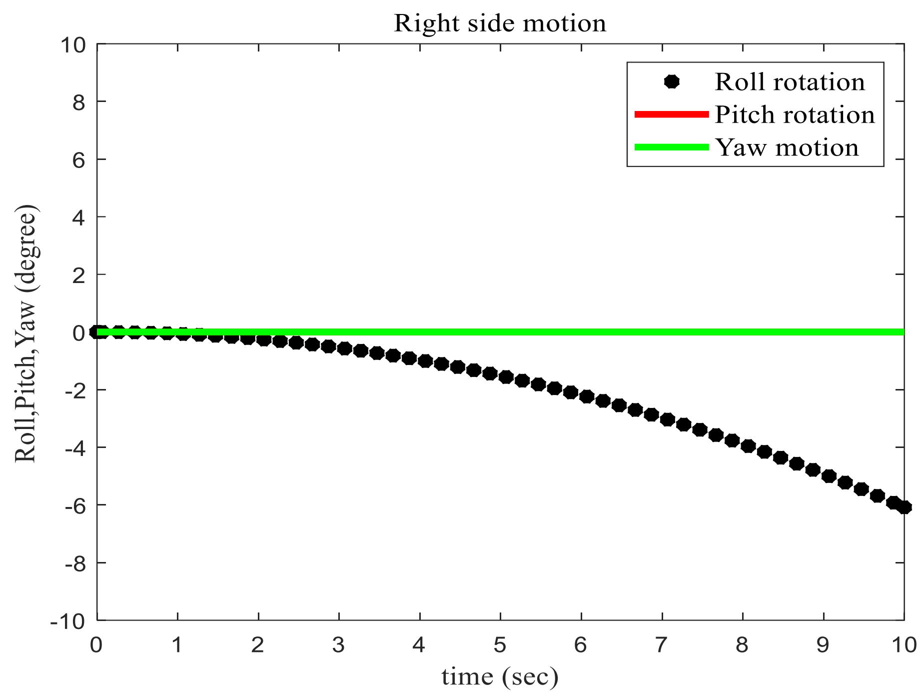


Figure 4.8: Open-loop response of Right side motion of $\phi$

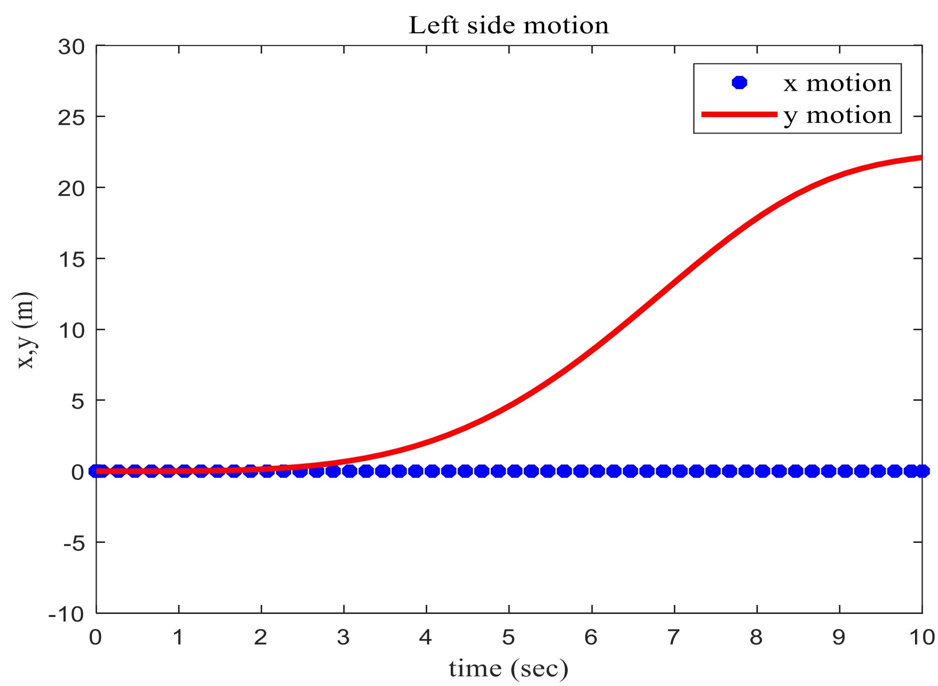


Figure 4.9: Open-loop response of Left side motion $y$

Simulation results of Figure 4.9 and Figure 4.10 show the open-loop response effect of $U_2$ on $y$ position and Roll angle when $\omega_1 = \omega_4 = 314.16 rad/\sec$. The roll angle is shown in Figure 4.10 and it shows an unstable response. Yaw motion - change the direction at the front of the craft facing, so there is yaw left and yaw right. When the two counterclockwise motors $\omega_2 = \omega_4 = 313 rad/\sec$ are spinning slower than clockwise motors $\omega_1 = \omega_3 = 314.16 rad/\sec$, the quadcopter to yaw right, push the left stick to the right. The body rotates in the opposite direction with more torque, and they are spinning. This causes the body to yaw to the left and pushes the left stick to the left.

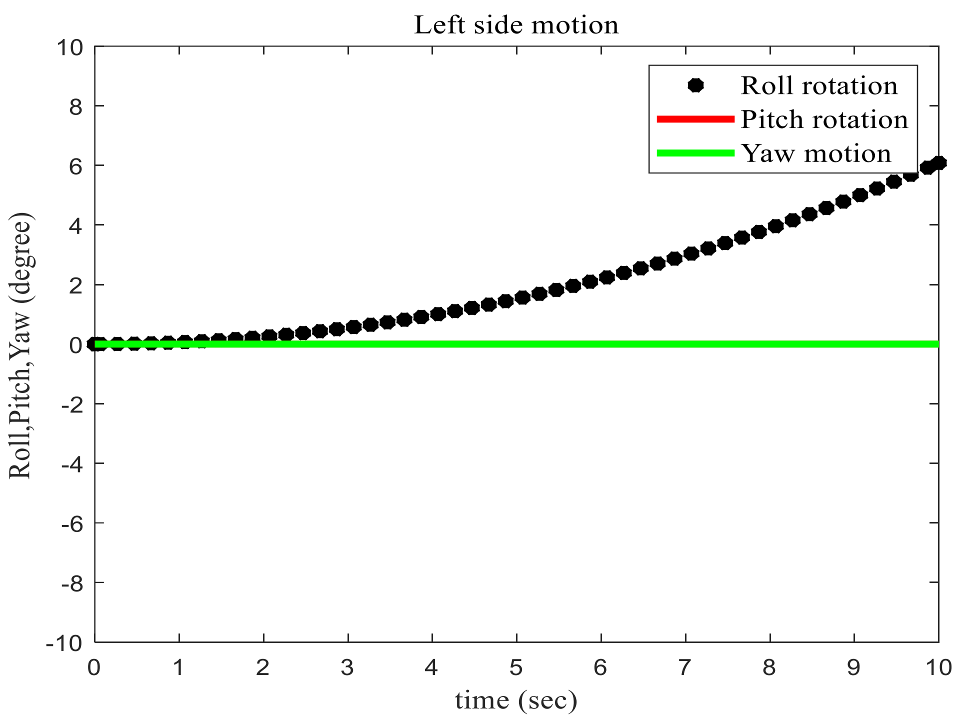


Figure 4.10: Open-loop response of Left side motion of $\phi$

The effects of the dynamics of state, which is called roll dynamic $\omega_1 = \omega_2 = 313\ rad/\sec$ the response shows the unstable system and how to small change in motor speed affects the system. The quadcopter is coupled and highly nonlinear. The simulation result of Figure 4.11 shows the system's open-loop and its affects yaw angle state output and rotational dynamics.

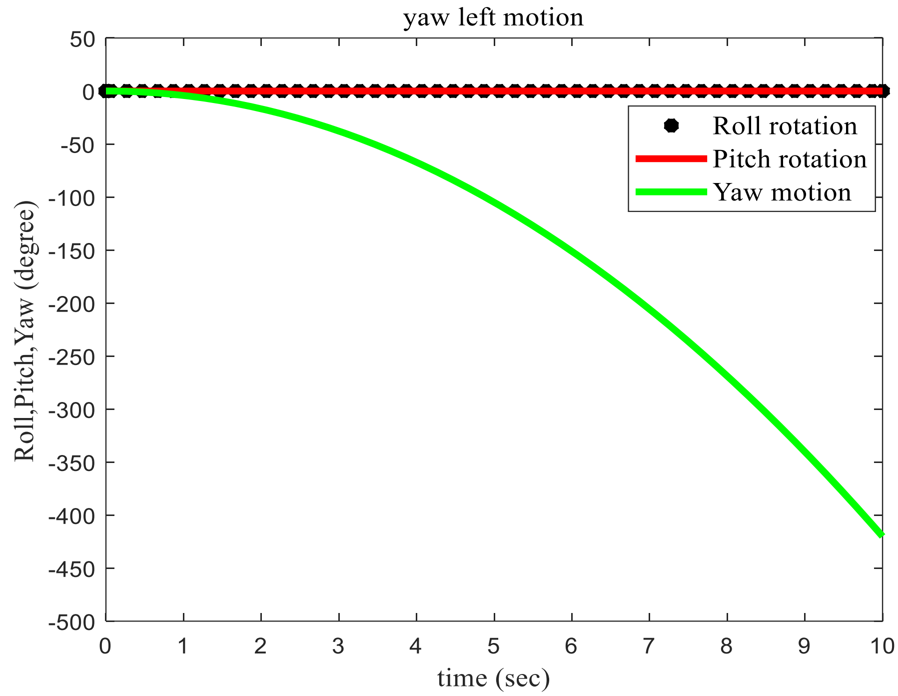


Figure 4.11: Open-loop Response of nonlinear yaw left motion

Generally, all simulation results show that while performing all motions of the quadcopter, the result goes to infinity and is not bound to the limited values. This caused the system to become unstable.

## 4.2. PID Control of Quadcopter-type UAV

A closed-loop control mechanism used to improve the system identifies the performance whether the designed system and controlled system nonlinear systems or linear. In this thesis work, quadcopter-type UAV is a highly non-linear system. There are two nested closed-loop control, the inner and outer loop. The inner loop is designed for controlling the three angular motions ($\phi,\theta,\psi$) of quadcopter-type UAV, while the outer loop closed-loop control is designed for controlling the three linear motions ($x, y, z$) of quadcopter-type UAV. For instance, start from the simplest and the most popular control mechanism called PID controller. However, it is a classical control strategy and is effective for linear and SISO systems. PID controllers in Figure 4.12 show the block diagram, which combines the three control terms described.

$$U(t) = k_p e(t) + k_i \int_0^t e(t)dt + k_d \frac{de(t)}{dt} \tag{4.3}$$

where $k_p$ is the proportional gain, $k_i$ is the integral gain, $k_d$ is the derivative gain. $e(t)$ is the error between the desired and actual output. Each of the brunches contributes to controlling the quadcopter, the integral to remove the steady-state error, and the derivative to increase the performance of the system by keeping the system from overshooting.

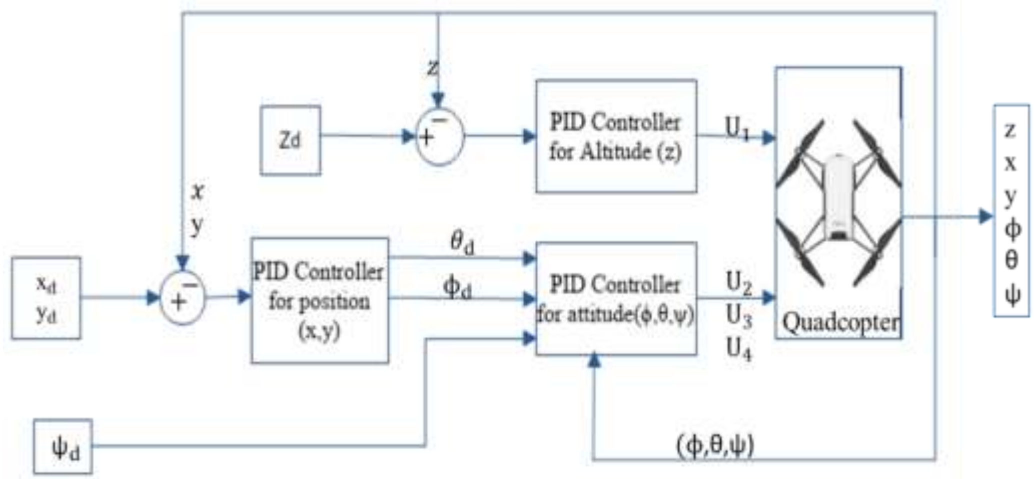


Figure 4.12: PID of the control of quadcopter-type UAV (Waliszkiewicz et al., 2020)

The linear PID control scheme may perform and control the quadcopter by using a linearization mechanism, but for the nonlinear model of the quadcopter, the controller has a low ability and cannot handle the disturbance. Figure 4.13 shows the x and y position Response for PID with wind disturbance at 25sec. The reference $[8\sin(0.4t); 10\sin(0.4t + \pi/2)]$ and response demonstrate the actual value of x, and y-position goes to $10^6$ (m), which means the system cannot follow the given trajectory track. Figure 4.14 shows the Roll and Pitch angle Response for PID with wind disturbance at 25sec. For all the magnitude of disturbance, velocity is 5m/s. From the plot, the roll angle goes to $10^4$ (degree), and the pitch angle is $10^6$ (degree). Figure 4.15 shows the yaw angle Response for PID with wind disturbance at 25sec. The result shows the controller can follow the reference until wind disturbance is exerted on the quadcopter, but after 25 sec, the PID controller cannot reject the wind disturbance and is not robust. The system is not stabilized, and the result is an unacceptable response, very high steady-state error, and the quadcopter becomes damaged.

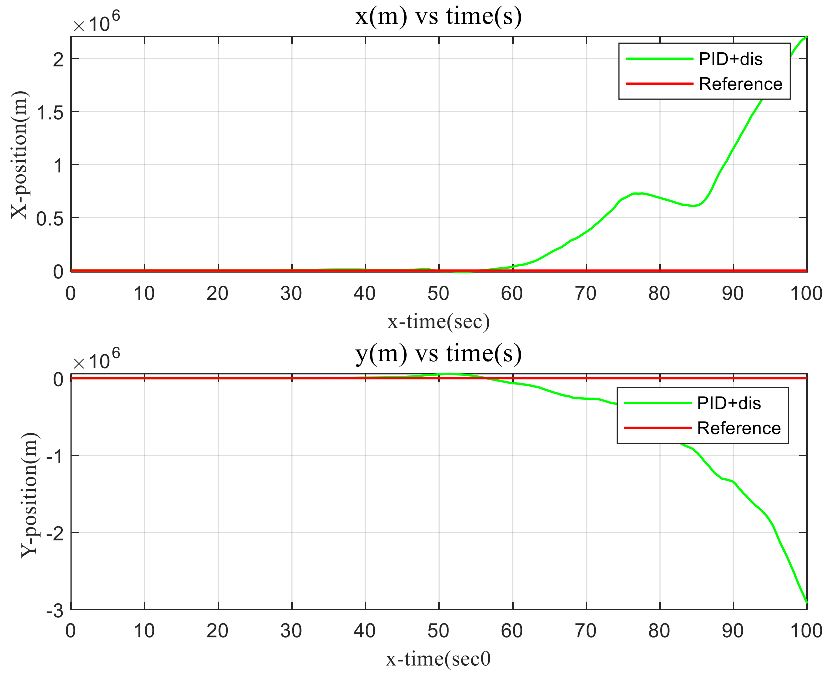


Figure 4.13: X and Y position Response for PID with wind disturbance at 25 sec

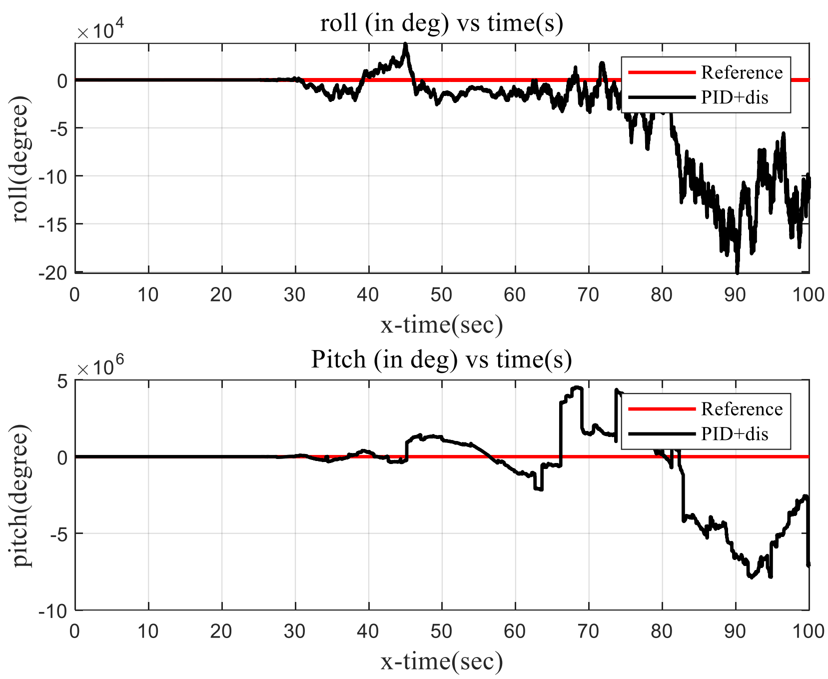


Figure 4.14: roll and pitch angle for PID with wind disturbance at 25 sec

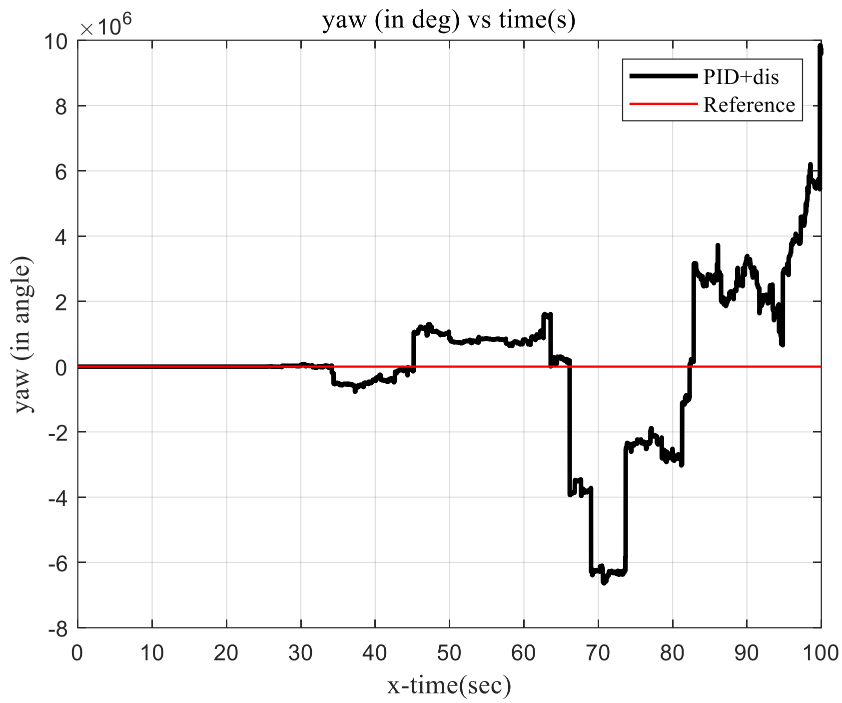


Figure 4.15: yaw angle for PID with wind disturbance at 25 sec

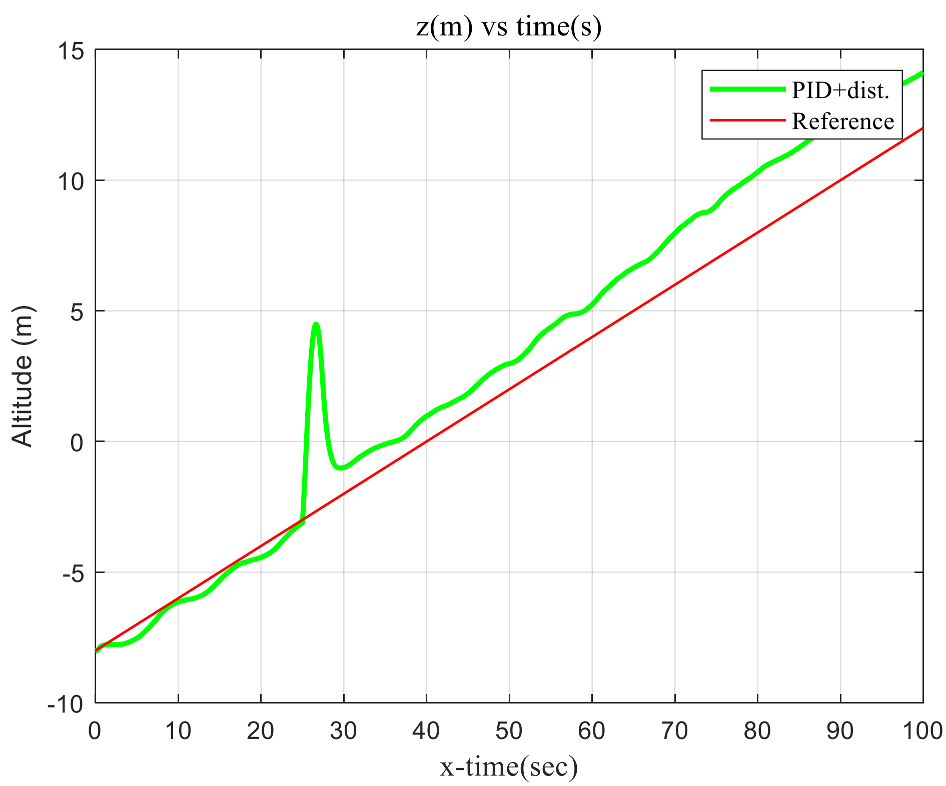


Figure 4.16: Altitude for PID with wind disturbance at 25 sec

## 4.3. Integral-Backstepping Control for Quadcopter-type-UAV System

Integral-backstepping control is chosen to improve performance and stabilize the proposed system. The block diagram proposed nonlinear control strategy is shown in Figure 4.17 to stabilize the quadcopter and design control law for the whole system so that the state trajectory for all output x = $[\phi \quad \theta \quad \psi \quad z \quad x \quad y]$ of the quadcopter system can track the desired reference.

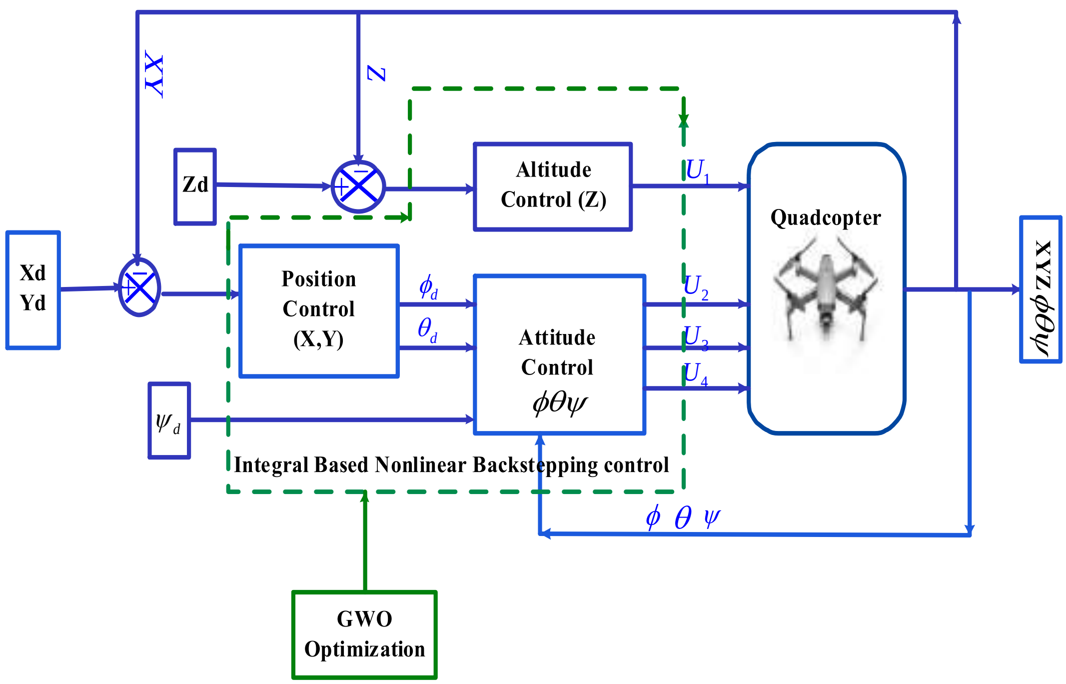


Figure 4.17: Block diagram of the proposed control system

As shown in the block diagram of the proposed control, there are two closed-loops: the outer loop and the inner loop. The outer loop produces the desired value for the pitch angle ($\theta_d$) and roll angle ($\phi_d$) internally. The inner one is the angle ($\phi, \theta, \psi$) control. To avoid the singularities of the system, sufficient assume all angles are bounded $\phi = [-\pi/2, \pi/2]$ $\theta = [-\pi/2, \pi/2]$, $\psi = [-\pi, \pi]$. The design steps of the Integral-backstepping controller designed of the quadcopter are similar for each one of the six controllable DOF. In this work, only one of them is explained in detail for simplicity. Depending on the sequence of state variables defined in the Equation (3.33), the Equation (3.34) the methodical design of integral based nonlinear backstepping control (IBC) is described as follows:

## A. For roll angle control ($\phi$):

Take the first two states variables (4.4) , and from that equation, it is strictly feedback form(Saibi et al., 2022). The input control law affects only the second state, and the subsystem is:

$$\begin{cases} \dot{x}_1 = \dot{\phi} = x_2 \\ \dot{x}_2 = \ddot{\phi} = b_1 u_2 + a_1 x_4 x_6 + a_2 x_4 \omega_r \end{cases} \tag{4.4}$$

Step 1: Defining the tracking error and its rate of change: $\phi = x_1$

$$e_1 = \phi_d - \phi \tag{4.5}$$

Where $\phi_d$ represents the desired roll angle that is specified by a reference model. Then, the derivative of the tracking error can be represented as:

$$\dot{e}_1 = \dot{\phi}_d - \dot{\phi} \tag{4.6}$$

The first Lyapunov function is chosen easier and positive definite in the function of $(e_1, p_1)$ as:

$$v_1(e_1, p_1) = \frac{1}{2} e_1^{\,2} + \frac{1}{2} \lambda_1 p_1^{\,2} \tag{4.7}$$

Where $p_1 = \int_0^t e_1(\tau) d\tau$ the integral term is added to the backstepping control to eliminate the error, the time derivative of the first Lyapunov faction defined in Equation(4.7) is:

$$\dot{v}_1(e_1, p_1) = e_1 \dot{e}_1 + \lambda_1 p_1 e_1 = e_1(\dot{\phi}_d - \dot{\phi} + \lambda_1 p_1) \tag{4.8}$$

Based on the given state is guaranteed to be stable if Equation (4.8) becomes negative semidefinite. Then $\dot{v}_1 = -c_1 e_1^{\,2} \leq 0$ is bounded to $\dot{v}_1$, where $c_1$ positive constant, and $\lambda_1$ is the gain for the integral term and backstepping consider the state variables as virtual controls and designing them as intermediate control laws (Mathematics, 2019). it is also a positive constant, and for inequality, the condition sets the virtual control $(\dot{\phi})_d$ as:

$$(\dot{\phi})_d = \dot{\phi}_d + \lambda_1 p_1 + c_1 e_1 \tag{4.9}$$

Step 2: Define the tracking error of the second state $\dot{\phi} = x_2$ defined as:

$$e_2 = (\dot{\phi})_d - \dot{\phi} = \dot{\phi}_d + \lambda_1 p_1 + c_1 e_1 - \dot{\phi} \tag{4.10}$$

The derivative of $e_2$ is expressed as:

$$\dot{e}_2 = \ddot{\phi}_d + c_1(-\lambda_1 p_1 - c_1 e_1 + e_2) + \lambda_1 e_1 - b_1 U_2 - a_2 \omega_r x_4 - x_4 x_6 a_1$$

The second Lyapunov function is defined in the function of $(e_1, e_2, p_1)$ for the second state to get the positive definite $v_2$:

$$v_2(e_1, e_2, p_1) = v_1 + \frac{1}{2} e_2{}^2 = \frac{1}{2} e_1{}^2 + \frac{1}{2} e_2{}^2 + \frac{1}{2} \lambda_1 p_1{}^2 \tag{4.11}$$

The time derivative of (4.11) and substitute for the model of $\dot{x}_2$ is defined as:

$$\begin{aligned} \dot{v}_2(e_1, e_2, p_1) = -c_1 e_1{}^2 + e_2 (1 + \lambda_1 - c_1{}^2) e_1 + \ddot{\phi}_d - c_1 \lambda_1 p_1 + c_1 e_2 \\ - b_1 U_2 - a_2 \omega_r x_4 - x_4 x_6 a_1) \end{aligned} \tag{4.12}$$

$$\dot{v}_2(e_1, e_2, p_1) \le -(c_1 e_1^2 - c_2 e_2^2) \tag{4.13}$$

Step 3: For satisfying the Lyapunov negative semidefinite and inequality condition of Equation (4.13), solve for the control input $U_2$ and select as:

$$U_2 = \frac{1}{b_1}((1 + \lambda_1 - c_1^2) e_1 + \ddot{\phi}_d - c_1 \lambda_1 p_1 + (c_1 + c_2) e_2 - a_2 \omega_r x_4 - x_4 x_6 a_1) \tag{4.14}$$

where $c_2$ is a positive constant of second controller gain and the term $c_2 e_2$ is added to stabilize the tracking error. Therefore, the control law will become asymptotically and satisfy the stable criteria of the system. The same steps are followed to extract to design $U_1, U_3, U_4, u_x,$ and $u_y$ control law for all parameters and, in short, given as:

**B. For pitch angle control $(\theta)$:**

It is the second subsystem for pitch angle control is:

$$\begin{cases} \dot{x}_3 = \dot{\theta} = x_4 \\ \dot{x}_4 = \ddot{\theta} = b_2 u_3 + a_3 x_2 x_6 + a_4 x_2 \omega_r \end{cases} \tag{4.15}$$

and defines the error track of the actual angle and the desired pitch angle $\theta = x_3$, the integral action added to backstepping control of pitch angle to reduce the error, and the virtual control $x_4$ error given as:

$$\begin{cases} e_3 = \theta_d - \theta \\ p_2 = \int_0^t e_3(\tau) d\tau \\ e_4 = (\dot{\theta}_d) - \dot{\theta} = \dot{\theta}_d + \lambda_2 p_2 + c_3 e_3 + \dot{\theta} \end{cases} \tag{4.16}$$

Where $p_2$ is the second integral action added to the backstepping control of pitch angle control and $\lambda_2$ is the integral action gain, and $c_3$ is the positive constant. The pitch angle is strictly feedback, and only the second equation of the subsystem is influenced $U_3$. That helps us to define the positive-definite of the Lyapunov function defined as:

$$v_3(e_3, p_2) = \frac{1}{2} {e_3}^2 + \lambda_2 \frac{1}{2} {p_2}^2 \tag{4.17}$$

And $e_3$ the error actual pitch angle and reference pitch angle. The time derivative of $v_3$:

$$\dot{v}_3(e_3, p_2) = e_3 \dot{e}_3 + \lambda_2 p_2 e_3 = e_3(\dot{\theta}_d - \dot{\theta} + \lambda_2 p_2) \tag{4.18}$$

Based on the given state is guaranteed to be stable if the Equation (4.18) becomes negative semidefinite. Then $\dot{v}_3 = -c_3 {e_3}^2 \leq 0$ is bounded to $\dot{v}_3$, Then define second of the Lyapunov function for this subsystem and the fourth for the total quadcopter system defined as:

$$v_4(e_3, e_4, p_2) = v_3 + \frac{1}{2} {e_4}^2 = \frac{1}{2} {e_3}^2 + \frac{1}{2} {e_4}^2 + \lambda_2 \frac{1}{2} {p_2}^2 \tag{4.19}$$

The time derivative of $v_4$ and becomes negative semidefinite:

$$\begin{gathered} \dot{v}_4(e_3, e_4, p_2) = -c_3 {e_3}^2 + e_4(1 + \lambda_2 - {c_3}^2) e_3 + \ddot{\theta}_d - c_3 \lambda_2 p_2 + c_3 e_4 \\ -b_2 U_3 - a_4 \omega_r x_2 - x_2 x_6 a_3) \end{gathered} \tag{4.20}$$

The time derivative of the equation must agree to be stable, $\dot{v}_4(e_3, e_4, p_2) \leq 0$. $\dot{v}_4(e_3, e_4, p_2)$ $\leq -(c_3 e_3^2 - c_4 e_4^2)$ is negative semidefinite, $c_4$ is the positive constant and became then satisfy the asymptotically global stable. Solve for the control input $U_3$ and select as:

$$U_3 = \frac{1}{b_2}((1+\lambda_2 - c_3{}^2)e_3 + \ddot{\theta}_d - c_3\lambda_2 p_2 + (c_3 + c_4)e_4 - a_4\omega_r x_2 - x_2 x_6 a_3) \tag{4.21}$$

**C. For yaw angle control** ($\psi$)**:**

The subsystem of yaw angle control from the total quadcopter and the control law affects only the $x_6$, and given as:

$$\begin{cases} \dot{x}_5 = \dot{\psi} = x_6 \\ \dot{x}_6 = \ddot{\psi} = a_5 x_2 x_4 + b_3 u_4 \end{cases} \tag{4.22}$$

The defined error between the desired yaw angle and actual yaw angle, integral added to the yaw angle backstepping control to reduce the error, and the virtual control $x_6$ error defined as:

$$\begin{cases} e_5 = \psi_d - \psi \\ p_3 = \int_0^t e_5(\tau)d\tau \\ e_6 = (\dot{\psi})_d - \dot{\psi} = \dot{\psi}_d + \lambda_3 p_3 + c_5 e_5 - \dot{\psi} \end{cases} \tag{4.23}$$

Where the term $p_3$ is the second integral added to the backstepping control of yaw angle control and $\lambda_3$ is the integral action gain. The Lyapunov function of the state of the subsystem and function for total the quadcopter system define as:

$$v_5(e_5, p_3) = \frac{1}{2}e_5{}^2 + \lambda_3 \frac{1}{2} p_3{}^2 \tag{4.24}$$

Based on the given state is guaranteed to be stable if the Equation (4.24) becomes negative semidefinite. Then $\dot{v}_5 = -c_5 e_5{}^2 \le 0$ is bounded to $\dot{v}_5$, and $c_5$ is the positive constant. Then define the second of the Lyapunov function for this subsystem and the sixth for the total quadcopter system defined as:

$$v_6(e_5, e_6, p_3) = v_5 + \frac{1}{2}e_6{}^2 = \frac{1}{2}e_5{}^2 + \frac{1}{2}e_6{}^2 + \lambda_3 \frac{1}{2} p_3{}^2 \tag{4.25}$$

The time derivative of $v_6$ and becomes negative semidefinite $\dot{v}_6(e_5, e_6, p_3) \le 0$:

$$\dot{v}_6 = -c_5 e_5{}^2 + e_6(1+\lambda_3 - c_5{}^2)e_5 + \ddot{\psi}_d - c_5\lambda_3 p_3 + c_5 e_6 - b_3 U_4 - x_2 x_4 a_5) \tag{4.26}$$

The time derivative of the equation must agree to be stable, $\dot{v}_6(e_5, e_6, p_3) \le 0$ and $\dot{v}_6(e_5, e_6, p_3)$ $\le -(c_5e_5^2 - c_6e_6^2)$ is negative semidefinite, $c_6$ is the positive constant, and became then satisfy the asymptotically global stable. Solve for the control input $U_4$ and select as:

$$U_4 = \frac{1}{b_3}((1+\lambda_3 - c_5{}^2)e_5 + \ddot{\psi}_d - c_5\lambda_3 p_3 + (c_5 + c_6)e_6 - x_2x_4a_5) \tag{4.27}$$

### D. For linear Z motion control:

The subsystem of altitude control of the quadcopter gives as follows:

$$\begin{cases} \dot{x}_7 = \dot{z} = x_8 \\ \dot{x}_8 = \ddot{z} = g - \dfrac{u_1}{m}(\cos(x_1)\cos(x_3)) \end{cases} \tag{4.28}$$

The defined error between the desired altitude and actual altitude of the quadcopter, integral action added to the backstepping control to reduce the error, and the virtual control, $x_8$ error defined as:

$$\begin{cases} e_7 = z_d - z \\ p_4 = \int_0^t e_7(\tau)d\tau \\ e_8 = (\dot{z})_d - \dot{z} = \dot{z}_d + \lambda_4 p_4 + c_7e_7 + \dot{z} \end{cases} \tag{4.29}$$

Where the term $p_4$ is the second integral action added to the backstepping control the altitude control and $\lambda_4$ is the integral action gain. The Lyapunov function of the first state and the second state of the subsystem and the seventh and the eighth function for total the quadcopter system define as:

$$v_7(e_7, p_4) = \frac{1}{2}e_7{}^2 + \lambda_4\frac{1}{2}p_4{}^2 \tag{4.30}$$

Based on the given state is guaranteed to be stable if the equation (4.30) becomes negative semidefinite. Then $\dot{v}_7 = -c_7e_7{}^2 \le 0$ is bounded to $\dot{v}_7$, and $c_7$ is the positive constant. Then define the second of the Lyapunov function for this subsystem and the sixth for the total quadcopter system defined as:

$$v_8(e_7,e_8,p_4)=v_7+\frac{1}{2}e_8{}^2=\frac{1}{2}e_7{}^2+\frac{1}{2}e_8{}^2+\lambda_4\frac{1}{2}p_4{}^2 \tag{4.31}$$

The time derivative of (4.31) and becomes negative semidefinite $\dot{v}_8(e_7,e_8,p_4)\le 0$:

$$\dot{v}_8=-c_7e_7{}^2+e_8(1+\lambda_4-c_7{}^2)e_7+\ddot{z}_d-c_7\lambda_4p_4+c_7e_8+g-\frac{U_1(\cos x_1\cos x_3)}{m}) \tag{4.32}$$

The time derivative of the equation must agree to be stable, $\dot{v}_8(e_7,e_8,p_4)\le 0$ and $\dot{v}_8(e_7,e_8,p_4)$ $\le -(c_7e_7^2-c_8e_8^2)$ is negative semidefinite, $c_8$ is the positive constant, and became then satisfy the asymptotically global stable. Solve for the control input $U_1$ and select as:

$$U_1=\frac{m}{\cos x_1\cos x_3}((1+\lambda_4-c_7{}^2)e_7+\ddot{z}_d-c_7\lambda_4p_4+(c_7+c_8)e_8+g) \tag{4.33}$$

### E. For linear $y$ motion control:

The subsystem of x-position control of the quadcopter gives as:

$$\begin{cases}\dot{x}_9=\dot{y}=x_{10}\\ \dot{x}_{10}=\ddot{y}=\dfrac{u_1}{m}u_y\end{cases} \tag{4.34}$$

The tracking error between the desired x-position and actual position, the integral action added to backstepping control of x-position control to reduce the error, and the virtual control $x_{10}$ error is defined as:

$$\begin{cases}e_9=y_d-y\\ p_5=\int_0^t e_9(\tau)d\tau\\ e_{10}=(\dot{y})_d-\dot{y}=\dot{y}_d+\lambda_5p_5+c_9e_9+\dot{y}\end{cases} \tag{4.35}$$

Define the first Lyapunov function of the x-position control subsystem for the first state stabilize

$$v_9(e_9,p_5)=\frac{1}{2}e_9{}^2+\lambda_5\frac{1}{2}p_5{}^2 \tag{4.36}$$

The state is guaranteed to be stable if Equation (4.36) becomes negative semidefinite. Then $\dot{v}_9 = -c_9 e_{79}{}^2 \leq 0$ is bounded to $\dot{v}_9$, and $c_9$ is the positive constant. Then define the second of the Lyapunov function for the second state of this subsystem. The quadcopter system is defined as:

$$v_{10}(e_9, e_{10}, p_5) = v_9 + \frac{1}{2} e_{10}{}^2 = \frac{1}{2} e_9{}^2 + \frac{1}{2} e_{10}{}^2 + \lambda_5 \frac{1}{2} p_5{}^2 \tag{4.37}$$

The time derivative of (4.37) and becomes negative semidefinite $\dot{v}_{10}(e_9, e_{10}, p_5) \leq 0$:

$$\dot{v}_{10}(e_9, e_{10}, p_5) = -c_9 e_9{}^2 + e_{10}(1 + \lambda_5 - c_9{}^2) e_9 + \ddot{y}_d - c_9 \lambda_5 p_5 + c_9 e_{10} + \frac{U_1}{m} u_y) \tag{4.38}$$

The time derivative must agree to be stable, and $\dot{v}_{10}(e_9, e_{10}, p_5) \leq -(c_9 e_9^2 - c_{10} e_{10}^2)$ is negative semidefinite, $c_{10}$ is the positive constant, and became then satisfy the asymptotically global stable. Solve for the control input $u_x$ and select as:

$$u_y = \frac{m}{U_1}((1 + \lambda_5 - c_9{}^2) e_9 + \ddot{y}_d - c_9 \lambda_5 p_5 + (c_9 + c_{10}) e_{10}) \tag{4.39}$$

## F. For linear x motion control:

The subsystem for x-position control of the quadcopter is given as:

$$\begin{cases} \dot{x}_{11} = \dot{x} = x_{12} \\ \dot{x}_{12} = \ddot{x} = \dfrac{u_1}{m} u_x \end{cases} \tag{4.40}$$

The tracking error between the desired x-position and an actual position of the quadcopter, $p_6$ the integral added to the backstepping control to minimize the error, $\lambda_6$ is the integral gain, and the virtual control $x_{12}$ error is defined as:

$$\begin{cases} e_{11} = x_d - x \\ p_6 = \int_0^t e_{11}(\tau) d\tau \\ e_{12} = (\dot{x})_d - \dot{x} = \dot{x}_d + \lambda_6 p_6 + c_{11} e_{11} + \dot{x} \end{cases} \tag{4.41}$$

The Lyapunov function of the quadcopter system's first state of subsystem function. Define as:

$$v_{11}(e_{11}, p_6) = \frac{1}{2}e_{11}{}^2 + \lambda_6 \frac{1}{2} p_6{}^2 \tag{4.42}$$

The given first state is guaranteed to be stable if the equation (4.42) becomes negative semidefinite. Then $\dot{v}_{11} = -c_{11}e_{11}{}^2 \le 0$ is bounded to $\dot{v}_{11}$, and $c_{11}$ is the constant positive gain. Then define the second of the Lyapunov function to guarantee the stability of the second state of this subsystem quadcopter system y-position defined as:

$$v_{12}(e_{11}, e_{12}, p_6) = v_{11} + \frac{1}{2}e_{12}{}^2 = \frac{1}{2}e_{11}{}^2 + \frac{1}{2}e_{12}{}^2 + \lambda_6 \frac{1}{2} p_6{}^2 \tag{4.43}$$

The time derivative of (4.43) and becomes negative semidefinite $\dot{v}_{12}(e_{11}, e_{12}, p_{64}) \le 0$ :

$$\dot{v}_{12}(e_{11}, e_{12}, p_6) = -c_{11}e_{11}{}^2 + e_{12}(1 + \lambda_6 - c_{11}{}^2)e_{11} + \ddot{x}_d - c_{11}\lambda_6 p_6 + c_{11}e_{12} + \frac{U_1}{m}u_x) \tag{4.44}$$

The time derivative of the equation must agree to be stable, and $\dot{v}_{12}(e_{11}, e_{12}, p_6)$ $\le -(c_{11}e_{11}^2 - c_{12}e_{12}^2)$ is negative semidefinite, $c_{12}$ is the positive constant, and became then satisfy the asymptotically global stable. Solve for the control input $u_y$ and select as:

$$u_x = \frac{m}{U_1}((1 + \lambda_6 - c_{11}{}^2)e_{11} + \ddot{x}_d - c_{11}\lambda_6 p_6 + (c_{11} + c_{12})e_{12}) \tag{4.45}$$

Where the backstepping control gain $c_i,_{i=1,2,3...12}$ and the integral gain $\lambda_j,_{j=1,2,...6}$ are positive constants from the equation (3.17) $\phi_d$ and $\theta_d$ can be calculated as:

$$\begin{cases} \ddot{x} = \dfrac{U_1}{m}(\cos\phi_d \cos\psi \sin\theta_d + \sin\psi \sin\phi_d) \\ \ddot{y} = \dfrac{U_1}{m}(\cos\phi_d \sin\theta_d \sin\psi - \cos\psi \sin\phi_d) \end{cases} \tag{4.46}$$

Assume the angle is slight $\sin\theta_d \cong \theta_d, \sin\phi_d \cong \phi_d$ and $\cos\phi_d \cong \cos\theta_d \cong 1$;

$$\begin{bmatrix} \ddot{x}_d \\ \ddot{y}_d \end{bmatrix} = \frac{U_1}{m}\begin{bmatrix} \sin\psi & \cos\psi \\ -\cos\psi & \sin\psi \end{bmatrix}\begin{bmatrix} \phi_d \\ \theta_d \end{bmatrix} \tag{4.47}$$

$$\begin{bmatrix} \phi_d \\ \theta_d \end{bmatrix} = \frac{m}{U_1}\begin{bmatrix} \sin\psi & -\cos\psi \\ \cos\psi & \sin\psi \end{bmatrix}\begin{bmatrix} \ddot{x}_d \\ \ddot{y}_d \end{bmatrix} \tag{4.48}$$

# CHAPTER FIVE

# 5. RESULT AND DISCUSSION

This chapter contains the analysis and discussion of the simulation result of the quadcopter with the proposed backstepping controller. The system parameter shown in Table 5.1 used in the simulation is taken from the Space Technology Institute (STI) center of Excellence of Adama Science and Technology University (ASTU).

Table 5.1: The Quadcopter model parameter specification

| Description | Parameter | Value | Unit |
|---|---|---|---|
| Total Mass of the quadcopter | $m$ | *1.5* | $kg$ |
| Gravitational acceleration | $g$ | *9.81* | $m/s^2$ |
| MOI about body frame's x-axis | $I_x$ | $7.5 \times 10^{-3}$ | $kg.m^2$ |
| MOI about body frame's y-axis | $I_y$ | $7.5 \times 10^{-3}$ | $kg.m^2$ |
| MOI about body frame's z-axis | $I_z$ | $1.3 \times 10^{-2}$ | $kg.m^2$ |
| Rotor inertia | $J_r$ | $6 \times 10^{-5}$ | $kg.m^2$ |
| Moment arm | $l$ | 0.55 | $m$ |
| Aerodynamic force constant | $b$ | $3.1 \times 10^{-5}$ | $N.s^2$ |
| Aerodynamic moment constant | $d$ | $7.5 \times 10^{-7}$ | $Nm.s^2$ |

The analysis is done under different conditions to evaluate the performance and test the robustness of the proposed controller under external disturbance, considering unmolded parameter uncertainty such as the mass of quadcopter as with varying load the position and altitude control of quadcopter, the simulator was designed using MATLAB2021a /Simulink. Figure 5.1 shows the thrust input to the quadcopter $U_1$, $U_2$, $U_3$, and $U_4$. The significant errors are penalized by estimating the root mean square errors (RMSE). RMSE tells us how the actual values are around the desired value of best fit, and there is no extremely good or bad threshold but the smallest RMSE, the better one.

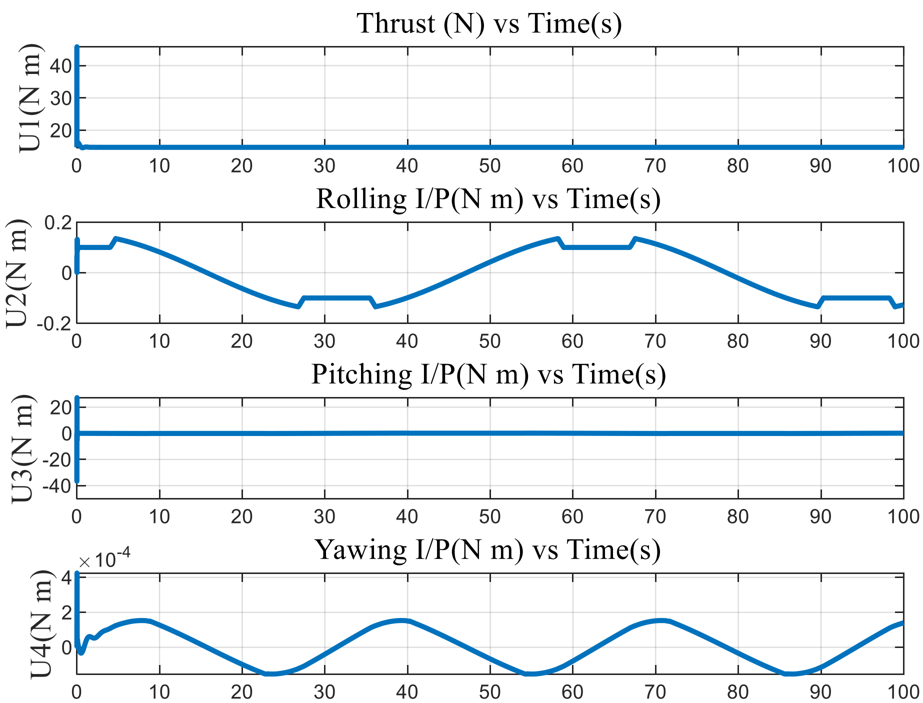


Figure 5.1: Simulation response of $U_1$, $U_2$, $U_3$, and $U_4$ control law

## 5.1. Altitude and Attitude Control of Integral-Backstepping Controller

### 5.1.1. Simulation Result of Altitude Control

The vertical motion of the quadcopter indicates the altitude or the height of the quadcopter is to fly upward from the ground and hover at the given height. In this thesis work, the simulation of the Altitude of the quadcopter represent by the z-axis and initially starts from -8 to show the global stability and with slopes from 0.2, and the total height of the quadcopter is 20m. Figure 5.2 shows the simulation result altitude control of quadcopter with Integral based nonlinear Backstepping controller (IBS) without any disturbance and parameter uncertainty. The control law $U_1$is the thrust force of the quadcopter's altitude represented in Figure 5.1. The result shows that the system follows the given reference trajectory, and the simulation time is 100secs. From the simulation result, the quadcopter starts from any initial and follows the given tracking points with a small steady-state error, and the controller improves the stability.

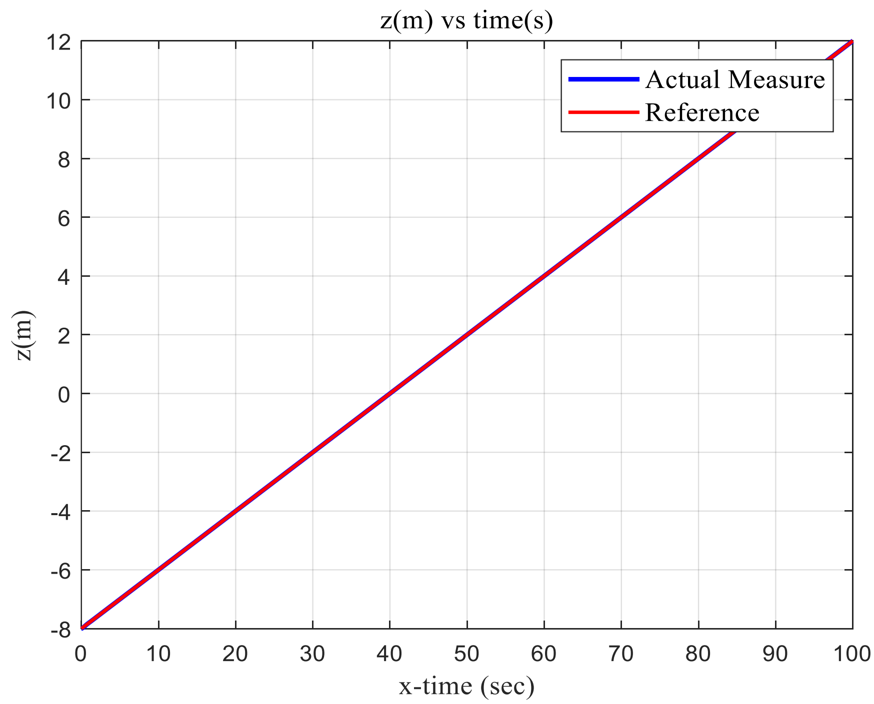


Figure 5.2: Response of altitude of IBC with ramp input

On the other hand, the quadcopter flies up from the initial and hovers at the desired height with a small steady-state error. The error in the z(m) is shown in Figure 5.5. and RMSE in Table 5.3

### 5.1.2. Simulation Result for Attitude Control

During the stabilization of the attitude of a quadcopter, the controller performed by reducing the error. In this thesis work, the desired angle roll and pitch angles are calculated internally, corresponding to their motion in the x and y-tracking, and the desired yaw angle is $0^{\circ}$. The Control law of the three-angle is shown in Figure 5.1. The simulation response in Figure 5.3 is shown the result of IBS for the three angular rotations roll, pitch, and yaw angles of the quadcopter. The IBS controller takes its desired value provided from the outer loop and performs the stabilized and tracking of the desired value by reducing the error in roll pitch, and the yaw angle is analyzed using the RMSE error analysis method for the nonlinear system in Table 5.3. The pitch angle is controlled with a small error than the roll angle control, and the actual yaw angle is less than $1 \times 10^{-18\circ}$, Figure 5.5 shows that the steady-state error in the yaw angle is zero.

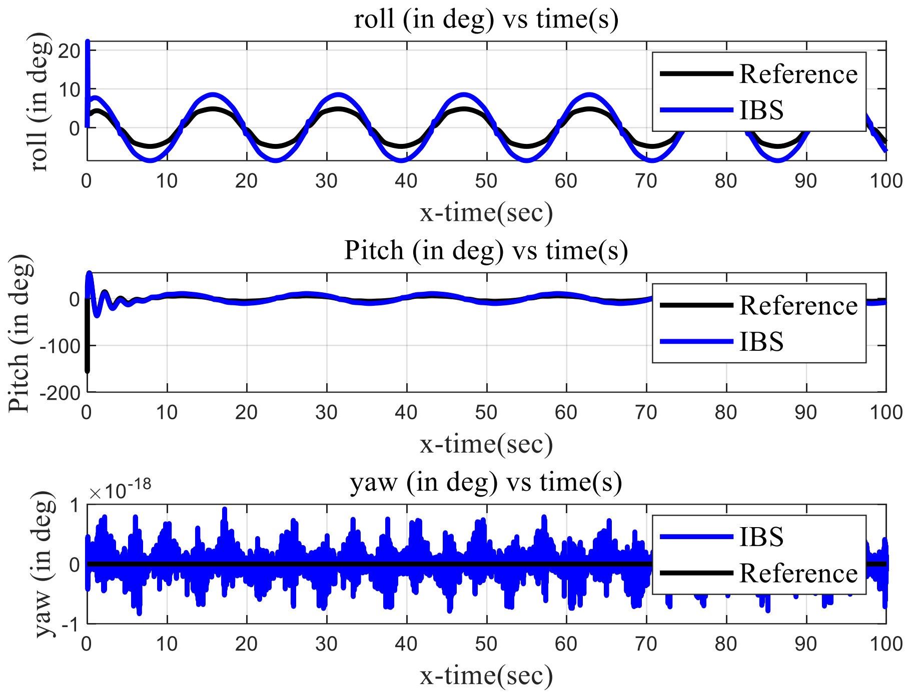


Figure 5.3: Simulation response of IBS roll, pitch, yaw angle vs time

### 5.1.3. Translational Position Control of the IBS Controller

The horizontal motion of the quadcopter is containing both x-position and y-position translation positions. Figure 5.4 shows the simulation response of the x-position and y-position of the IBS controller without any disturbance and uncertainty. The initial is [0; 10], and desired helical trajectory of the system define as $[x;\ y] = [8\sin(0.4t); 10\sin(0.4t + \pi/2)]$. The result shows that the IBS controller gives good performance and the maximum error can be zoomed in for each response as shown in Figure 5.4 and analyzed by the RMSE in Table 5.3 and the quadcopter tracks the given trajectory and small steady state error as shown in Figure 5.5. the result of the error shows the error in x-position is vary between -0.5m and 1m and for y-position varies between -0.05m and 0.05m.

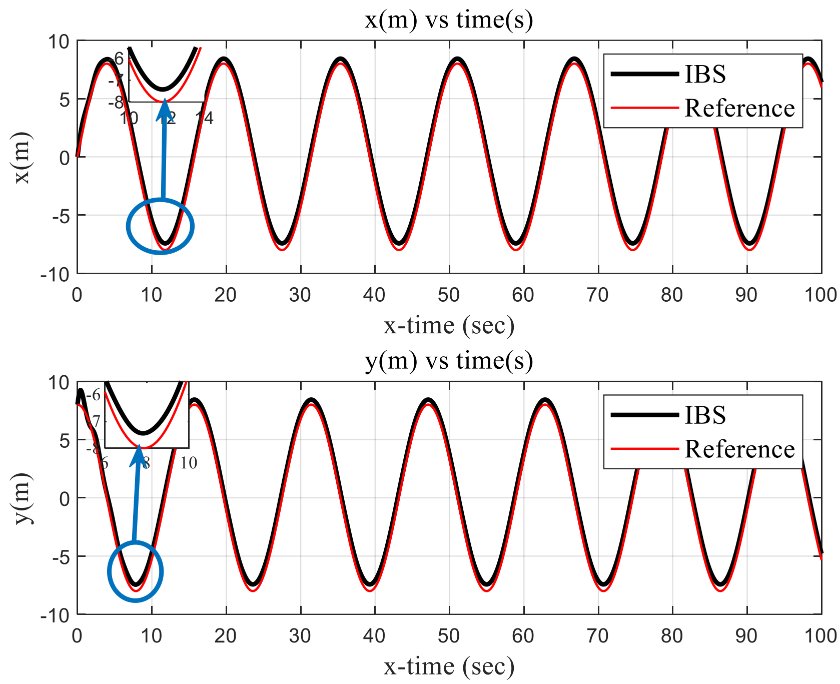


Figure 5.4: Simulation response of x and y position for IBS controller

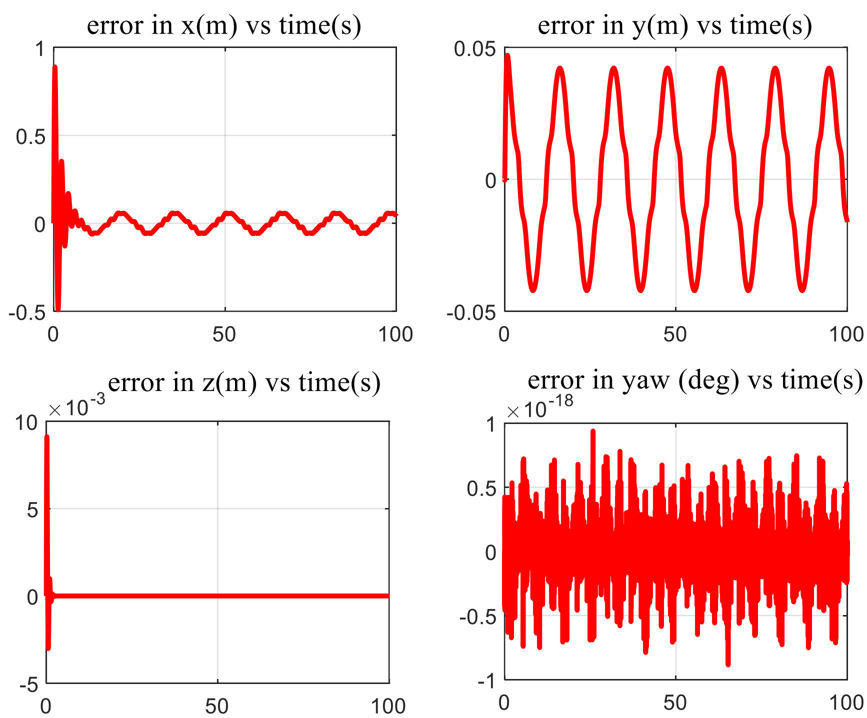


Figure 5.5: Error in x, y, z-position, and yaw angle of IBS control

## 5.2. GWO-IBS Controller of Attitude and Altitude Control

The GWO optimization was applied to tuning the control gains Table 5.2 designed for the integral nonlinear backstepping controller has 12 ($c_1, c_2, c_3, c_4, c_5, c_6, c_7, c_8, c_9, c_{10}, c_{11}$, and $c_{12}$) gains and for the integral control, has 6 ($\lambda_1, \lambda_2, \lambda_3, \lambda_4, \lambda_5$, and $\lambda_6$) gains.

Table 5.2: The best solution obtained by GWO

| | Roll angle ($\phi$) | Pitch angle ($\theta$) | Yaw angle ($\psi$) | z | x | y |
|---|---|---|---|---|---|---|
| GWO -IBS gains | $\lambda_1 = 0.453$<br>C1=66.665<br>C2=36.362 | $\lambda_2 = 6.600$<br>C3=30.177<br>C4=44.730 | $\lambda_3 = 7.383$<br>C5=25.215<br>C6= 81.612 | $\lambda_4 = 20$<br>C7=6.938<br>C8=0.747 | $\lambda_5 = 1.158$<br>C9= 7.216<br>C10= 8.777 | $\lambda_6 = 4.572$<br>C11=9.042<br>C12=5.801 |

### 5.2.1. Simulation Result of GWO-IBS Controller for Altitude Control

The altitude control of GWO-IBS performs looks similar to the IBS controller but there is a slight small difference in steady state error, which means the proposed control mechanism reduced the steady state error and tracks the desired trajectory more than the IBS controller. Figure 5.6 shows the simulation result of altitude or z(m) of a quadcopter with a GWO-IBS controller without wind disturbance and parameter uncertainty and the RMSE analysis is done.

### 5.2.2. Simulation of GWO-IBS Controller for Translational Position Control

The translation motion of the quadcopter is referring to the movement along the x-position and y-position. The x-position performs the left and right-side movement of the quadcopter whereas y-position causes to move forward and backward motion. Figure 5.7 shows the simulation result of the proposed GWO-IBS controller has better performance than IBS and that the quadcopter follows the given trajectory. The magnified plot in Figure 5.7 is used to display how the proposed controller is follow the given trajectory in both positions and the RMSE analysis is done.

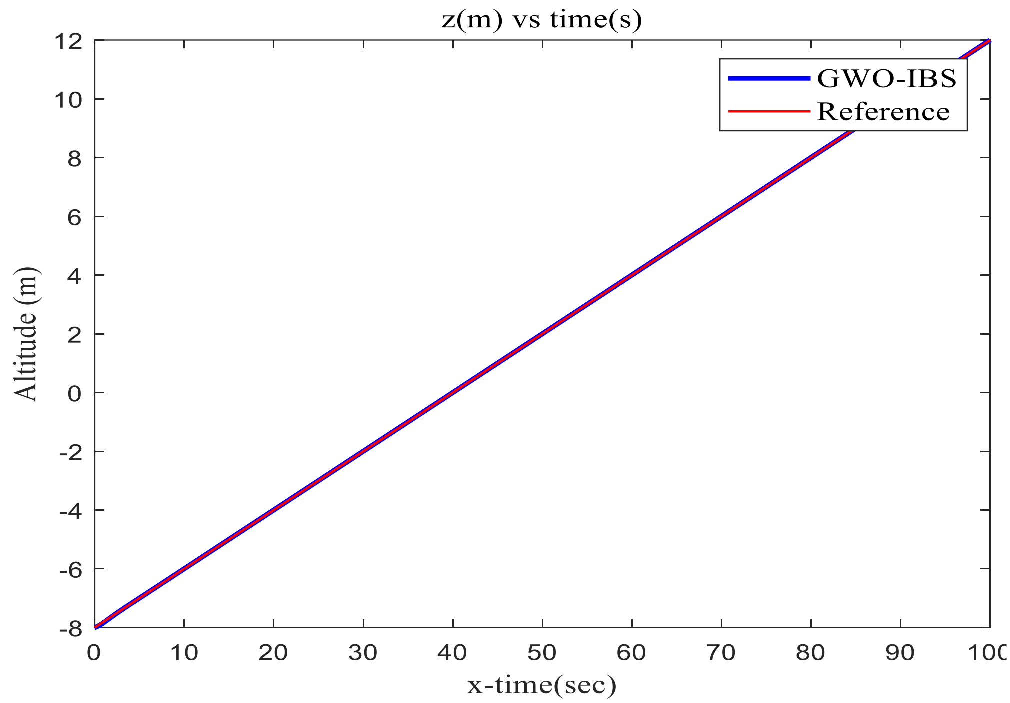


Figure 5.6: GWO-IBS Result of Altitude control vs time

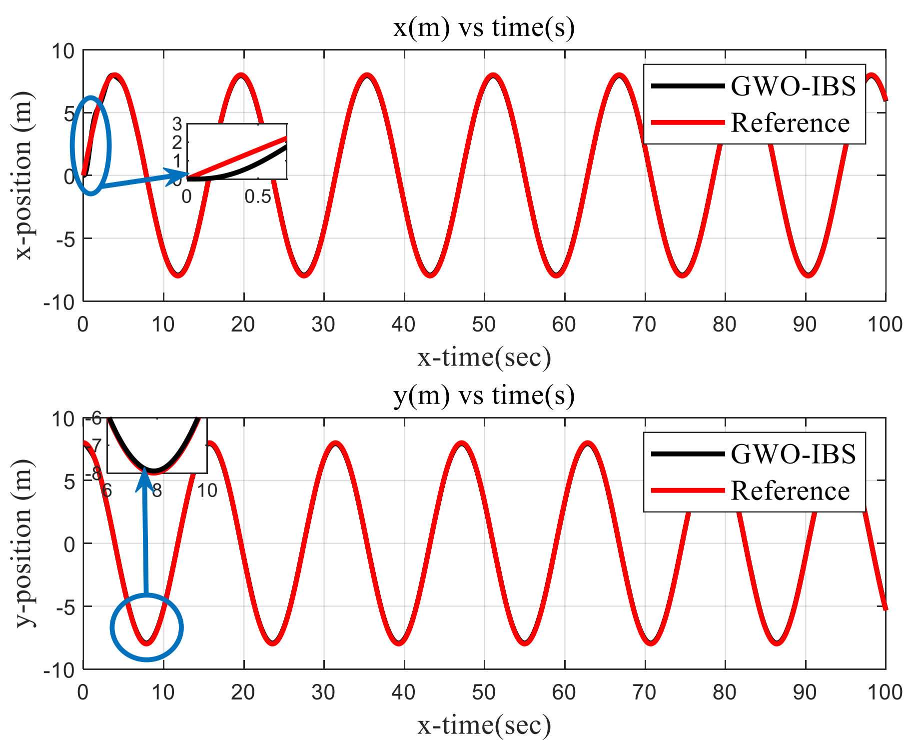


Figure 5.7: GWO-IBS Result of x-position and y-position vs time

### 5.2.3. Simulation of GWO-IBS Controller for Attitude Control

The roll attitude is the rotation of the quadcopter along the x-axis and causes the system to move to the rolling right side and the rolling left along with the horizontal motion while the pitch attitude is the rotation along the y-axis that caused the quadcopter to move to forward and backward. Figure 5.8 shows GWO-IBS control of pitch and roll angle (degree). The proposed controller behaves with better performance and the desired reference trajectory of roll angle is reached with a small steady state error GWO-IBS controller can control the pitch angle with better performance than the IBS controller and the quadcopter follows the desired trajectory track. The yaw attitude is the rotation of the quadcopter along the z-axis. The yaw angle is also controlled and the desired reference is reached. Figure 5.9 shows the GWO-IBS control of yaw angle(degree) and the GWO-IBS nearer to zero ( $2.5 \times 10^{-19}$) degree.

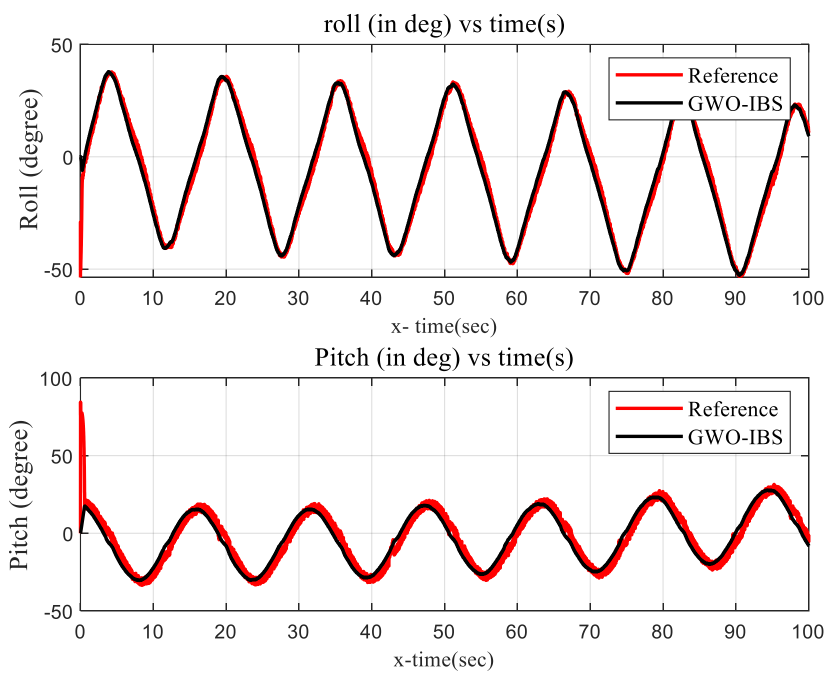


Figure 5.8: GWO-IBS control of roll and pitch angle(degree) vs time

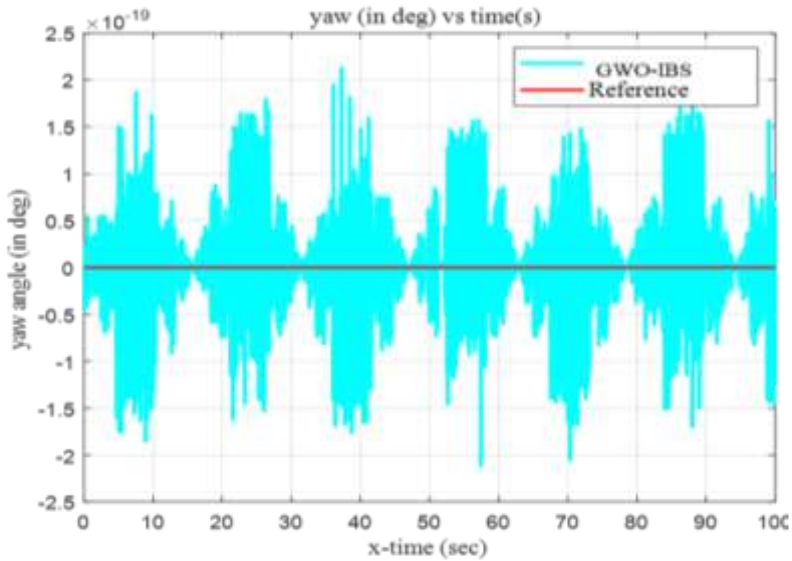


Figure 5.9: GWO-IBS control of yaw angle(degree) vs time

## 5.3. Test Robustness of Controller

The proposed control mechanism checked the robustness of the controller by assuming there is sudden wind disturbance force and model parameter uncertainty. In this thesis work, the parameter uncertainty of the model is the quadcopter dynamic on the translational motion by variation mass of the payload.

### 5.3.1. Test Integral-Backstepping Controller

*Scenario 1:* Robustness test with Wind Disturbance

The sudden disturbances added to the quadcopter consider variable wind disturbance with velocity $V_{wind} = 5i + 5j + 5k\ m/s$ and are applied as step input within the time of 25 sec to test the ability to reject the disturbance of the controller. Figure 5.10 shows the simulation result of altitude Z(m) with uniform disturbance and the yawing angle IBS controller with the wind disturbance. From the response, the quadcopter is following the given desired reference before the disturbance, but after 25 secs the quadcopter is away from the desired reference, IBS controller not robust. The desired power consumed is 0.577watts to reach the desired altitude of the quadcopter 20m, and to reach the hovering state. But due to the wind disturbance, the actual power consumed due to is 26.699 watts because the vehicle pushes upward for 2.765 sec and away from the given reference trajectory by 4.98m. These affect the battery capacity of the quadcopter as well as the flight time and cause damage.

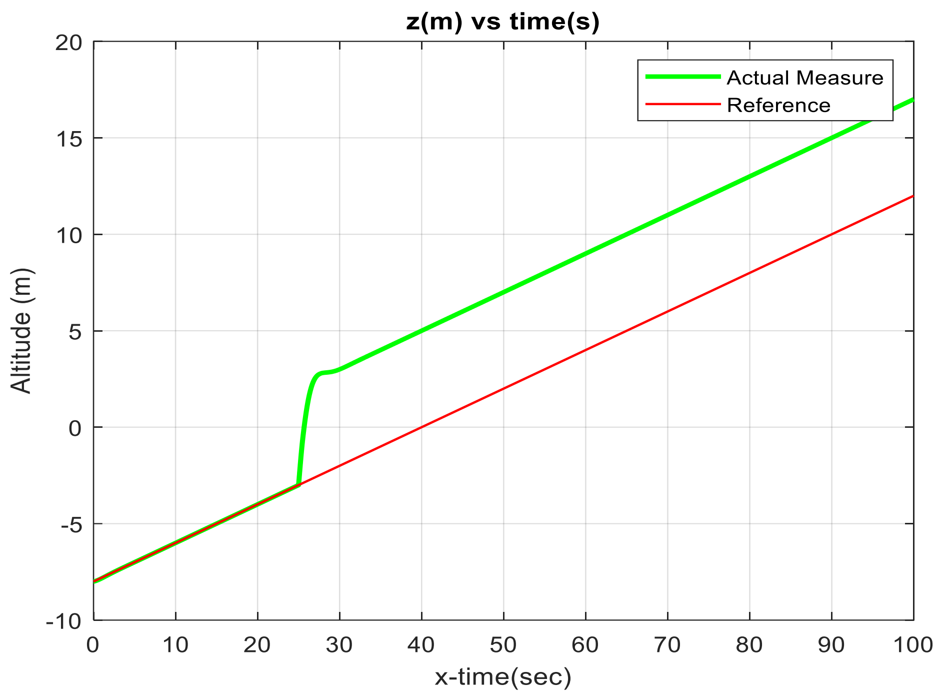


Figure 5.10: Response altitude z(m) IBS with uniform wind disturbance at 25se

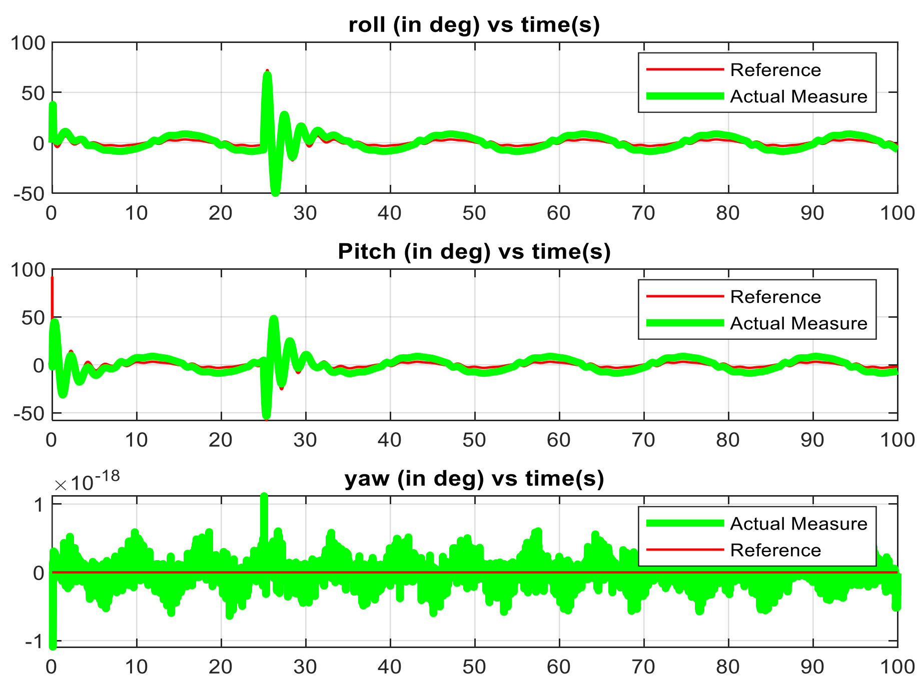

Figure 5.11: Roll, Pitch, and yaw angle for IBS with wind disturbance at 25 sec

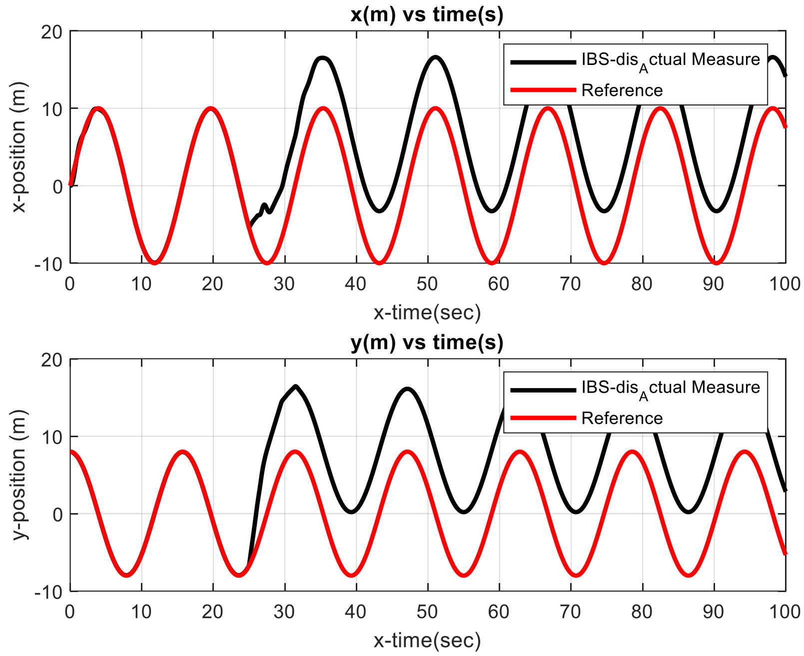


Figure 5.12: x and y position for IBS with wind disturbance at 25 sec

As shown in Figure 5.11 the IBS controller performs well with acceptable error and the quadcopter track within the desired pitch angle. The response x and y-position for IBS with sudden wind disturbance are shown in Figure 5.12. The result of IBS the black one moves away from the reference the red. IBS control is not robust during the existence of external disturbances. But in both roll angle and pitch angle at the starting point and wind force exist in the system there is a small error and analyses the error to know how the actual value is closed to the desired reference trajectory in terms of RMSE. The error between the desired value and the reference trajectory of IBS with disturbance is shown in Figure 5.13. and the RMSE analysis is done in Table 5.3

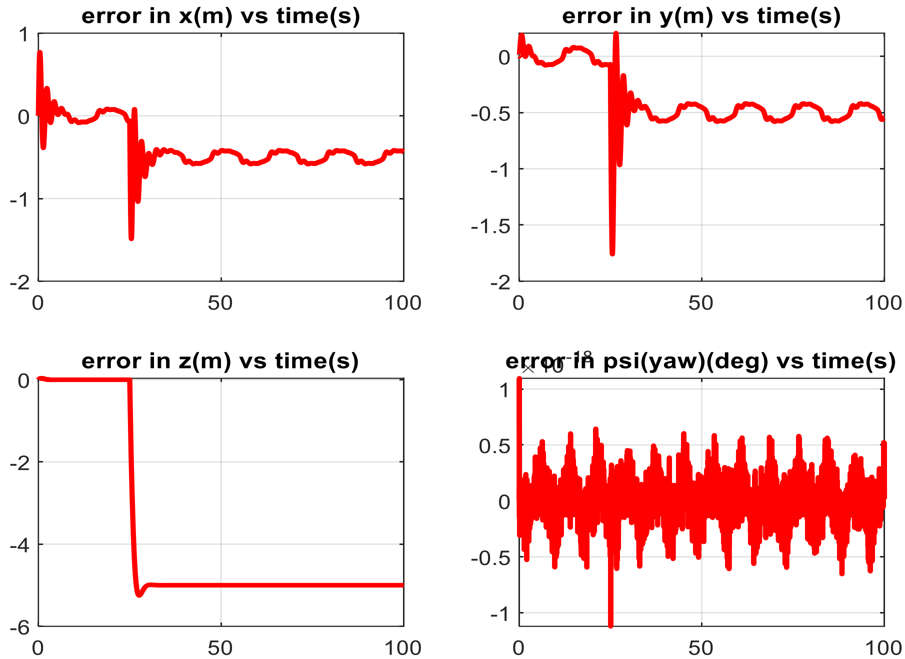


Figure 5.13: Error x, y, z, and yaw angle IBS with wind disturbance at 25 sec

### 5.3.2. Grey Wolf Optimization Based Integral-Backstepping (GWO-IBS)

The optimized proposed control mechanism performs better than the non-optimized one in control of the altitude of the quadcopter speed of wind disturbance change from the magnitude 2 to 10 m/s in is $[i, j, k]$ direction wind at 25 secs. Figure 5.14 shows that the GWO-IBS with uniform and multiform wind disturbance is applied to the quadcopter, and as the simulation, the result shows the controller reject the disturbance from the system and settles within a short period, the proposed controller is robust in the existence of disturbance and the quadcopter is followed the desired reference trajectory with very small acceptable error as shown in the Figure 5.19 and the Table 5.3 analyses in terms of RMSE. The result demonstrates that the GWO-IBS performs better at altitude even the velocity of wind disturbance changes.

In the case of attitude or z-trajectory control, the GWO-IBS controller eliminates the oscillation that exists in the IBS at the starting point and during the disturbance. Figure 5.15 shows the simulation result of the roll angle of the proposed controller with $V_{wind} = 5i + 5j + 5k\ m/s$ wind disturbance at 25 sec. The proposed controller is better performing the roll angle control of the quadcopter than IBS with the existence of variable wind disturbance at the level applied to the quadcopter for them. The quadcopter rotates the roll angle with the desired reference trajectory with a very small error and settled in a short time as shown in Figure 5.19. during the existence of wind disturbance reduces the system handles the effect of wind by the steady state error, and error analysis is done by RMSE.

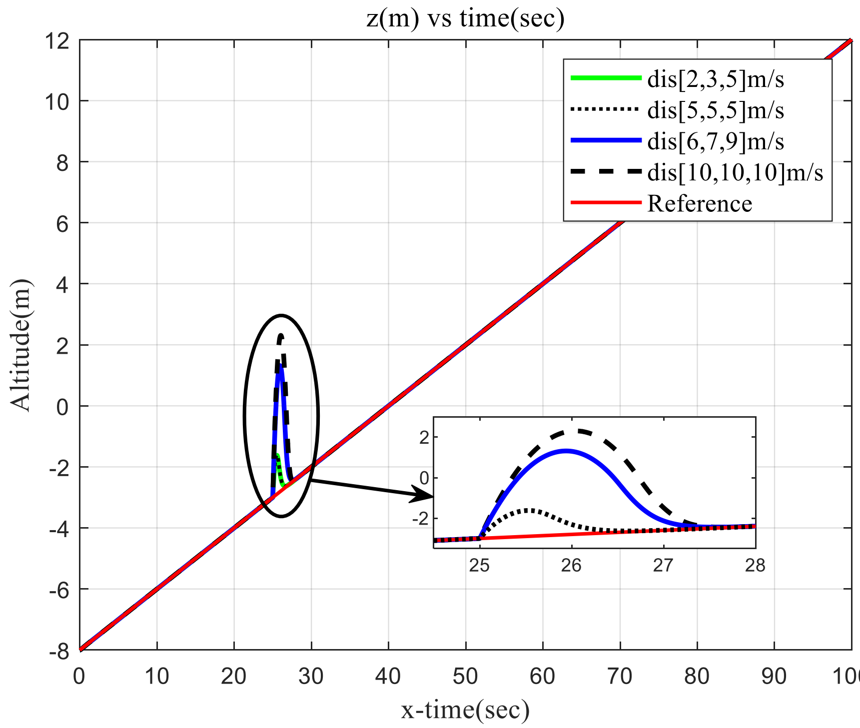


Figure 5.14: Altitude z(m) of GWO-IBS with wind disturbance at 25 sec

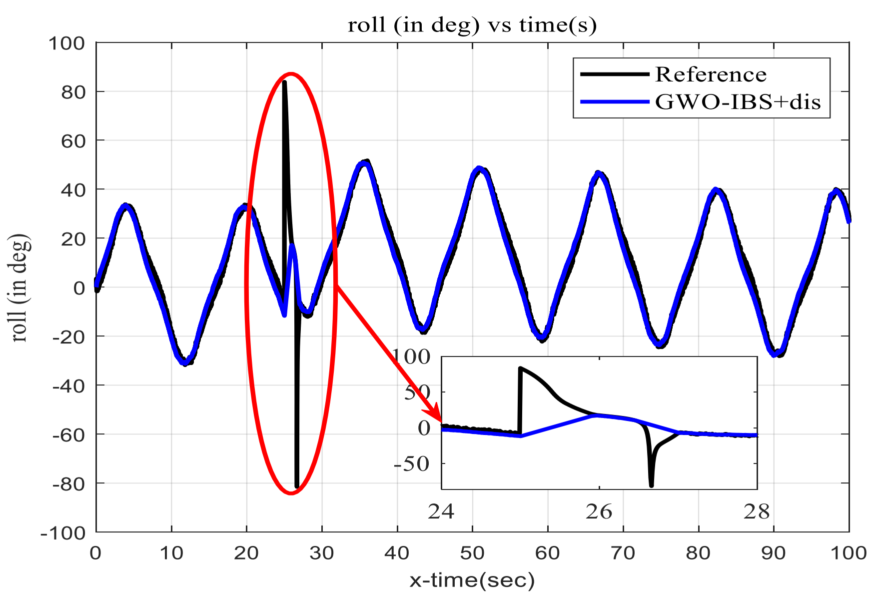


Figure 5.15: Roll angle of GWO- IBS with wind disturbance at 25 sec

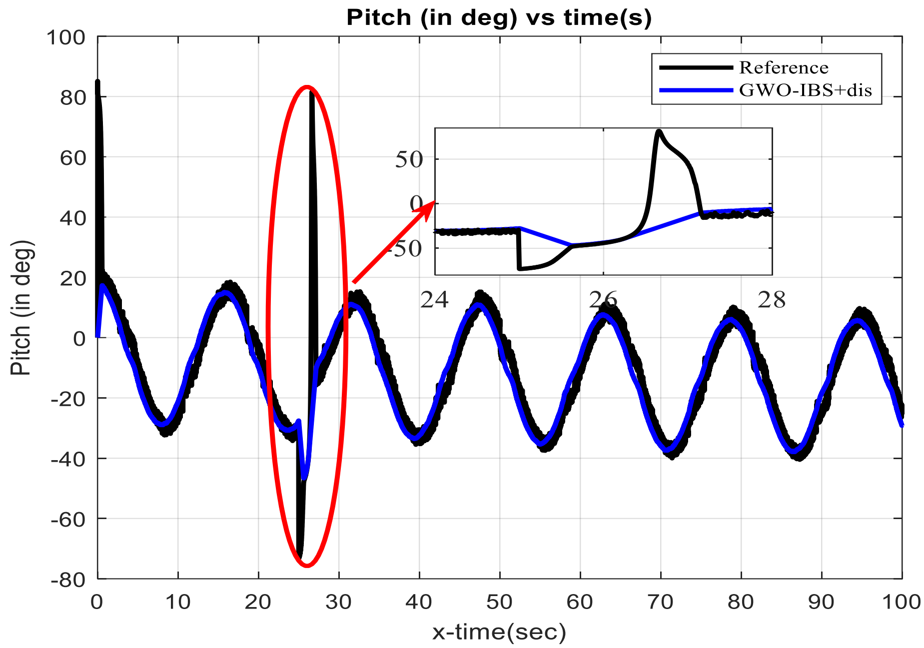


Figure 5.16: Pitch angle of GWO- IBS with wind disturbance at 25 sec

Figure 5.16 represents the simulation result of pitch angle with the GWO-IBS controller and the result shows the proposed controller has better performance than the IBS controller. GWO-IBS is the handle of uniform wind disturbance and becomes robust and Figure 5.18 show the response of the proposed controller for y, and x trajectory under uniform wind disturbance applied to the quadcopter. The result shows that the GWO-IBS can reject the disturbance rapidly and perform within the trajectory. The multiform wind disturbance was also tested, and the simulation response from the result the controller is robust and better perform until the magnitude of wind disturbance is 10. Steady state error is shown in Figure 5.19, and the performance numerically in Table 5.3 determined through the RMSE.

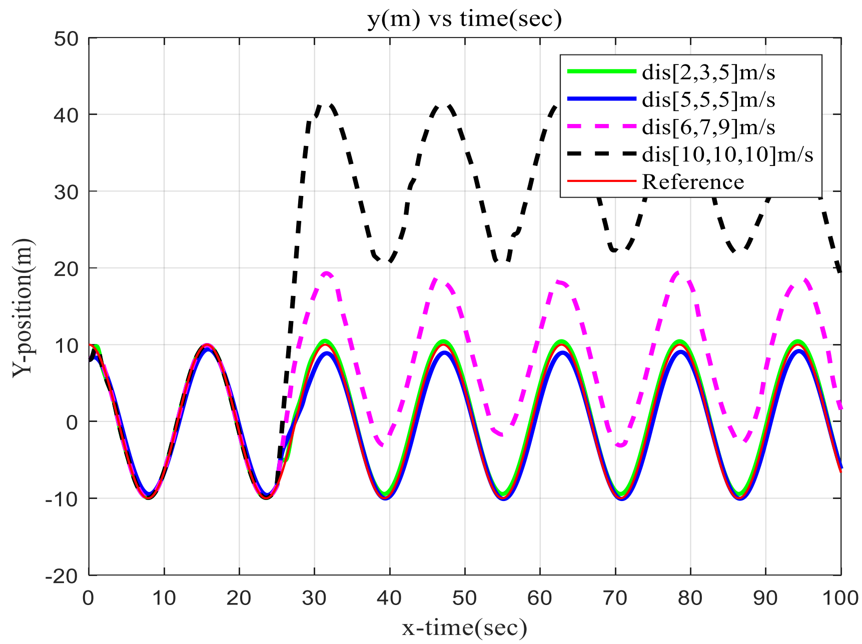


Figure 5.17: y-position of GWO-IBS with wind disturbance at 25 sec

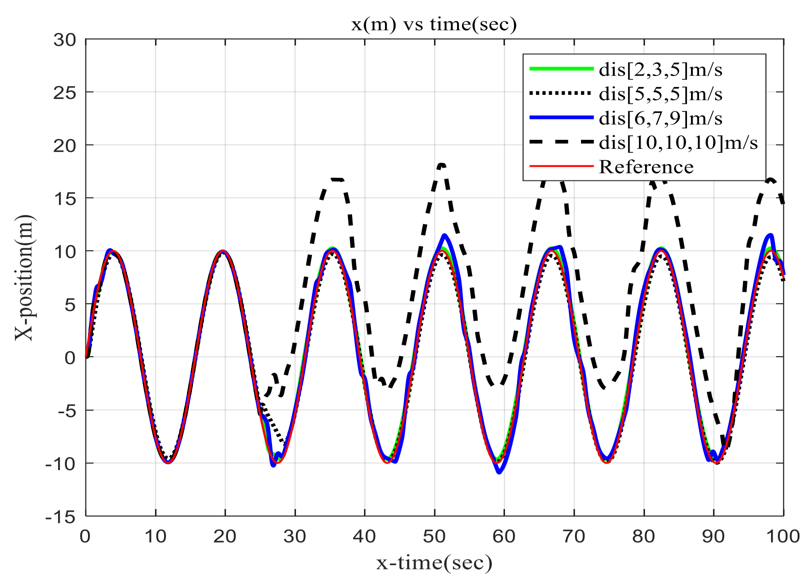


Figure 5.18: x-position of GWO-IBS with wind disturbance at 25 sec

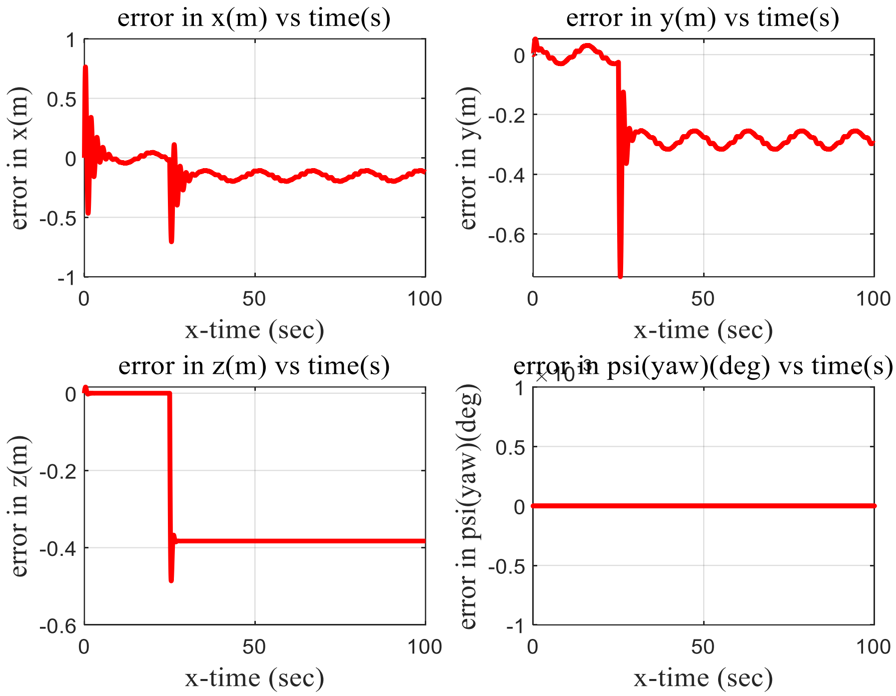


Figure 5.19: Error x, y, z-position, and yaw angle GWO-IBC with wind disturbance

*Scenario 2:* Robustness with parameter uncertainty of mass variation

The variable mass of the quadcopter control is the most challenging one. To evaluate the robustness of the proposed controller, consider the variation of the mass of the quadcopter. For instance, From the dynamic model of the quadcopter equation (3.28), when the quadcopter is applicable in healthcare for the delivery propose of packed blood or small medication equipment for emergency, there is a payload added to the design system which is the mass of the load. Most small medication types of equipment mentioned in Table B.1 each have a mass of less than 5.5kg shown in Appendix B. for blood delivery single bag blood of has a 0.555kg weight this is equal to 37% of the original quadcopter mass.

Figure 5.20 shows the simulation result of GWO-IBS for x and y-positions when the mass increased to 4kg. The proposed control can handle the variation in masses by tracking the reference trajectory with the best performance than IBS. The result shows the reference trajectory in red and the trajectory obtained by the controller with the GWO-IBS controller the black. The proposed GWO-IBS controller gives better performance and is robust.

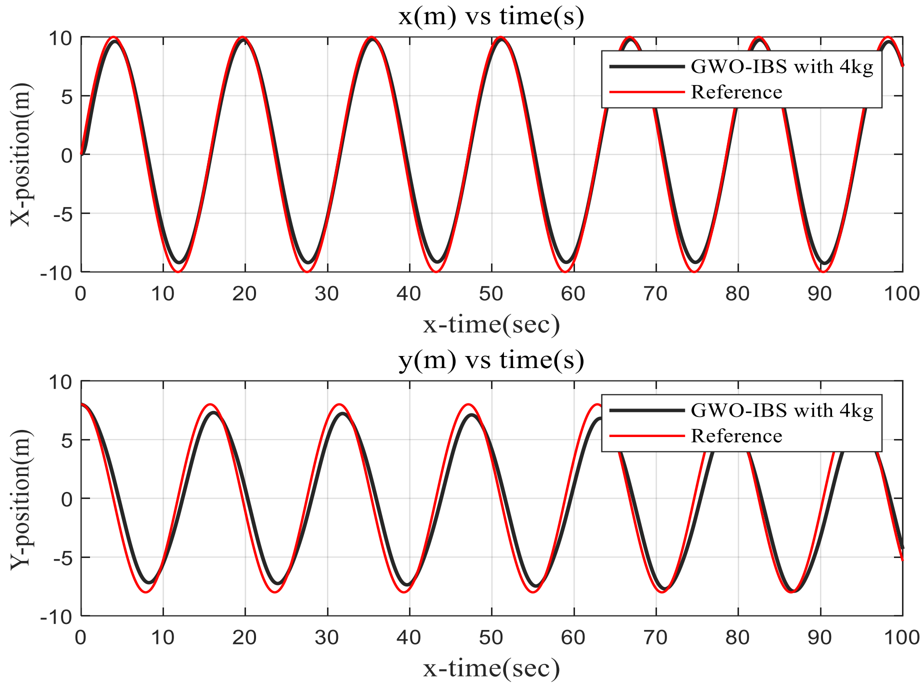


Figure 5.20: GWO-IBS for x and y-positions when the mass increased to 4kg

*Scenario 3*: Robustness with parameter uncertainty variation of moment inertia

Another parameter that affects system parameter uncertainty which ΔI is considered arbitrarily in $(0\sim25\%) \times$ I is added and indicates that the moment of inertia $I + \Delta I$is calculated. In this thesis work, test the robustness of the proposed controller varies the 10% and 25% of the original and add it to the original inertial moment of the quadcopter Table 5.3 contains values of error analysis of root mean square error. In the wind disturbance scenario, the value root mean square error analyzed when the disturbance is uniform at the magnitude of wind speed is 5. From the dynamic of the quadcopter, from the Equation (3.27) the moment inertia used in this thesis simulation is small and its effects on the system. Identifying the effect of the moment of inertia is difficult in this way it may measure by testing experimentally.

Table 5.3: Root Mean Square error Values the proposed IBS and GWO-IBS

| Controllers | $RMSE_X$ | $RMSE_Y$ | $RMSE_Z$ | $RMSE_\psi$ | $RMSE_\phi$ | $RMSE_\theta$ |
|---|---|---|---|---|---|---|
| IBS without dist. | 0.4537 | 0.4523 | 0.3081 | 1.54e-18 | 4.3395 | 4.5468 |
| IBS with dist. | 0.5017 | 0.5108 | 4.9837 | 2.27e-18 | 4.2766 | 4.5209 |
| GWO-IBS without dist. | 0.0831 | 0.0274 | 4.30e-04 | 1.73e-19 | 2.6696 | 2.6696 |
| GWO-IBS with dist. | 0.0884 | 0.0605 | 0.0037 | 1.53e-19 | 4.3374 | 4.5451 |
| IBS with 4kg mass | 0.3422 | 0.3539 | 0.8495 | 0.1084 | 4.9311 | 4.9311 |
| GWO-IBS with 4kg mass | 0.1252 | 0.5720 | 0.4424 | 0.1081 | 0.9157 | 0.9157 |
| GWO-IBS when I ↑ by10% | 0.2702 | 0.5979 | 0.3410 | 0.1116 | 2.8199 | 2.8199 |
| GWO-IBS when I ↑ by 25% | 0.2486 | 0.5688 | 0.2634 | 0.1152 | 2.8196 | 2.8196 |

Note: dist. is disturbance

Generally, the proposed GWO-IBS controller has improved the performance and stability of the system without wind disturbance and no parameter uncertainty, in the position scenario 1, the error was evaluated numerically. Based on the result and from Table 5.3 the GWO-IBS give better improvement with 81.68% for x- trajectory, 93.65% for y-trajectory, and 99.86% for z-trajectory, 48.38% for roll angle, 41.29% for pitch angle, and 88.77% for yaw angles than IBS. For scenario 2, the error was reduced by 82.38% for x-trajectory, 88.12% for y- trajectory, 99.93% for altitude z- trajectory, 37.26% for both roll, pitch angles, and 93.26% for, and yaw angles than IBS. Therefore, the proposed control mechanism has a strong ability in the rejection disturbance. the GWO-IBS reduced the error and give better with 68.40%, 70.65%, and 99.9% for x, y, and z- trajectory's and 57.2%, 57.2%, and 100% for roll, pitch, and yaw angles the quadcopter than IBS. Thus, stabilization and trajectory tracking control of a quadcopter-type UAV system achieved using GWO-IBS controller.

# 6. CONCLUSION AND RECOMMENDATION

## 6.1. Conclusion

The nonlinear mathematical model of the system was discussed in detail. The system Open-loop analysis shows that the quadcopter is unstable without using any control techniques. This thesis develops the integral based nonlinear backstepping control scheme designed based on the Lyapunov stability criteria and Grey Wolf Optimization for altitude, attitude and horizontal motion control of quadcopter. The simulation has done with various initial value for all inputs and the able to guarantee global stability, robust, and better trajectory tracking that force the quadcopter system the desired position. The proposed nonlinear control has been applied to the system and: -

- ✓ The integral action increases the response time and minimizes the error.
- ✓ The GWO Algorithm provided the globally optimal value of all gains.
- ✓ Improved global stability
- ✓ It is robust under the existence of wind disturbance
- ✓ Strongly handle uncertainty and perform better when the extra load mass is added
- ✓ Track the designed helical trajectory

Generally, the proposed GWO-IBS control have been ensured the stability system under the wind disturbance and parameter uncertainty of variation of mass as a load and moment of inertia. In this work, the effect of moment of inertial to the can performed with does not show on the simulation graph. But the performance of quadcopter evaluated through the RMSE. the comparisons of proposed control techniques with the IBS have been done, the result shows that the GWO-IBS has better and small RMSE in the acceptable value than IBS. Numerous simulation results show that the proposed control system can achieve high-precision response.

## 6.2. Recommendation

This thesis doesn’t consider pass planning of quadcopter with battery performance and controlling of motor dynamics of the quadcopter, for the next researchers developing path planning for automated, and this research have implement on a quadcopter that can be applied for the delivery of small medication equipment. Additionally, GWO-IBS based on exact mathematical model of the system and has several gains to be optimized. Although it does robust in a limited range of disturbances is increased and becomes unstable when the range of uncertainty and disturbance is too high because the optimized gain value is fixed gain. For further work recommend that, the solution can be used as model free adaptive integral nonlinear backstepping controller. An adaptive control provides the best solution during the existence of uncertain system dynamics.

**Acknowledgements:** This thesis work is funded by Adama Science and Technology University under the grant number of ASTU/SM-R/532/22, Adama, Ethiopia

# REFERENCES


Abdelhay, S., & Zakriti, A. (2019). Modeling of a Quadcopter Trajectory Tracking System Using PID Controller. Procedia Manufacturing, 32, 564–571. https://doi.org/10.1016/j.promfg.2019.02.253

Abeywickrama, H. V., Jayawickrama, B. A., He, Y., & Dutkiewicz, E. (2018). Empirical Power Consumption Model for UAVs. IEEE Vehicular Technology Conference, 2018-Augus, 1–5. https://doi.org/10.1109/VTCFall.2018.8690666

Akhtar, S. N. (2017). The use of modern tools for modelling and simulation of UAV with haptic. M. Sc. Res. Thesis, Cranfield Univ., Shrivenham, UK. https://core.ac.uk/download/pdf/83926716.pdf

Alkamachi, A., & Erçelebi, E. (2017). Modelling and Genetic Algorithm Based-PID Control of H -Shaped Racing Quadcopter. https://doi.org/10.1007/s13369-017-2433-2

Balamurugan, C. R., Revathy, S. M., & Vijayakumar, P. (2020). Quadcopter based emergency medikit delivery system for hill stations. International Journal of Reconfigurable and Embedded Systems (IJRES), 9(3), 201. https://doi.org/10.11591/ijres.v9.i3.pp201-212

Basri, M. A. M., Abidin, M. S. Z., & Subha, N. A. M. (2018). Simulation of Backstepping-based Nonlinear Control for Quadrotor Helicopter. Applications of Modelling and Simulation,2,

Bjälemark, A. (2013). Quadcopter Control using Android-based Sensing Hannes Bergkvist. http://lup.lub.lu.se/student-papers/record/4933972

Bouabdallah, S. (PhD T. (2007). design and control of quadrotors with application to autonomous flying Samir BOUABDALLAH THÈSE N O 3727 (2007). 3727. https://infoscience.epfl.ch/record/95939/files/EPFL_TH3727.pdf

Bouadi, H., Bouchoucha, M., & Tadjine, M. (2007). Modelling and stabilizing control laws design based on backstepping for an UAV type-quadrotor. In IFAC Proceedings Volumes (IFAC-PapersOnline) (Vol. 6, Issue PART 1). IFAC. https://doi.org/10.3182/20070903-3-fr-2921.00043

Can, E., & Içmez, S. ˙. (2014). Trajectory Tracking of a Quadrotor Unmanned Aerial Vehicle (Uav) Via Attitude and Position Control a Thesis Submitted To the Graduate School of Natural and Applied Sciences of Middle East Technical University. Middle East Technical University, November. https://doi.org/10.13140/2.1.4660.064

Chamola, V., Kotesh, P., Agarwal, A., Naren, Gupta, N., & Guizani, M. (2021). A Comprehensive Review of Unmanned Aerial Vehicle Attacks and Neutralization Techniques. Ad Hoc Networks, 111, 102324. https://doi.org/10.1016/j.adhoc.2020.102324

Cheng, H., & Yang, Y. (2017). Following of an Unmanned Quadrotor Helicopter. 768–773.

Ding, L., He, Q., Wang, C., & Qi, R. (2021). Disturbance Rejection Attitude Control for a Quadrotor: Theory and Experiment. International Journal of Aerospace Engineering, 2021. https://doi.org/10.1155/2021/8850071

DING, X., GUO, P., XU, K., & YU, Y. (2019). A review of aerial manipulation of small-scale rotorcraft unmanned robotic systems. Chinese Journal of Aeronautics, 32(1), 200–214. https://doi.org/10.1016/j.cja.2018.05.012

Dynamics, M. V., & Equations, Q. (2018). Autonomy in Motion Modeling Vehicle Dynamics – Quadcopter Equations of Motion (pp. 1–22).

Fessi, R., Rezk, H., & Bouallègue, S. (2021). Grey Wolf optimization based tuning of terminal sliding mode controllers for a quadrotor. Computers, Materials and Continua, 68(2), 2265–2282. https://doi.org/10.32604/cmc.2021.017237

Ganapathy Subramanian, R., & Elumalai, V. K. (2016). Robust MRAC augmented baseline LQR for tracking control of 2 DoF helicopter. Robotics and Autonomous Systems, 86, 70–77. https://doi.org/10.1016/j.robot.2016.08.004

Gao, P., Zhang, G., Ouyang, H., & Mei, L. (2019). A Sliding mode control with nonlinear fractional order pid sliding surface for the speed operation of surface-mounted pmsm drives based on an extended state observer. Mathematical Problems in Engineering, 2019. https://doi.org/10.1155/2019/7130232

Gao, Y., Li, R., Shi, Y., & Xiao, L. (2022). Design of path planning and tracking control of quadrotor. Journal of Industrial and Management Optimization, 18(3), 2221. https://doi.org/10.3934/jimo.2021063

Gouta, H., Said, S. H., & M'Sahli, F. (2016). Predictive and backstepping control of double tank process: A comparative study. IETE Technical Review (Institution of Electronics and Telecommunication Engineers, India), 33(2), 137–147. https://doi.org/10.1080/02564602.2015.1052580

Han, S. (2021). applied sciences Grey Wolf and Weighted Whale Algorithm Optimized IT2 Fuzzy Sliding Mode Backstepping Control with Fractional-Order Command Filter for a

Nonlinear Dynamic System.

Hsieh, T.-C., Hung, M.-C., Chiu, M.-L., & Wu, P.-J. (2020). Challenges of UAVs Adoption for Agricultural Pesticide Spraying : A Social Cognitive Perspective. January, 1–16. https://doi.org/10.20944/preprints202001.0121.v1

Huang, Q., & Wingo, B. (2016). Mathematical Modeling of Quadcopter Dynamics. Rose-Hulman Undergraduate Research Publications, 14.

Kandeel, H. M., Abdelmaksod, E. A., & Elnady, A. O. (2022). Modeling and Control of X-Shape Quadcopter. February. https://doi.org/10.9790/1684-1901034657

Kim, K., Kim, H. G., Song, Y., & Paek, I. (2019). Design and simulation of an LQR-PI control algorithm for medium wind turbine. Energies, 12(11), 1–18. https://doi.org/10.3390/en121

Kohli, M., & Arora, S. (2018). Chaotic grey wolf optimization algorithm for constrained optimization problems. Journal of Computational Design and Engineering, 5(4), 458–472. https://doi.org/10.1016/j.jcde.2017.02.005

Leal, I. S., Abeykoon, C., & Perera, Y. S. (2021). Design, simulation, analysis and optimization of pid and fuzzy based control systems for a quadcopter. Electronics (Switzerland), 10(18). https://doi.org/10.3390/electronics10182218

Lin, X., Yu, Y., & Sun, C. yin. (2019). A decoupling control for quadrotor UAV using dynamic surface control and sliding mode disturbance observer. Nonlinear Dynamics, 97(1), 781–795. https://doi.org/10.1007/s11071-019-05013-6

Liu, C., Pan, J., & Chang, Y. (2016). PID and LQR Trajectory Tracking Control for An Unmanned Quadrotor Helicopter : Experimental Studies. 10845–10850.

Luis, F., & Moncayo, G. (2021). Backstepping Control of Nonlinear Dynamical Systems (S. Vaidyanathan (Ed.)).

Lyapunov Function. (2008). In Encyclopedia of Neuroscience (pp. 2196–2196). https://doi.org/10.1007/978-3-540-29678-2_2854

Mamo, M. B. (2020). Trajectory Control of Quadcopter by Designing Second Order SMC Controller. Journal of Electrical Engineering, Electronics, Control and Computer Science, 7(23), 11–20.

Mathematics, A. (2019). LaSalle Invariance Principle for Ordinary Differential Equations and Applications Okolie , Ogochukwu Uni . No 40673 Prof . Khalli Ezzinbi.

Mirjalili, S., Mirjalili, S. M., & Lewis, A. (2014). Grey Wolf Optimizer. Advances in Engineering Software, 69, 46–61. https://doi.org/10.1016/j.advengsoft.2013.12.007

Munjani, P. R., Soni, D. P., Patel, H. J., Pathrudkar, S. Y., & Baghel, R. (2021). Design and Fabrication of Ambulance Drone with Navigation. 10(3). https://doi.org/10.15680/IJIRSE-T.2021.1003160

Niemiec, R., & Gandhi, F. (2016). A comparison between quadrotor flight configurations. 42nd European Rotorcraft Forum 2016, 1, 186–197.

Nithyavathy, N., Pavithra, S., Naveen, M., Logesh, B., & James, T. (2020). Design and development of drone for healthcare. International Journal of Scientific and Technology Research, 9(1), 2676–2680.

Oh, H., & Yoo, S. (2021). Development of Drone Mounted BLDC Motor Stator using Multi Stacked Structure of Cartridge. 12(6), 602–607.

Pan, C., Si, Z., Du, X., & Lv, Y. (2021). A four-step decision-making grey wolf optimization algorithm. Soft Computing, 25(22), 14375–14391. https://doi.org/10.1007/s00500-021-06194-2

Pattern, F. (2021). Working Principle and Components of Drone How do drones fly in air ? Which drone is more popular ? Introduction to Drone or UAV. 1–29.

Pérez, R. I., Galvan, G. R., Pérez, I., Galvan, R., Lara, D., Jonathan, A., & Alabazares, D. L. (2018). Attitude Control of a Quadcopter Using Adaptive Attitude Control of a Quadcopter Using Adaptive Control Technique Control Technique. https://doi.org/10.5772/intec hopen 71382

Rodríguez-Abreo, O., Garcia-Guendulain, J. M., Hernández-Alvarado, R., Rangel, A. F., & Fuentes-Silva, C. (2020). Genetic algorithm-based tuning of backstepping controller for a quadrotor-type unmanned aerial vehicle. Electronics (Switzerland), 9(10), 1–24. https://doi.org/10.3390/electronics9101735

Roy, R., Islam, M., Sadman, N., Mahmud, M. A. P., Gupta, K. D., & Ahsan, M. M. (2021). A Review on Comparative Remarks, Performance Evaluation and Improvement Strategies of Quadrotor Controllers.Technologies,9(2),37.https://doi.org/10.3390/technologies902 0037

Sabatino, F. (2015). Quadrotor control: modeling, nonlinear control design, and simulation. KTH Electrical Engineering, June.

Saibi, A., Boushaki, R., & Belaidi, H. (2022). Backstepping Control of Drone. January, 4. https://doi.org/10.3390/engproc2022014004

Setyawan, G. E., Kurniawan, W., & Gaol, A. C. L. (2019). Linear Quadratic Regulator Controller (LQR) for AR. Drone's Safe Landing. Proceedings of 2019 4th International Conference on Sustainable Information Engineering and Technology, SIET 2019, July 2020, 228–233. https://doi.org/10.1109/SIET48054.2019.8986078

Shah, J., Okasha, M., & Faris, W. (2018). Gain scheduled integral linear quadratic control for quadcopter. International Journal of Engineering and Technology(UAE), 7(4), 81–85. https://doi.org/10.14419/ijet.v7i4.13.21334

Shauqee, M. N., Rajendran, P., & Suhadis, N. M. (2021). An effective proportional-double derivative-linear quadratic regulator controller for quadcopter attitude and altitude control. Automatika, 62(3–4), 415–433. https://doi.org/10.1080/00051144.2021.1981527

Sheng, Z., & Wei-qi, Q. (2017). Dynamic systems backstepping control for pure-feedback nonlinear systems. 1–20.

Singh, N., & Wolf, G. (2020). A Modified Variant of Grey Wolf Optimizer. August 2018. https://doi.org/10.24200/SCI.2018.50122.1523

Singhal, G., Bansod, B., & Mathew, L. (2018). Unmanned Aerial Vehicle Classification , Applications-and-Challenges :AReview.Preprint, November, 1–19. https://doi.org/10.209-44/preprints201811.0601.v1

Siti, I., Mjahed, M., Ayad, H., & Kari, A. El. (2019). applied sciences New Trajectory Tracking Approach for a Quadcopter Using Genetic Algorithm and Reference Model Methods. https://doi.org/10.3390/app9091780

Suresh, H., Sulficar, A., & Desai, V. (2018). Hovering control of a quadcopter using linear and nonlinear techniques. International Journal of Mechatronics and Automation, 6(2–3), 120–129. https://doi.org/10.1504/IJMA.2018.094488

Tps, H. T., & Tp, H. T. (2018). Medical Drones Are Saving Lives in Africa - The Drones World MEDICAL DRONES AS PART OF AF RICA ’ S NEW I NF RA ST RU CTU RE Medical Drones Are Saving Lives in Africa - The Drones World. 1–8.

Turabieh, H. (2016).A Hybrid ANN-GWO Algorithm for Prediction of Heart Disease. American Journal of Operations Research, 06(02), 136–146. https://doi.org/10.4236/ajor.2016. 62016

USAID. (2019). Ethiopia Fact sheet Maternal and Child Health. Nursing and Midwifery Board of Australia, 035(September), 1–3.

Usman, M. (2020). Quadcopter modelling andcontrolwith MATLAB/Simulink implementation. Bachelor’s Thesis 2019 LAB University of Applied Sciences Technology Lappenranta, 68. https://doi.org/10.9790/1684-1901034657

Vishal, & Ohri, J.(2015).GA tuned LQR and PID controller for aircraft pitch control. India

International-Conferenceon-Power-Electronics,IICPE,2015-May(October).https://doi.org/ 10.1109/IICPE.2014.7115839

Waliszkiewicz, M., Wojtowicz, K., Rochala, Z., & Balestrieri, E. (2020). The design and implementation of a custom platform for the experimental tuning of a quadcopter controller y. Sensors (Switzerland), 20(7). https://doi.org/10.3390/s20071940

Xuan-Mung, N., & Hong, S. K. (2019). Improved altitude control algorithm for quadcopter unmanned aerial vehicles. Applied Sciences (Switzerland), 9(10). https://doi.org/10.3390/-app9102122

Yang, F., Xue, X., Cai, C., Sun, Z., & Zhou, Q. (2018). Numerical simulation and analysis on spray drift movement of multirotor plant protection unmanned aerial vehicle. Energies, 11(9). https://doi.org/10.3390/en11092399

Zhou, L., Zhang, J., She, H., & Jin, H. (2019). Quadrotor uav flight control via a novel saturation integral backstepping controller. Automatika, 60(2), 193–206. https://doi.org/10.1080/00051144.2019.1610838

# APPENDIX A: DERIVATION OF THE TRANSFORMATION MATRIX

## A.1 Rotational Matrix R

The body frame has been transformed from the inertial frame. The first rotational matrix:

$$R(\psi) = \begin{pmatrix} \cos\psi & \sin\psi & 0 \\ -\sin\psi & \cos\psi & 0 \\ 0 & 0 & 1 \end{pmatrix} \tag{A.1}$$

The inertia frame has been obtained with the rotation of the body about its Y-axis with pitch angle $\theta$. The inertia frame has been transformed from the body frame by:

$$R(\theta) = \begin{pmatrix} \cos\theta & 0 & -\sin\theta \\ 0 & 1 & 0 \\ \sin\theta & 0 & \cos\theta \end{pmatrix} \tag{A.2}$$

The body frame has been found from the rotation of the inertia frames about its X-axis. The body frame has been transformed from the inertia frame by

$$R(\phi) = \begin{pmatrix} 1 & 0 & 0 \\ 0 & \cos\phi & \sin\phi \\ 0 & -\sin\phi & \cos\phi \end{pmatrix} \tag{A.3}$$

Finally, the transformation from inertial to body frame is given by

$$R_e^b = R(\phi)R(\theta)R(\psi) \tag{A.4}$$

$$R = \begin{pmatrix} 1 & 0 & 0 \\ 0 & \cos\phi & \sin\phi \\ 0 & -\sin\phi & \cos\phi \end{pmatrix} \begin{pmatrix} \cos\theta & 0 & -\sin\theta \\ 0 & 1 & 0 \\ \sin\theta & 0 & \cos\theta \end{pmatrix} \begin{pmatrix} \cos\psi & \sin\psi & 0 \\ -\sin\psi & \cos\psi & 0 \\ 0 & 0 & 1 \end{pmatrix} \tag{A.5}$$

The Sequentially ordered product (A.4) is the reverse of the ordered product and the rotational matrix $R(\phi)R(\theta)R(\psi)$. Transformation matrix from the body frame to inertial the previous $R_e^b$ the rotation matrix is becoming transposed.

$$R = (R_e^b)^T = R_b^e \tag{A.6}$$

$$R_e^b = \begin{pmatrix} \cos\theta\cos\psi & \cos\psi\sin\theta\sin\phi - \sin\psi\cos\phi & \cos\psi\sin\theta\cos\phi + \sin\psi\sin\phi \\ \sin\psi\cos\theta & \sin\theta\sin\psi\sin\phi + \cos\psi\cos\theta & \cos\phi\sin\psi\sin\theta - \cos\psi\sin\phi \\ -\sin\theta & \sin\phi\cos\theta & \cos\theta\cos\phi \end{pmatrix} \quad \text{(A.7)}$$

## A.2 Euler Rates

The relationship between Euler rate and angular body rates expressed in the equation (3.3) is given as follows (Shauqee et al., 2021)

$$\begin{bmatrix} p \\ q \\ r \end{bmatrix} = R(\dot{\phi})\begin{bmatrix} \dot{\phi} \\ 0 \\ 0 \end{bmatrix} + R(\phi)R(\dot{\theta})\begin{bmatrix} 0 \\ \dot{\theta} \\ 0 \end{bmatrix} + R(\phi)R(\theta)R(\dot{\psi})\begin{bmatrix} 0 \\ 0 \\ \dot{\psi} \end{bmatrix} \quad \text{(A.8)}$$

The assumption angle in quadcopter-type UAV is small made and the time derivative of each Euler rate becomes small, then, $\cos(\phi) = \cos(\theta) = 1$ and $\sin(\theta) \cong \sin(\phi) \cong 0$ $R(\dot{\phi}) = R(\dot{\theta}) = R(\dot{\psi}) = \mathrm{I}$.

$$\begin{bmatrix} p \\ q \\ r \end{bmatrix} = I\begin{bmatrix} \dot{\phi} \\ 0 \\ 0 \end{bmatrix} + R(\phi)I\begin{bmatrix} 0 \\ \dot{\theta} \\ 0 \end{bmatrix} + R(\phi)R(\theta)I\begin{bmatrix} 0 \\ 0 \\ \dot{\psi} \end{bmatrix} \quad \text{(A.9)}$$

$$= \begin{bmatrix} \dot{\phi} - \sin\theta\dot{\psi} \\ \cos\phi\dot{\theta} + \sin\phi\cos\theta\dot{\psi} \\ -\sin\phi\dot{\theta} + \cos\phi\cos\theta\dot{\psi} \end{bmatrix} \quad \text{(A.10)}$$

$$\xi = \begin{bmatrix} 1 & 0 & -\sin(\theta) \\ 0 & \cos(\phi) & \sin(\theta)\cos(\theta) \\ 0 & -\sin(\phi) & \cos(\phi)\cos(\theta) \end{bmatrix}\begin{bmatrix} \dot{\phi} \\ \dot{\theta} \\ \dot{\psi} \end{bmatrix} \quad \text{(A.11)}$$

If the angles are assumed as small, then the S matrix becomes the identity matrix

$$\begin{bmatrix} p \\ q \\ r \end{bmatrix} = s\begin{bmatrix} \dot{\phi} \\ \dot{\theta} \\ \dot{\psi} \end{bmatrix} \quad \text{(A.12)}$$

And the angular rates are equal to the time derivative of the Euler angles. Otherwise when the inverse matrix of S is given as:

$$s^{-1} = \begin{bmatrix} 1 & \sin(\phi)\tan(\theta) & \cos(\phi)\tan(\theta) \\ 0 & \cos(\phi) & -\sin(\phi) \\ 0 & \sin(\phi)/\cos(\theta) & \cos(\phi)/\cos(\theta) \end{bmatrix} \tag{A.13}$$

$$\begin{bmatrix} \dot{\phi} \\ \dot{\theta} \\ \dot{\psi} \end{bmatrix} = \begin{bmatrix} 1 & \sin(\phi)\tan(\theta) & \cos(\phi)\tan(\theta) \\ 0 & \cos(\phi) & -\sin(\phi) \\ 0 & \sin(\phi)/\cos(\theta) & \cos(\phi)/\cos(\theta) \end{bmatrix} \begin{bmatrix} p \\ q \\ r \end{bmatrix} \tag{A.14}$$

## APPENDIX B: RELATED INFORMATION FOR CALCULATION OF POWER FOR THE QUADCOPTER-TYPE UAV

i. Power calculations for vertical motion of the quadcopter

The thrust force required to lift the quadcopter(Page & Lutus, 2010) (Abeywickrama et al., 2018)is equal to its weight,

$$F = mg \tag{B.1}$$

And this causes the gravitational potential energy (GPE) to be equal to the weight of the quadcopter times the height to which it's lifted.

$$\text{GPE} = \text{kg x } 9.8 \text{ m/s2 x m} = \text{joules.}$$

Then, the quantity of energy produced per a given time (in seconds) is power, and calculated as:

$$P = \frac{mgh}{t} \text{ in watt} \tag{B.2}$$

ii. Power calculation for Climbing a Hill motion of the quadcopter

To determine how much power is needed to achieve a specified climb rate or the reference trajectory. Here are the details:

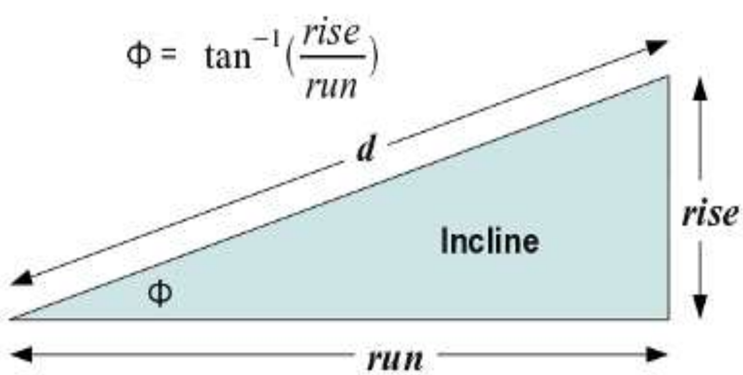


Figure B.1: Slope Diagram

Quadcopter mass m: 1.5 kilograms

Hill slope (rise/run): 0.2

Hill angle φ = tan−1(rise/run) = 11.31°

Desired velocity v: 20m/100 s=0.2m/s

When climbing, the gravitational force is less than in a vertical lift. The force equation for this case is:

$$F = m\ g \sin(\varphi) \tag{B.3}$$

Now that we know how to compute the force, we can find the power required to meet the desired velocity goal of 0.2 m/s.

The Power desired for 20m is calculated as:

$$\text{Power}_{des} = f\ v = f\ v = m\ g \sin(\varphi)\ v = 1.5 \times 9.81 \times \sin\ (11.31°)\ \times 0.2 = 0.577 \text{ watts}$$

iii. The weight of the quadcopter and load is affecting the fighting time of the quadcopter

If the Lithium polymer battery Pack (LiPo) 8000mAh 6S 35C/70C(Munjani et al., 2021)

Number of motors = 4

$$\text{Thrust requir} = \text{ Quadcopter weight} \times \text{ Power} - \text{to} \\ - \text{weight ratio per number of the motor}$$

$$= 1500 \times \frac{3}{4} = 1125$$

iv. Battery discharge converts mAh to Ah

$$= \frac{8000}{1000} = 8\text{Ah}$$

v. The maximum discharge of the battery for 80%, Efficiency capacity

$$= 8 \times 0.8 = 6.4\text{A}$$

vi. The thrust produced by each motor

$$= \frac{1500}{4} = 375\ gm\ per\ motor$$

The Average Amps is 10.43Amp.

finally, flight time = $\text{capacity} \times \frac{\text{discharge}}{\text{Average Amps}} \times 60 = 29.45\text{min.}$

Table B.1 Typical weight for major medical items with less than 20 % accuracy

| Infusions | | Sutures | Weight |
|---|---|---|---|
| 1-liter infusion in the plastic pouch | 1.3kg | 36 single pieces | 0.2kg |
| Ampoules | | X-Ray films | |
| 100 amps. 2ml | 0.6kg | 100 films 24x30cm | 2.7kg |
| 100 amps. 5ml | 1.0kg | 100 films 30x40cm | 3.7kg |
| 100 amps. 10ml | 1.6kg | 100 films 35x43cm | 5.6kg |
| Vials | | Gauze compresses | |
| 100 vials | 3.5kg | Big 100m x 1 m | 3.0kg |
| Tablets | | 100 sterilized gauze compresses 10x20cm | 0.3kg |
| 1000 small tablets | 0.3kg | 25 packs of 2 sterile compresses | 0.6kg |
| 1000 large tablets | 0.8kg | Elastic gauze bandages | |
| POP (Plaster of Paris) | | 10 elastic gauze bandages 10cm | 0.2kg |
| 10 POP 10cm | 1.8kg | Elastic bandages | |
| 10 POP 15cm | 2.7kg | 10 elastic bandages 10cm | 0.5kg |
| 10 POP 20cm | 3.6kg | Urine bags | |

# APPENDIX C: SIMULINK BLOCK DIAGRAM OF THE DYNAMIC MODEL OF QUADCOPTER-TYPE UAV

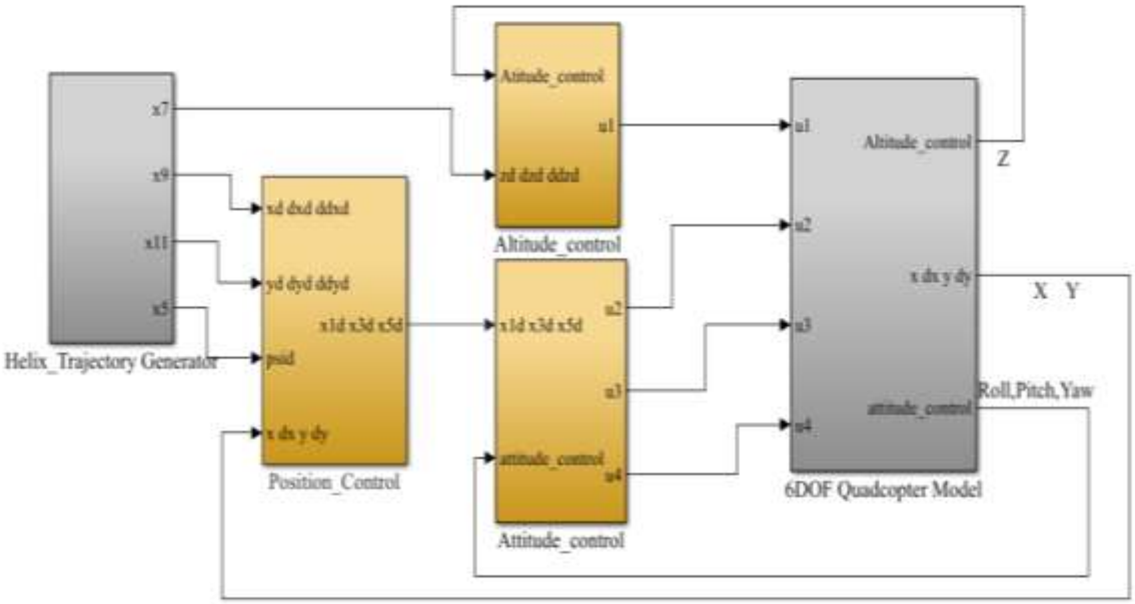


Figure C.1: Generic Simulink block of system with the proposed controller

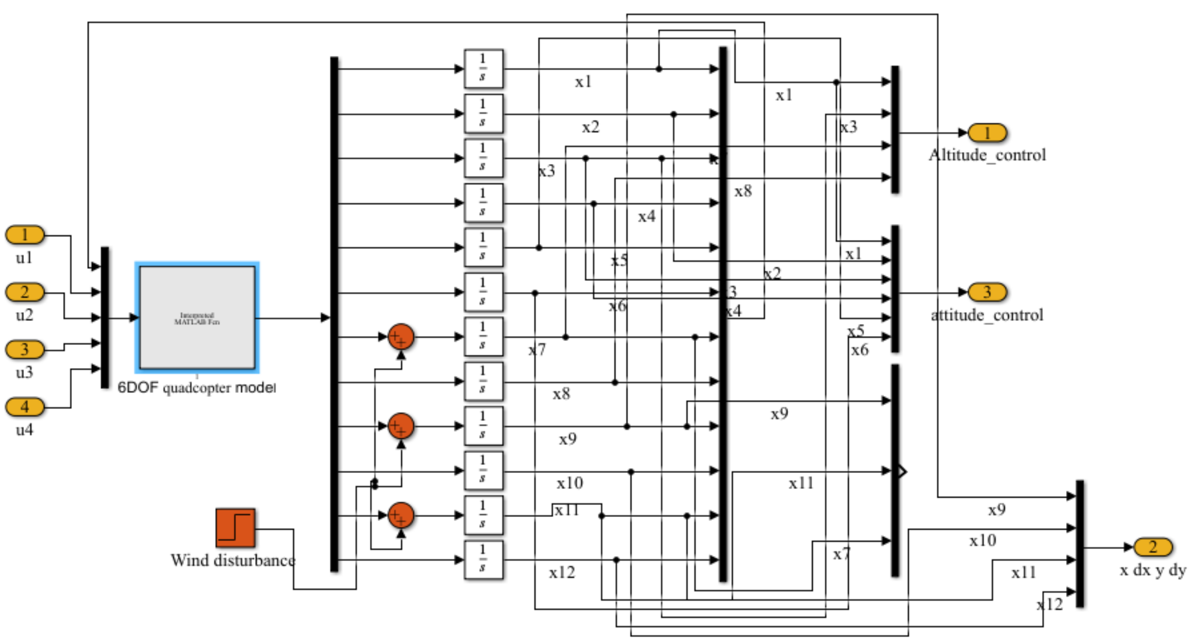


Figure C.2: Six-DOF Quadcopter Model Subsystem

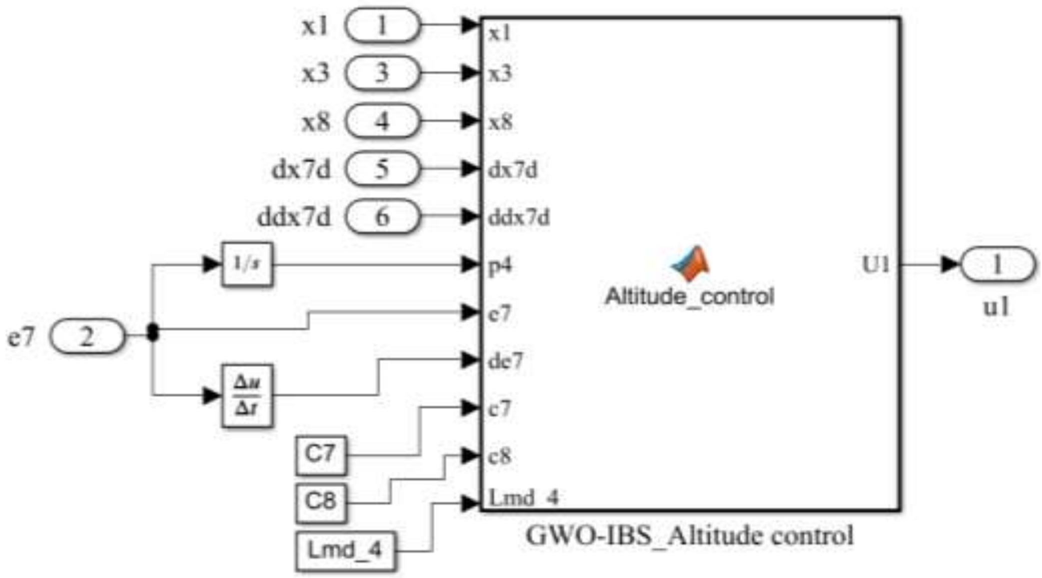


Figure C.3: GWO-IBS Altitude control Simulink block

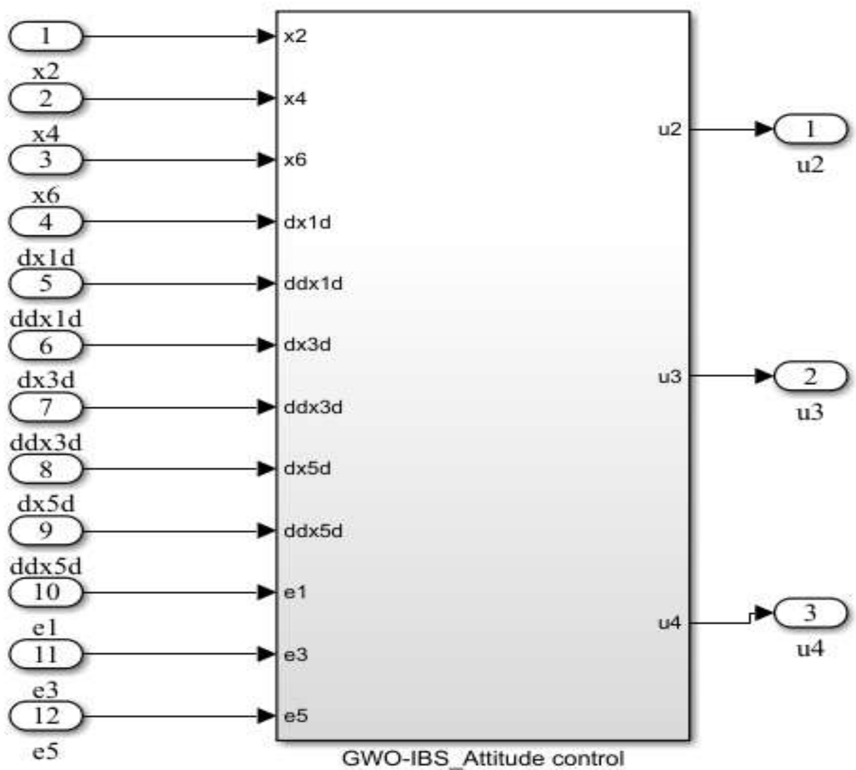


Figure C.4: GWO-IBS Attitude control Simulink block

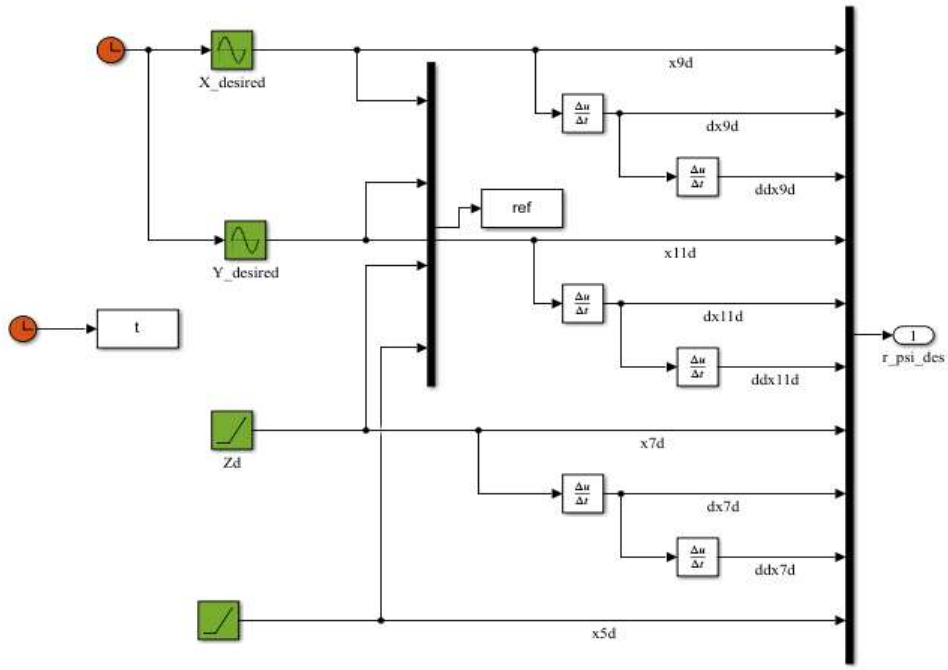


Figure C.5: Helical Trajectory and desired set point Simulink block

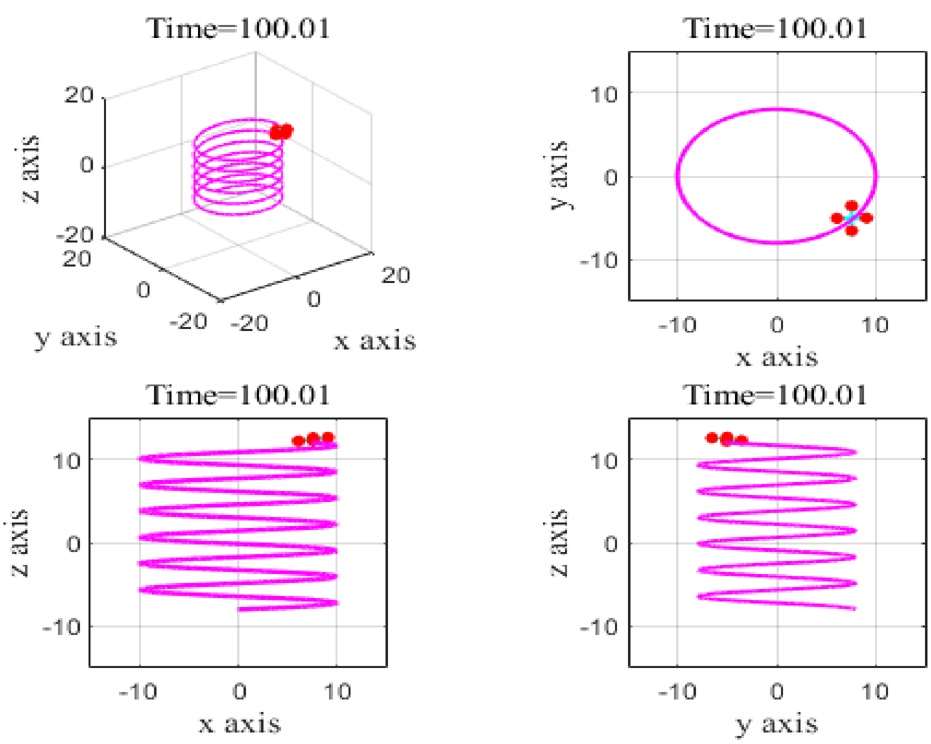


Figure C.6: Quadcopter tracking of a 3D helical trajectory.

Appendix D: Matlab m.code of function

```
%%%%%% quadcopter 6DOF model
function [dx1,dx2,dx3,dx4,dx5,dx6,dx7,dx8,dx9,dx10,dx11,dx12]=...
    model(u1,u2,u3,u4,x1,x2,x3,x4,x5,x6,x8,x10,x12)
m = 1.5;%
I = [7.5e-3,   0,        2.55e-6;
     0,        7.5e-3,   0;
     2.55e-6,  0,        1.3e-2];
g=9.8;
Ixx=I(1,1); Iyy=I(2,2); Izz=I(3,3);
a1=(Iyy-Izz)/Ixx; b1=1/Ixx;
a2=(Izz-Ixx)/Iyy; b2=1/Iyy;
a3=(Ixx-Iyy)/Izz; b3=1/Izz;
b4=1/m;
dx1=x2;
dx2=a1*x4*x6+b1*u2;
dx3=x4;
dx4=a2*x2*x6+b2*u3;
dx5=x6;
dx6=a3*x2*x4+b3*u4;
dx7=x8;
dx8=-g+b4*cos(x1)*cos(x3)*u1;
dx9=x10;
dx10=b4*(cos(x5)*sin(x3)+cos(x3)*sin(x1)*sin(x5))*u1;
dx11=x12;
dx12=b4*(sin(x5)*sin(x3)-cos(x3)*sin(x1)*cos(x5))*u1;
```

%%%%Altitude control subsystem

```
Function[Ux,Uy]==Altitude_control(x1,x3,x10,dx9d,ddx9d,p5,e9,de9,c9,c10,Lmd5,
x12,dx11d,ddx11d,p6,e11,de11,c11,c12,Lmd6)
m = 1.5;% 4;7;
g=9.8;
b4=1/m;
z8=x8-dx7d-Lmd_4*p4-c7*(e7);
U1=1/(b4*(cos(x1)*cos(x3)))*(-(c7+c8)*z8+g+ddx7d+c7*de7+(1-
Lmd_4+c7^2)*e7+Lmd_4*p4);
```

%%%%position control subsystem

```
function U1=position_control(x1,x3,x8,dx7d,ddx7d,p4,e7,de7,c7,c8,Lmd_4)
```

```
m = 1.5;% 4;7;
g=9.8;
b4=1/m;
z10=x10-dx9d-Lmd_5*p5-c9*(e9);
Ux=U1/(b4*(cos(x1)*cos(x3)))*(-(c9+c10)*z10+g+ddx9d+c9*de9+(1-
Lmd5+c7^2)*e9+Lmd_ 5*p5);
```

%%% Y-control%%%%%

```
z12=x12-dx11d-Lmd_6*p6-c11*(e11);
Uy=U1/(b4*(cos(x1)*cos(x3)))*(-(c11+c12)*z12+g+ddx11d+c11*de11+(1-Lmd6+c11^2
)*e11 + Lmd_6*p6);
```

%%%%%%%Attitude control subsystem

```
function [u2,u3,u4]=attitude_control(x2,x4,x6,...
    dx1d,ddx1d,dx3d,ddx3d,dx5d,ddx5d,e1,de1,e3,de3,e5,de5,p1,p2,p3,...
    c1,c2,c3,c4,c5,c6,Lmd_1,Lmd_2,Lmd_3)
h=0.01;
m = 1.5;%4;7;
I = [7.5e-3,   0,         2.55e-6;
     0,        7.5e-3,   0;
     2.55e-6,   0,         1.3e-2];
g=9.8;
Ixx=I(1,1); Iyy=I(2,2); Izz=I(3,3);
a1=(Iyy-Izz)/Ixx;
b1=1/Ixx;
a2=(Izz-Ixx)/Iyy ;
b2=1/Iyy;
a3=(Ixx-Iyy)/Izz;
b3=1/Izz;
z2=x2-dx1d-c1*e1-Lmd_1*p1;
u2=(1/b1)*(ddx1d+c1*de1-(c1+c2)*z2+(1-Lmd_1+c1^2)*e1-a1*x4*x6+Lmd_1*p1);
```

%%%%%pitch control

```
z4=x4-dx3d-c3*e3-Lmd_2*p2;
u3=(1/b2)*(ddx3d+c3*de3-(c3+c4)*z4+(1-Lmd_2+c3^2)*e3-a2*x2*x6+Lmd_2*p2);
```

%%%%%% yaw control

```
z6=x6-dx5d-c5*e5-Lmd_3*p3;
u4=(1/b3)*(ddx5d+c5*de5-(c5+c6)*z6+(1-Lmd_3+c5^2)*e5-a3*x2*x4+Lmd_3*p3);
```